AFAMRL-TR-83-016

AD A129517

A FOUNDATION FOR SYSTEMS ANTHROPOMETRY: LUMBAR/PELVIC KINEMATICS

H. M. REYNOLDS, Ph.D.
SIK-CHUEN LEUNG, Ph.D.

MICHIGAN STATE UNIVERSITY
EAST LANSING, MICHIGAN 48824

FEBRUARY 1983

Approved for public release; distribution unlimited.

AIR FORCE AEROSPACE MEDICAL RESEARCH LABORATORY
AEROSPACE MEDICAL DIVISION
AIR FORCE SYSTEMS COMMAND
WRIGHT-PATTERSON AIR FORCE BASE, OHIO 45433

NOTICES

When US Government drawings, specifications, or other data are used for any purpose other than a definitely related Government procurement operation, the Government thereby incurs no responsibility nor any obligation whatsoever, and the fact that the Government may have formulated, furnished, or in any way supplied the said drawings, specifications, or other data, is not to be regarded by implication or otherwise, as in any manner licensing the holder or any other person or corporation, or conveying any rights or permission to manufacture, use, or sell any patented invention that may in any way be related thereto.

Please do not request copies of this report from Air Force Aerospace Medical Research Laboratory. Additional copies may be purchased from:

National Technical Information Service
5285 Port Royal Road
Springfield, Virginia 22161

Federal Government agencies and their contractors registered with Defense Technical Information Center should direct requests for copies of this report to:

Defense Technical Information Center
Cameron Station
Alexandria, Virginia 22314

TECHNICAL REVIEW AND APPROVAL

AFAMRL-TR-83-016

This report has been reviewed by the Office of Public Affairs (PA) and is releasable to the National Technical Information Service (NTIS). At NTIS, it will be available to the general public, including foreign nations.

This technical report has been reviewed and is approved for publication.

FOR THE COMMANDER

CHARLES BATES, JR.
Chief
Human Engineering Division
Air Force Aerospace Medical Research Laboratory

REPORT DOCUMENTATION PAGE

READ INSTRUCTIONS BEFORE COMPLETING FORM

1. REPORT NUMBER
AFAMRL-TR-83-016

2. GOVT ACCESSION NO.
AD-A129 517

3. RECIPIENT'S CATALOG NUMBER

4. TITLE (and Subtitle)
A FOUNDATION FOR SYSTEMS ANTHROPOMETRY: LUMBAR/PELVIC KINEMATICS

5. TYPE OF REPORT & PERIOD COVERED
Final Report
22 Feb. 1981 - 22 Feb. 1982

6. PERFORMING ORG. REPORT NUMBER

7. AUTHOR(s)
H.M. Reynolds, Ph.D.
Sik-Chuen Leung, Ph.D.

8. CONTRACT OR GRANT NUMBER(s)
F33615-81-C-0506

9. PERFORMING ORGANIZATION NAME AND ADDRESS
Department of Biomechanics
Michigan State University
East Lansing, Michigan 48824

10. PROGRAM ELEMENT, PROJECT, TASK AREA & WORK UNIT NUMBERS
61102F, 2313-V1-31

11. CONTROLLING OFFICE NAME AND ADDRESS
AFAMRL, Human Engineering Division,
AMD, AFSC, Wright-Patterson AFB OH 45433

12. REPORT DATE
11 May 1983

13. NUMBER OF PAGES
104

14. MONITORING AGENCY NAME & ADDRESS (if different from Controlling Office)

15. SECURITY CLASS. (of this report)

15a. DECLASSIFICATION/DOWNGRADING SCHEDULE
N/A

16. DISTRIBUTION STATEMENT (of this Report)

DISTRIBUTION STATEMENT A
Approved for public release;
Distribution Unlimited

17. DISTRIBUTION STATEMENT (of the abstract entered in Block 20, if different from Report)

18. SUPPLEMENTARY NOTES

AFAMRL Monitor: Mr. Charles E. Clauser, AFAMRL/HEG, Tele: 513 255 5779

19. KEY WORDS (Continue on reverse side if necessary and identify by block number)

Anthropometry	Screw Axis
Linkage System	Stereoradiography
Kinematics	Lumbar/Pelvis
Three-Dimensional	Anatomical Frames of Reference

20. ABSTRACT (Continue on reverse side if necessary and identify by block number)
Research protocol and results from System Anthropometry Laboratory's three-dimensional investigation of the lumbar/pelvis linkage system are presented. A stereoradiographic system measures three-dimensional coordinates of implanted targets in the skeletal system of an unembalmed cadaver seated in a wooden seat conforming to Air Force specifications. The cadaver is experimentally positioned to obtain three-dimensional data on lumbar extension, flexion, and lateral sidebending motions. Data are analyzed to provide a screw axis description of the instantaneous axis of rotation for each change of position.

(continued on reverse side)

SECURITY CLASSIFICATION OF THIS PAGE(When Data Entered)

20. Abstract, cont'd.

In addition, position vectors are calculated that describe locations of the bones in the lumbar/pelvic linkage system and a point on the screw axis closest to the origin of the bone frame of reference. The data are presented in three-dimensional coordinates measured in a laboratory with a spatial accuracy of approximately ±0.03 cm. The extensive references to measurement and measurement techniques studies offer a listing not presented elsewhere in the literature, or in other reviews of the literature, and with particular application to systems anthropometry, from the fields of anthropometry, osteology, kinematics, and three-dimensional measurement techniques.

SECURITY CLASSIFICATION OF THIS PAGE(When Data Entered)

PREFACE

Research reported herein was conducted under contract F33615-81-C-0506 with the Air Force Aerospace Medical Research Laboratory, U.S. Air Force, Wright-Patterson Air Force Base. This research investigation has been conducted in Systems Anthropometry Laboratory which has been constructed and supported by funds from the Air Force Office of Scientific Research, Air Force Aerospace Medical Research Laboratory, and the College of Osteopathic Medicine. Principal investigator is Herbert M. Reynolds, Ph.D., Associate Professor, Department of Biomechanics, Department of Anthropology, Michigan State University. Mr. Charles E. Clauser, Workload and Ergonomics Branch, Wright-Patterson Air Force Base, Ohio, acted as contract monitor; and Intz Kaleps, Ph.D., Chief, Mathematics and Analysis Branch, Biodynamics and Bioengineering Division, Wright-Patterson Air Force Base, Ohio, acted as Senior Technical Advisor.

The authors would also like to acknowledge the support of Dr. Robert W. Little, Chairperson, Department of Biomechanics, and Dr. Myron S. Magen, Dean, College of Osteopathic Medicine. Ms. Laurie J. Batzer and Mr. June Lai provided excellent technical assistance in the conduct of this research program. Ms. Ann D. Eschtruth, Ms. Laura Hayes and Ms. Therese Thelen, Department of Biomechanics, edited and prepared the manuscript for publication.

TABLE OF CONTENTS

List of Tables

List of Illustrations

1.0 INTRODUCTION

1.1 STATEMENT OF LABORATORY RESEARCH OBJECTIVES

This report describes research conducted in the Systems Anthropometry Laboratory (SAL) at Michigan State University, from 21 February 1981 to 23 February 1982. This research represents a one-year effort within a continuing investigation of the three-dimensional Systems Anthropometry of the human body.

Basic laboratory research has been conducted in three-dimensional anthropometry for application in simulation studies of the human body. The multidisciplinary investigation of the three-dimensional position and mobility of the skeletal system has developed a methodology whereby kinematics, mass distribution properties, and muscle and ligament attachments can be described in comparable anatomical frames of reference. As a result, three-dimensional anthropometry can describe basic geometry of the human body for mathematical simulations.

1.1.1 Three-dimensional systems anthropometry

Anthropometry, as a subdiscipline of physical anthropology, has been used extensively to describe the static size and shape of the human body in the U.S. military for the past 40 years. With the advent of the high speed digital computer, and the development of computer-based simulations of the human body, functional body geometry (e.g., link length and segment mass) has been derived from anthropometric techniques and instruments developed in the nineteenth century to measure external body dimensions for human variation studies. The traditional dimensions of anthropometry are scalar quantities, representing body size and shape unique to the position in which the body is measured. To satisfy the more rigorous mathematical requirements of computer simulations and biomechanically representative anthropomorphic dummies, dimensions in anthropometry must be in vector quantities that are independent of body position. Establishing a three-dimensional anthropometry that meets this requirement has been the major objective of research in Systems Anthropometry for the past five years.

The new anthropometric data measure the spatial geometry of the whole body relative to a three-dimensional frame of reference, i.e. traditional anthropometric scalars are replaced with position vectors. A dedicated stereoradiographic laboratory has been constructed at Michigan State University and the basic research design has been described previously (Reynolds 1976, 1977, 1978, 1981). This report will provide data and analytical procedures illustrating Systems Anthropometry.

1.1.2 Improve biofidelity of human simulations

Simulations of the human body are currently used to model both ergonomic and dynamic environments. Increasingly difficult demands are made on the human operator with respect to the mental and physiological workload. For example, the need for accurate design of a workstation to fit the human operator is critical: ease of reaching for controls and sighting of instrument panels is highly related to work efficiency and fatigue. Furthermore, as the significance of the task increases, psychological

stress becomes a major factor in the ability of the human operator to perform the task. The physical environment must therefore be designed to accommodate the ergonomic geometry of different operators in the most efficient manner possible in order to reduce this element of fatigue (Frisch and D'Aulerio, 1980; Kroemer, 1973).

Equally as important to geometric accommodation is the design of the pilot's environment to minimize the risk of injury during a crash or ejection (Mohr, Brinkley, Kazarian, and Millard, 1969). Of particular importance, for example, is the question of how to position the pilot for an ejection event so that forces are distributed through the body in the least harmful manner. Thus, the position and mobility of the human body, especially the spinal column, must be carefully studied in order to design the best cockpit for personal protection in a high acceleration environment.

As research continues in the Systems Anthropometry Laboratory, data on the position and mobility of the human body in three-dimensional space will be measured and analyzed with the aim of providing accurate three-dimensional anthropometric and kinematic data for improving biosimulations. As a result, more accurate predictions of performance and response of the anthropomechanical system can be made with computer simulations.

1.1.3 Position and mobility of skeletal system

The human body can be modeled as a system of mechanical links that represent bones and joints: each bone represents a physical link connected at joints by soft connective tissue. Each bone, analytically, is a rigid body; two bones, including the intervening soft tissue, compose a relative motion segment. In the living body, muscles generate internal forces acting on bones across an anatomical (fulcrum) joint thereby creating motion or resistance to motion. The human body is, therefore, a living, moving mechanical system, with its relative link positions providing the geometry for all subsequent potential motions.

Continuing the analogy, in three-dimensional space, each of the approximately 68 links (excluding hands and feet) in the human body have six degrees of freedom. If the linkage system were not constrained by soft tissue, potential positions and motions of the human body which result from this linkage system would clearly be unmanageable in both number and complexity. An objective of this research program has been to develop a methodology that measures each link with six degrees of freedom in the anatomical system. A research design has been developed to measure motions in the whole intact body so that soft tissue constraints on joint mobility and segment position are representative of the living human body. In addition, mass distribution and moments which act passively on the spinal column and pelvis are similar to the living subject. Body positions have been limited to the seated subject and motions restricted to the lumbar and pelvic linkage system.

1.2 CURRENT LABORATORY RESEARCH OBJECTIVES

Current research objectives in SAL are twofold. First, the position of the skeletal system in an unembalmed cadaver has been measured with respect to an Air Force seat geometry. Second, the three-dimensional kinematics of the lumbar and pelvic linkage systems have been investigated in unembalmed cadavers. This report will present body position geometry

and kinematics of lumbar and pelvic linkage systems in an experimental design that will measure data as representative of the living human body as possible.

1.2.1 Position and size of skeletal system

Position of the body is being investigated to establish a representative initial posture. Accurate positional data in comparable anatomical frames of reference for variety of seated positions are necessary. These data must represent vertebral column geometries that are loaded and constrained in a manner representative of the living body. Excised vertebral columns cannot provide the required data since preloads and moments acting on the column in the intact body are not known. These, measured body positions must represent carefully controlled body postures.

Since all simulations of the human body incorporate body size as a parameter, a three-dimensional description of the human skeletal system must be related to body size. Variability in skeletal size has been initially studied in an investigation of three-dimensional size and shape of the adult pelvis as a function of body size defined by stature and body weight (Reynolds, Snow, and Young, 1981).

1.2.2 Three-dimensional kinematics

The lumbar and pelvic linkage systems are normally composed of five lumbar vertebrae, a sacrum, right and left hip bones. Each of these bones, considered separately as rigid bodies in a human linkage system, is measured in seated positions of a cadaver. Data obtained on unembalmed cadavers measured with the spinal column as part of the whole body are unique. The primary purpose of these measurements is to quantify the motion characteristics of the lumbar and pelvic linkage systems in three-dimensional space.

These data are measured with the cadaver sitting in a seat that approximates Air Force seat specifications, thereby providing three-dimensional coordinate data on the position of the pelvis (e.g., the H-point, lumbo-sacral joint, and ischial tuberosities) and lumbar vertebrae relative to the Seated Reference Point (SRP). The three-dimensional description of motion will be described by an axis of rotation for each of the motions located in both the SRP frame of reference and an anatomical frame of reference. With the utilization of the anatomical axis frame, the location of the axis of rotation can be described relative to other anatomical features (e.g., articular facets, vertebral body, and intervertebral disc) and compared between subjects.

A major objective of every anthropometric study is to measure human variation. The present investigation has developed a methodology whereby relative motions in the skeletal system are comparable between subjects. With data obtained in such a manner, it will be possible to:

1) Collect data in a sample and estimate variability in the population;

2) Compare motions so that differences between subjects can be studied;

3) Test for a quantitative relationship between motion and skeletal geometry;

4) Evaluate the effect of other biological parameters, such as age and sex, in variability of motion parameters.

2.0 REVIEW OF LITERATURE

2.1 ANTHROPOMETRY AND OSTEOLOGY

Anthropometric investigations of the human body have seldom measured dimensions of the lumbar and pelvic linkage systems. Dempster (1955) established an anatomical linkage model for which he measured living subjects and cadavers to describe the link dimensions of the extremities, including the approximate location of the hip joint. For example, he described the hip joint as an area relative to Trochanterion, an anthropometric landmark in a measure of leg length (Martin, 1928). Dempster observed that Martin's definition of Trochanterion could be used to estimate the location of the hip joint center within a circle with a radius of approximately 1 cm.

Subsequent to Dempster's work, which did not investigate the spinal column, the Air Force Aerospace Medical Research Laboratory sponsored a program at The University of Michigan's Highway Safety Research Institute. The Torso Linkage Study conducted by Snyder et al.(1972) investigated the geometry of the spinal column relative to various locations of the elbow. The relationship between hip joint and shoulder joint was not established; and the formulations of joint kinematics in the vertebral column were described in predictive terms, thereby making the data difficult to utilize in other spinal simulations.

Another anthropometric program, sponsored by the automotive industry, measured the two-dimensional location of the hip joint center in an automotive seated position (Geoffrey, 1961). A review of engineering anthropometry for the automotive industry made by Robbins and Reynolds (1975) concluded that the current state of anthropometric data did not meet requirements of physical (e.g., anthropomorphic dummies) or computer simulations of the human body.

Lanier's osteological study of the presacral vertebrae (1939) has been used for initial estimates of vertebral geometry in a finite element model of the disc (Belytschko, Kulak, Schultz, and Galante, 1974) and a model of the spine and rib cage (Andriacchi, Schultz, Belytschko and Galante, 1974). More recent investigations of pelvic geometry have been those by Pope et al. (1977b) and Reynolds, Snow and Young (1981); the latter investigation provides the most extensive data available on three-dimensional pelvic geometry.

Several fundamental problems must be considered when traditional anthropometric and osteological data are utilized:

a) These data have been collected from different populations without sampling to match body size parameters.

b) The data are presented as scalar quantities from which estimates of position vectors must be made.

c) The geometry has not been related to joint kinematics and therefore requires major assumptions regarding range of motion and type of motion data derived from other studies.

In conclusion, an integrated set of anthropometric and osteological data are needed to provide the basic geometric data on the human skeleton for dynamic simulations.

2.2 JOINT KINEMATICS

Motions of the body, whether from internally or externally generated forces, are dependent upon the initial position of the rigid bodies composing the system. As will be pointed out in the following literature review on joint kinematics, anatomical structures place constraints on the kinematics of a motion segment. Thus, the position of the rigid body as well as the structure's geometry are independent parameters in human kinematics.

2.2.1 Position and skeletal geometry

Current state of knowledge of body position and skeletal geometry is reflected in current models such as developed by Andriacchi, Schultz, Belytschko and Galante (1974). Their model geometry is based upon investigations of vertebrae geometry (Lanier, 1939; Schultz, Benson, and Hirsch, 1974b), rib cage geometry (Schultz, Benson, and Hirsch, 1974a), and traditional anthropometric dimensions of embalmed cadavers (Clauser, McConville, and Young, 1969) and the living body (Damon, Stoudt, and McFarland, 1966). Thus, the basic geometry of the spinal column and rib cage is described by combining different, unrelated studies.

Two other parameters are needed for a complete definition of spinal geometry: intervertebral disc space (Todd and Pyle, 1928; Pope, et al., 1977a; Andersson, et al., 1981) and spinal curvature or posture (Keegan, 1953; Mohr, et al., 1969; Milne and Lauder, 1974; Patrick, 1976). There are, therefore, substantial sources of data for describing various spinal geometry parameters, but the precision of the total system geometry is weakened by the lack of a complete anthropometric investigation that describes relationships between all of these parameters.

2.2.2 Lumbar kinematics

Research investigations of joint kinematics in the lumbar linkage system may be divided into two categories. The first is composed of those investigations of living subjects in which range of motion either for the whole lumbar region or between vertebral pairs is made; the second is composed of investigations of cadaveric material. Most of these studies have measured motions of two vertebrae, intervening disc, and all attached ligaments (i.e., a motion segment).

Within those investigations of living subjects, there have been two measurement techniques used: radiographic (Bakke, 1931; Begg and Falconer, 1949; Olsson, Selvik, and Willmer, 1977) and goniometric (Clayson et al., 1962; Troup, Hood, and Chapman, 1968; Loebl, 1967; Anderson and Sweetman, 1975). Bakke (1931) studied the intervertebral ranges of motion in 24 females and 20 males ranging in age from 3 to 79 years. Using planar radiographs, he measured the intervertebral angle representing the range of motion in the sagittal (flexion-extension) and frontal (lateral side-bending) planes. Continuing the same type of study, although with a greater emphasis on clinical applications, Begg and Falconer (1949), Tanz (1953), Froning and Frohman (1968), and Pennal, et al., (1972) measured the two-dimensional range of motion in "normal" subjects and patients. Considerable variation between subjects was shown in these investigations.

All investigators acknowledged the difficulty of deriving accurate data from planar radiographs; but the potential benefit in using

radiographic findings to assist clinical diagnosis outweighed the difficulties. A particular clinical model describing low back pain etiology was investigated by Knutssen (1944) and Hagelstam (1949) in radiographic examinations which attempted to determine whether retroposition of a vertebrae was associated with disc degeneration. Their results were promising although limited by a two-dimensional radiographic technique.

The development of three-dimensional radiographic measurement techniques provided the possibility of a closer examination of differences arising from investigating a three-dimensional problem with two-dimensional methods. With three-dimensional capabilities, position with six degrees of freedom can be measured, enabling coupled motion (White and Panjabi, 1978), for example, in lateral bending of the lumbar spine, to be investigated.

Two different quantitative radiographic techniques to measure three-dimensional data have been developed. Biplanar radiography (Suh, 1974) has been used in clinical studies in the United States (Brown, Burstein, Nash, and Schock, 1976; Stokes, Medlicott and Wilder, 1980), whereas stereoradiography (Selvik, 1974) has been used more frequently in European clinical studies (Olsson, Selvik, and Willner, 1977; Egund et al., 1978).

In contrast, stereoradiographic investigations utilize implanted targets (Aronson, Holst, and Selvik, 1974); whereas biplanar radiographic investigations use anatomical features as landmark targets (Rab and Chao, 1977). The degree to which the same point can be identified on two separate, distinct views of the spinal column has been discussed (Sherlock and Aitken, 1980; Reynolds and Hubbard, 1980). Rab and Chao's investigation indicates an error due to point identification in three-dimensional data, the magnitude of which Marcus (1980) points out would produce loss of accuracy and precision in the screw axis analysis.

From clinical investigations of spinal motion, little data can be derived for describing normal motions, location of the instantaneous axis of rotation, or other quantitative properties of joint kinematics in the spinal column. Rolander (1966) conducted the most extensive investigation of the lumbar spine to date. He studied excised lumbar vertebrae: 71 motion segments (two vertebrae with ligaments and intervening disc) from 38 autopsy subjects with ages of 4 to 76 years. The specimens were sealed in bags and frozen at -29 °C until used in the experiment. The experimental tests were made without simulating an <u>in vivo</u> environment, thereby creating uncontrolled artifact in the data due to dehydration of the ligaments and intervertebral disc. Measurements of motions in the three cardinal planes were recorded for translation and rotation as a function of the relative location of the load. Data on all motion segments were grouped for analysis, thereby precluding the possibility of evaluating differences between them. However, the ranges of motions in the three cardinal anatomical planes were: 1° maximum rotation in the horizontal plane, 6° maximum rotation in the sagittal plane, and 5.5° maximum rotation in the frontal plane.

Rolander's results point out for lumbar vertebrae that:

1) there are small translatory components (± 1-2 mm) in normal motion segments;

2) there are changing instantaneous centers of rotation for normal spinal segments;

3) instantaneous centers of rotation for motion in the sagittal and frontal planes tend to lie in the disc on the side of a line passing through the disc center and opposite to the direction of motion (e.g., dorsal side for lumbar flexion, and ventral for lumbar extension);

4) the articular facets play an important role in determining the amount of motion in the vertebral motion segments.

Cossette, Farfan, Robertson and Wells (1971) measured the location of the instantaneous axis of rotation for motion in the horizontal plane. The L3-L4 motion segment was obtained from 12 unembalmed cadavers. A couple was applied to the third lumbar vertebral body, thereby generating a torque about the longitudinal axis for a maximum 6° or less rotation to one side. The centers of rotation were found to lie in the posterior region of the vertebral body and generally on the side in the direction of the rotation. The authors also point out that their experiment illustrates the significant role of the facets in determining the limits and range of motion in the lumbar vertebrae.

Gregerson and Lucas (1967) investigated in living normal males the amount of axial rotation in the transverse plane for motions in the thoracolumbar spine while walking on a treadmill, standing and sitting erect. They reported an increase in the total range of motion in axial rotation from the sacrum up through the lumbar and thoracic vertebrae with a total of 9° rotation between the first and fifth lumbar vertebrae in one subject in the standing position. Sitting significantly decreased the amount of rotation in the lumbar region, particularly at the lumbosacral joint (e.g., in one subject, 9° rotation standing versus 3° rotation sitting).

Based upon these studies and their interpretation of the results, White and Panjabi (1978) estimated the maximum amplitude range of rotatory motion in the lumbar spine about each of the cardinal axes. They estimate going up the column from L5-S1 to L1-L2 a range of motion in flexion-extension from 20° to 12° rotation, in lateral bending from 3° to 6° rotation, and in axial rotation 5° to 2° rotation. These values are less than those reported by Bakke (1931) as summarized in Schultz (1974). Thus, at present, the results in the literature on motion in the lumbar spine are inconclusive, particularly when a linkage representation is desired.

2.2.3 Pelvic kinematics

The pelvis has not traditionally been viewed as an anatomical structure within which there are physiological motions. Forces acting on the pelvis (Jensen and Davy, 1975) and hip joint (Hirsch, 1965; Rydell, 1965) have been investigated; hip joint sphericity has also been extensively studied (Blowers, Elson and Korley, 1972; Clarke, Fiske and Amstutz, 1979). Reynolds (1980) reviewed the literature on motions between the sacrum and hip bones, and reported preliminary data which suggested that 1°-2° rotation of the sacrum relative to the hip bone occurred during maximum movements of the leg. Weisl (1954a, 1954b, and 1955) had previously investigated the sacroiliac joint and found the greatest movement of the sacrum to be about an axis 5-10 cm vertically below the sacral promontory. Wilder, Pope and Frymoyer (1980) have proposed that axes of rotation vary considerably and occur with substantial relaxation of ligaments and corresponding separation between the joint surfaces. Their conclusions are

based upon a topographical examination of the sacroiliac joint in eleven anatomical subjects whose pelvic bones were removed, cleaned and measured. Weisl (1954b) had previously investigated the topography of the joint with the cartilage still attached. Weisl's studies imply that there are probably differences between kinematic inferences based upon a cartilagenous versus osteological preparation of the joint surface.

Consequently, the question of sacral motion remains open both with respect to amount and location. There is, however, a corollary question concerning the pubic symphysis. That is, do the two hip bones also move relative to each other, requiring motion at the pubic symphysis? Motion in the pelvis has been studied for clinical application (Reynolds, 1980), but its significance for simulation of the lumbar and pelvic linkage systems remains a matter for investigation.

3.0 EXPERIMENTAL PROTOCOL

3.1 DESCRIPTION OF LABORATORY: AN OVERVIEW

The Systems Anthropometry Laboratory was constructed in 1977-78 at Michigan State University. The laboratory consists of three rooms: x-ray room, darkroom, and computer analysis room. Quantitative data from stereoradiographs are gathered through a complex experimental design developed for this research investigation.

3.1.1 Radiographic facility and instrumentation

The radiographic facility is composed of two rooms: x-ray and darkroom. The x-ray room is equipped with two Dynamax 42-40 x-ray tubes (1.0-2.0 mm focal spots, 15 degree targets) and an AMRAD Craig I generator (maximum output 500 mA @ 125 kVp or 600 mA @ 100 kVp). The two x-ray tubes are mounted on a steel beam, which is attached to a three-dimensional Siemens tube mount that can be positioned with 5 degrees of freedom. The distance between the focal spots is 74.72 cm.

The film cassette holder consists of two parallel aluminum tracks which hold a Liebel-Flarsheim film grid (64"-85" focus, 12:1 grid ratio) in front of a 14" x 36" film cassette with 3M TRIMAX 12 intensifying screens for use with TRIMAX XD radiographic film. The film cassette holder moves with three degrees of freedom providing a film plane 146 cm wide by 272 cm high.

Quantitative stereoradiography in SAL requires a vertical film plane. Vertical and horizontal movements of the film cassette holder are made on stainless steel tracks. Two sets of tracks have two pillow blocks on each track with milled .635 cm aluminum plates mounted to define a vertical film plane. The vertical film plane is perpendicular to a horizontal plane defined by a bubble level accurate to 30 seconds of arc. Steel beams 1.27 cm x 7.62 cm x 261.62 cm are attached to each side of the vertical track channels. The channels are straightened by set screws spaced 15.24 cm apart along the length of the steel beams. As a result, the film moves in a vertical plane.

3.1.1.1 Laboratory axis system: wire grid The laboratory axis system (i.e., inertial axis system) is defined by a wire grid lying in a plane parallel to the film plane (Figure 3.1). When facing the wire grid, the origin of the axis system is located at the bottom lefthand intersection of two vertical and six horizontal wires.

The perpendicular distance of each wire grid intersection from a milled aluminum plate on the film cassette holder has been measured by a depth gauge. After careful alignment of the wire grid, the plate and wire grid are parallel within $\pm$ 0.0127 cm. The coordinates (Table 3.1) of all intersections between the vertical and horizontal tungsten wires have been measured with a vernier caliper. The coordinates of these 12 intersections are used in the digitizing program. When a film pair is digitized, the operator measures the same wire intersection (Figure 3.1) for each film. In this manner, the film plane is spatially tracked in the inertial frame of reference and can, therefore, be moved to any position behind the wire grid.

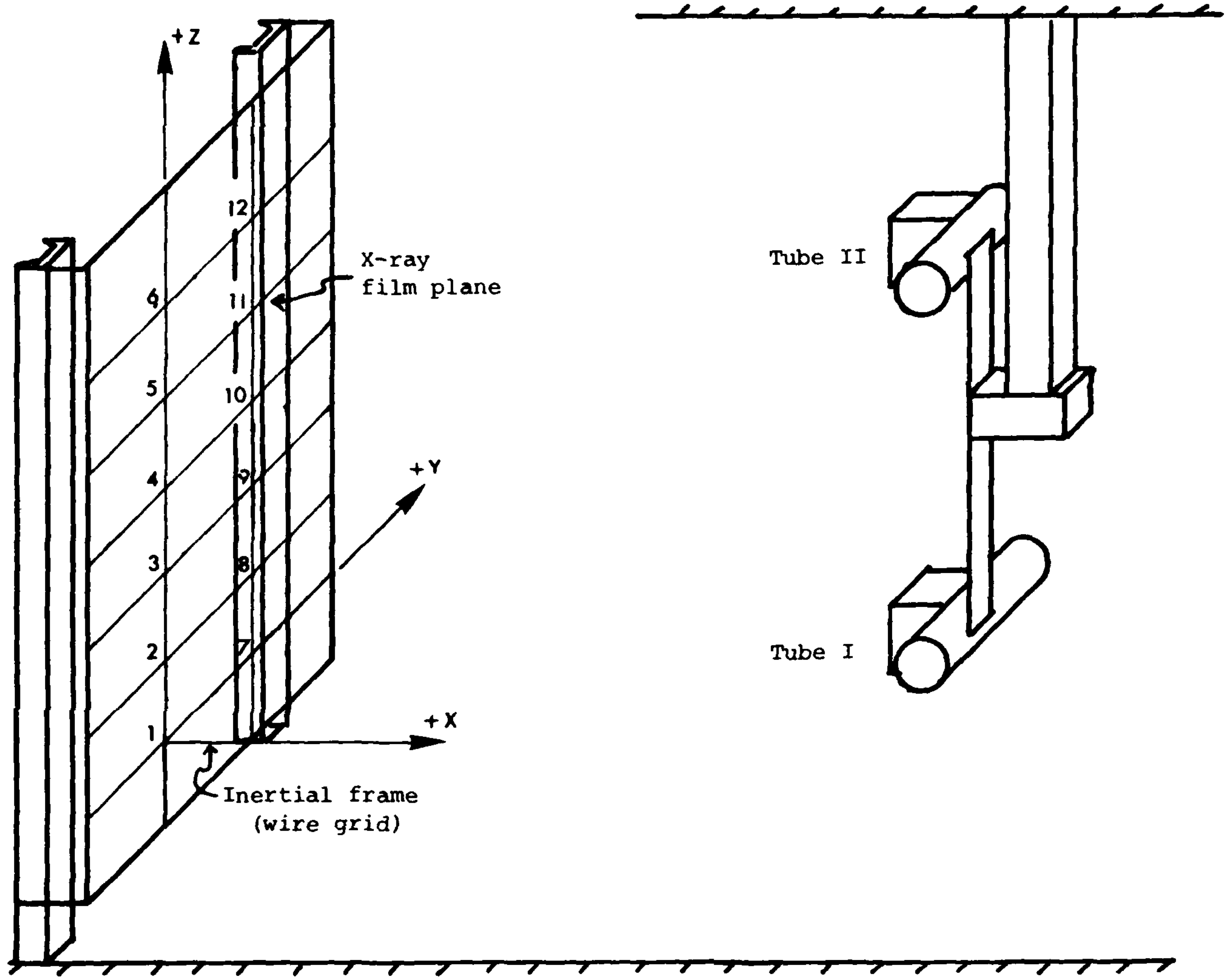

Figure 3.1. Schematic of laboratory wire grid, film plane, and X-ray tubes.

Target #	Coordinates Y (cm)	Z (cm)	Target #	Coordinates Y (cm)	Z (cm)
1	0.000	0.000	7	30.530	0.000
2	0.000	30.455	8	30.530	30.455
3	0.000	60.980	9	30.530	60.980
4	0.000	91.530	10	30.530	91.530
5	0.000	121.950	11	30.530	121.950
6	0.000	152.435	12	30.530	152.435

Table 3.1. Coordinates of wire grid intersection points.

This wire grid forms the yz plane of the laboratory axis system. The wire grid is 6.30 cm in front of the film plane. In Figure 3.1, a right-handed orthogonal axis system is depicted. The film plane is indicated, as well as the relative location of the x-ray tubes. All data labeled "inertial axis system" in this report will be in coordinates relative to the wire grid origin.

3.1.1.2 Chair design Investigations of the cadaver's seated positions are made in a hard seat, shown in Figure 3.2. The wooden seat, constructed at the Air Force Aerospace Medical Research Laboratory, represents a typical Air Force seat geometry. With respect to the horizontal (xy) plane, the seat pan forms a 6° angle and the seat back forms a 103° angle.

The seat back has been modified by SAL so that lumbar extension is experimentally controlled. A radio-translucent, adjustable support for the lumbar region has been constructed of a curved plexiglass plate mounted on a 2.54 cm diameter nylon screw with a ball-and-socket joint between plate and screw. This support device is adjustable for different heights on the chair back. The seat back, Seat Reference Point (SRP), and curved plexiglass plate are targeted with tungsten-carbide balls.

3.1.1.3 Calibration devices In the current digitizing algorithm, focal length calculation and merger of the two radiographic digital images use two targets on a glass rod. These two targets are designed on a line perpendicular to the film plane. In the present data, the targets are separated by a distance of 35.44 cm. (See arrowheads in Figure 3.2). In addition, a quartz cube with its corners targeted serves as a check for quality control in the digitizing.

3.1.2 Analytical facility and instrumentation

The analytical facility is composed of a Talos SR 640 x-y digitizer (accuracy ± 0.013 cm) and a General Automation 16/460 minicomputer (64K x 18 bit MOS parity memory). The digitizer is back-lighted with an active 76 cm x 101 cm electrostatic digitizing surface. Each film is digitized on this device which has output to both the minicomputer and a terminal. The digitizing program, described in Section 4.0, prompts the digitizer with the digitizing protocol. Upon completion of digitizing the three-dimensional coordinates are stored on hard disc. After the data are reviewed for errors, there is a Tektronix 4014 graphic terminal and a Tektronix 4662 x-y plotter available for graphical analysis.

Figure 3.2. Position of Air Force chair, glass rod, quartz cube in front of laboratory wire grid and film cassette holder ("0" marks origin of laboratory axis system on wire grid).

3.2 SUBJECT PROTOCOL

3.2.1 Subject selection and description

The availability of suitable cadavers has severely restricted the amount of data obtained. The main criteria are age (maximum age of 70 years), body size (no obese subjects), and general condition of the musculoskeletal system at time of death. Of the three criteria, age is the most restrictive for obtaining subjects.

As a result, only data and analysis on Subject #18 have been reported. The subject was a 59-year-old white male who died of an acute myocardial infarction. The anthropometric measures, made on the supine body according to procedures described in Chandler, et al.,(1974) are listed in Table 3.2.

Stature	173.6	cm
Weight	70.00	kg
Suprasternale Height	143.1	cm
Left ASIS Height	99.1	cm
Right ASIS Height	93.1	cm
Symphysion Height	89.0	cm

Table 3.2. Anthropometric dimensions of Subject #18.

3.2.2 Cadaver targets

After taking clinical radiographs to check for any observable pathology, e.g., osteoarthritis, etc., the cadaver is targeted with .8 mm diameter tungsten-carbide balls that are implanted with a spring-loaded instrument (Aronson, Holst and Selvik, 1974). Six balls are implanted in each vertebra: two on the dorsal spine and two each on the right and left sides of the neural arches and transverse processes. Each ball is pressed firmly into bone so that it moves with the bone.

The bones targeted for Subject #18 were as follows:

Cervical vertebra: 7
Thoracic vertebrae: 1, 4, 8, 11, 12
Lumbar vertebrae: 1, 2, 3, 4
Sacrum
Right and left hip bones (Innominates)

Subject #18 had a sacralized fifth lumbar vertebra and the twelfth thoracic vertebra had only a right rib. This subject has an anomalous spinal column (Wigh, 1980) with a transitional T12 and a sacralized L5.

3.2.3 Measurement positions

After each bone in the cadaver position investigation is targeted, the subject is positioned in the hard seat; and the torso is sequentially moved to different body positions in the sagittal and frontal planes. Ten positions have been measured: six in lumbar extension (LBAR 3.0 - 5.5); one seated erect position (SEATERCT); two in lumbar flexion (SEATEDP1 and SEATEDP2); and one lateral bending position to the subject's right (SIDEBEND).

Figure 3.3.a depicts the subject in the erect position. In order to place the body in this position, the buttocks are moved as far back into the seat as possible and retained there by a strap passing inferior to the anterior superior iliac spines and superior to the pubic symphysis. The torso is restrained against the chair back by a second strap across the chest. A rubber block is placed behind the neck, and the head is restrained by tape. This position approximates an erect seated position in a living body, but only passive body mass preloads the spinal column.

Figure 3.3.b is an example of a lumbar extension position. The curved plate of the lumbar device pushes on the back in the upper lumbar region. The experimental procedure begins with a maximum lumbar extension position and the curved plate is moved toward the seat back in 0.5 cm increments. The positions in lumbar extension are labeled LBAR 3.0-5.5, referring to the relative amount of displacement of the curved plate, with LBAR 5.5 being the maximum lumbar extension. The lumbar extension device is

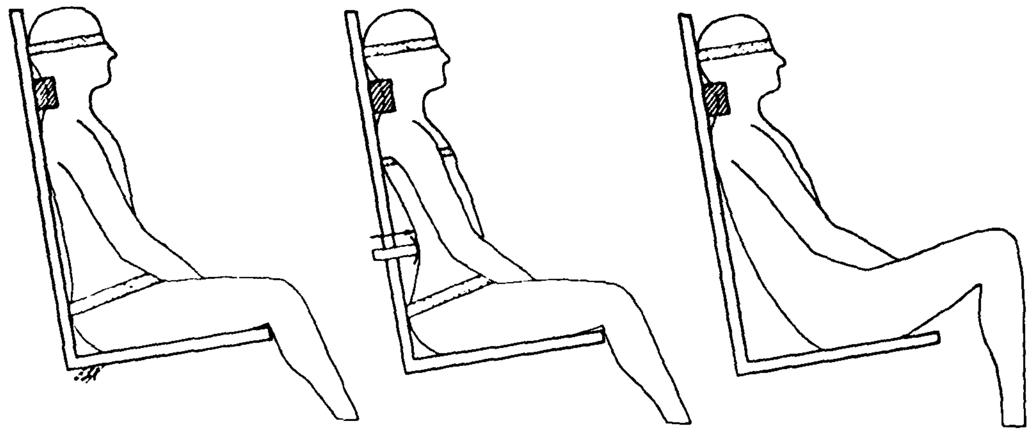

(a) (b) (c)

Figure 3.3 Subject seated in a) erect position (SEATERCT), b) lumbar extension position (LBAR), c) lumbar flexion position (SEATEDP1 and SEATEDP2).

positioned by finding a vertical location in which the lumbar vertebrae extend with minimum resistance.

Figure 3.3.c illustrates a lumbar flexed position with only the head and upper torso restrained against the chair back. The pelvis has been rotated away from the chair back and the posture is slumped. This position is typical of SEATEDP1 and SEATEDP2.

A right lateral side bending position (SIDEBEND) is not illustrated. As in lumbar flexion, only the head and upper torso are restrained.

3.2.4 Skeletal preparation and bone targets

Following completion of the radiographic study of body position, the bones of spinal column and pelvis are removed from the body. The bones are cleaned, and radiographs are made to locate and identify cadaver targets in the bones. For Subject #18, two targets remained in L4, one in L3-L2, three in L1, two in T12, three in the sacrum, and one in the right innominate.

The original location of missing targets has been estimated by measuring distances from the targets remaining in the bone. For bones with two targets remaining, a third target has been glued on the bone at the intersection of two radii representing the distances to a third target in the cadaver position data. In some instances, there is an impression in the bone where the target had been implanted, and the target is replaced.

After the cadaver targets are located, stereoradiographs are made and the target images are digitized. Three-dimensional distances are calculated between every pair of the three targets, providing a basis for evaluating the accuracy of target identification. Subsequent to identification of the cadaver targets on the cleaned bones, anatomical pointmark targets (.8 mm tungsten-carbide balls) are glued in place on each bone. A target is glued in the geometric middle of each facet on the vertebrae, at the ends of right and left transverse processes, on the

dorsal spine, and three targets on the rim of the inferior vertebral body surface. Three targets are glued on the base of the sacrum, and one target is positioned in both the sacroiliac joints at the intersection of two lines bisecting the superior and inferior poles of the joint surface. The innominate bone has a pointmark glued on corresponding to the sacroiliac junction point on the sacrum as well as a point representing the posterior superior iliac spine.

Stereoradiographs of the bones with both cadaver targets and anatomical pointmarks are made. To reduce the effect of experimental errors arising from experimental procedures, the bones are placed on the chair back at approximately their location during the cadaver study; and the coordinate locations of the quartz cube and glass rod are closely matched to the corresponding X, Y, Z coordinates in the cadaver motion film pairs. When the BONES steropairs meet these requirements, then the cadaver targets and anatomical pointmarks are digitized and added to the data base Subject #18.

4.0 FILM DATA REDUCTION

4.1 INTRODUCTION: OVERVIEW AND EQUIPMENT REQUIREMENTS

Radiographic images of targets on the skeletal system, glass rod, quartz cube, seat and wire grid are measured to describe the three-dimensional position of the seated cadaver. The three-dimensional coordinates of each target are calculated from measurements of two radiographic films comprising a stereoradiographic film pair (Figure 4.1). The data reduction process depends upon accurate measurements, an interactive computer program, and careful editing procedures to assure consistent data. A description of these procedures, including the basic stereoradiographic algorithm for calculating the three-dimensional coordinates, are presented in the following section.

4.1.1 Film data reduction

The film data reduction process consists of the following steps:

1) Target names are entered into a computer file. This computer file will be used throughout the film data reduction process to check for consistent use of the same target names.

2) A double exposure of the glass rod is measured to obtain focal length.

3) Targets on a stereoradiographic film pair of the cadaver are measured. Both Steps 2 and 3 use a program, "DIGITZ", which contains the complete algorithm, discussed in Section 4.2.

4) The three-dimensional coordinates calculated in "DIGITZ" are checked for consistent distances between every pair of targets on a bone in all body positions of the cadaver. If the distances are consistent, the three-dimensional coordinates are saved and used in the analysis of body position and mobility.

5) Stereoradiographic film pairs of the excised bones with cadaver targets amd anatomical pointmarks are made and digitized as in Steps 1, 2, and 3 above. The distances between cadaver targets, measured on films of the excised bones, are compared to distances representative of the target positions in all body positions of the cadaver. If the comparison establishes consistency in the data, the three-dimensional coordinates of cadaver targets and anatomical pointmarks are saved as BONES data and used in the analysis of body position and mobility.

6) Every stereoradiographic film pair is digitized several times, and the average and standard deviations are calculated. This procedure minimizes the effect of variation caused by human error in positioning the cursor of the digitizing board and inaccuracy of the digitizer. (Human error is approximately $\pm$ .02 cm and the Talos digitizer is specified at $\pm$ .013 cm.)

4.2 DIGITIZING ALGORITHM

The digitizing algorithm, outlined by Reynolds, Hallgren, and Marcus (1982), has had many subsequent versions with substantial improvements to the accuracy of the resulting data. The algorithm discussed in the

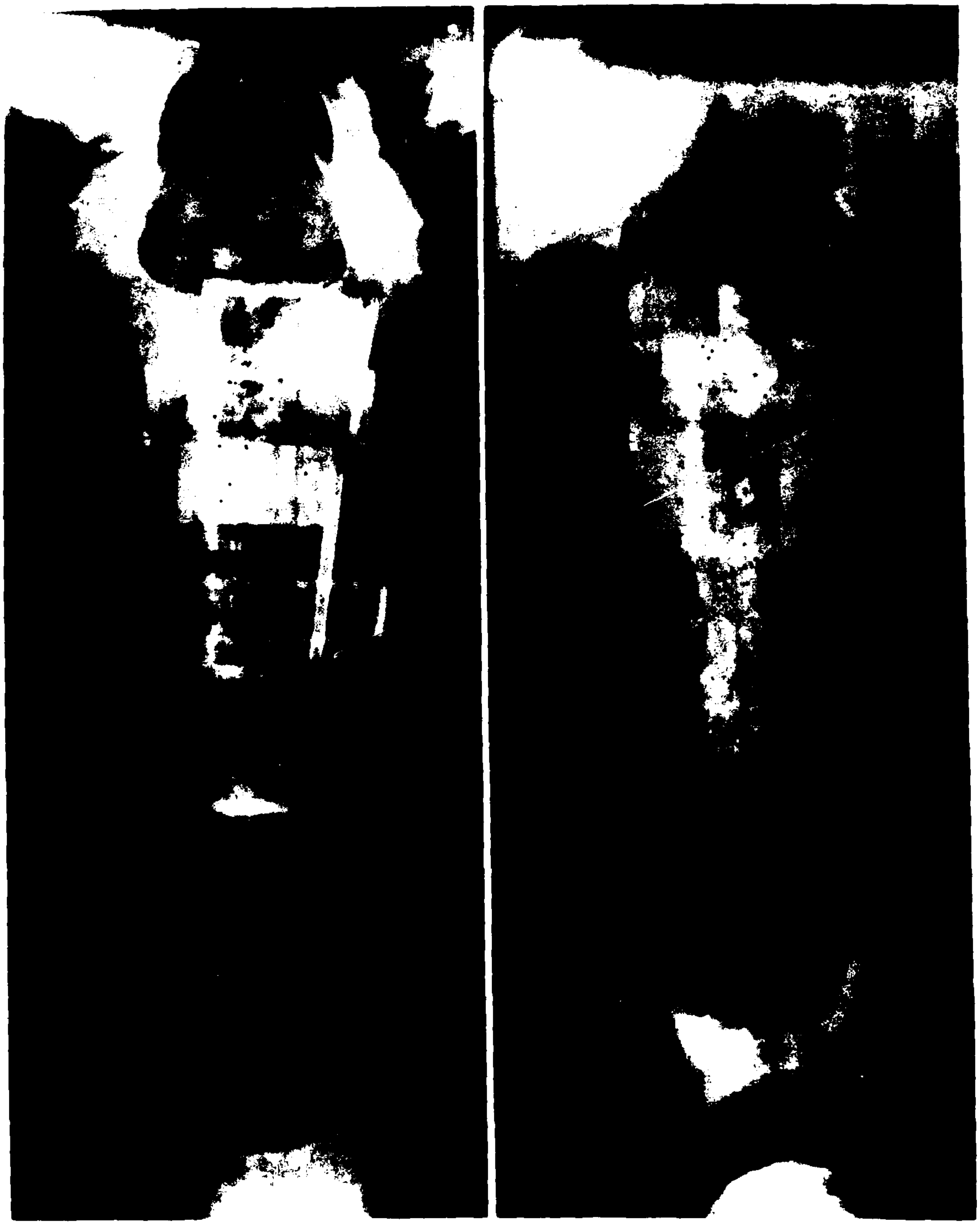

Figure 4.1. Stereoradiographic film pair of Subject #18. Tube II image is on left and Tube I image on right. Photographs have been retouched to indicate cadaver targets on film (.8 mm balls).

following section is based upon the current version. Suggested improvements will be discussed in this section, and they will be incorporated in subsequent versions.

4.2.1 Coordinate systems

The digitizer has a two-dimensional axis system. This axis system in which x- and y-coordinates of film targets are input to DIGITZ has its origin at the bottom left-hand corner of the digitizer board.

A film three-dimensional coordinate system is defined parallel to the laboratory axis system. The y-coordinate axis is parallel to the horizontal wire image; the z-coordinate axis is parallel to the vertical wire image; and x axis is normal to the film and is defined by the right-hand rule. Origin of this coordinate system is located at the tube II image of a selected wire target.

The stereobase coordinate system is defined in the film plane by the projection of a line joining the two focal spots of the x-ray tubes. The origin of this axis system lies at the midpoint of this focal spot line. $\hat{x}$, $\hat{y}$, and $\hat{z}$ are defined as shown in Figure 4.2.

The inertial frame of reference, discussed previously is the fixed laboratory coordinate system. Its origin is located at the lowest left intersection of the wire grid: the y-axis is the lowest horizontal wire, the z-axis is the left vertical wire, and the x-axis is normal to the wire grid plane defined by the right-hand rule (see Figure 4.3).

4.2.2 Focal length computation

All three-dimensional coordinates of cadaver targets, chair targets, etc., are calculated with measurements from a pair of films. Constants in the algorithm are the stereobase (SB = distance between focal spots of x-ray tubes), y and z coordinates of all wire targets, distance of wire grid from the film plane, and the distance separating the glass rod targets.

Focal length, distance of x-ray tubes from film plane (Figure 4.2), is calculated assuming the glass rod is perpendicular to the film plane,

$$FL = \frac{(\Delta_1 + SB)(\Delta_2 + SB)(LEN)}{SB(\Delta_1 - \Delta_2)} \qquad (1)$$

where LEN = length of glass rod, SB = stereobase length, Δ_1 = parallax for glass rod target on double exposure farthest from film, and Δ_2 = parallax for glass rod target on double exposure closest to film.

4.2.3 Target data input

DIGITZ is the computer program used to calculate three-dimensional coordinates. Operationally, the tube II film is digitized first, then the tube I film is digitized. On each film, wire targets, glass rod targets, quartz cube targets, cadaver targets, and chair targets are digitized. The wire, rod, and quartz cube targets are used first to merge the two-dimensional anatomical and chair data from the film into three-dimensional data in the inertial frame. Second, these targets are used to check the accuracy of the results.

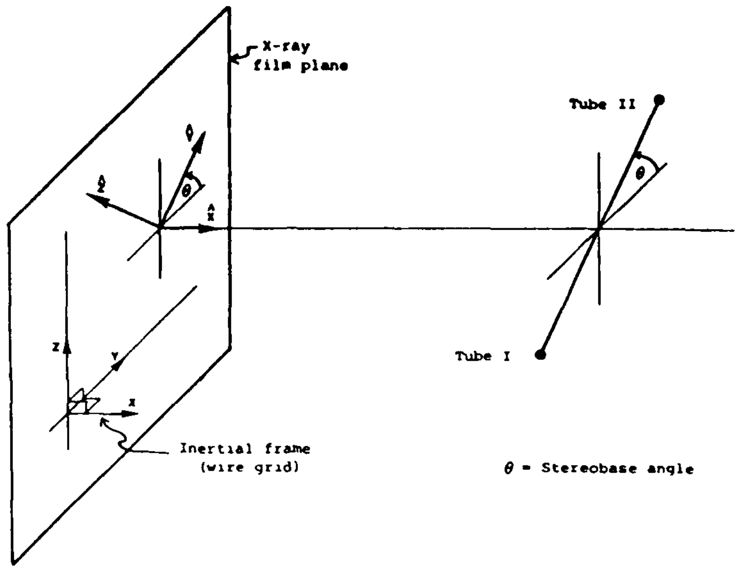

Figure 4.2. Stereobase axis system.

4.2.4 Stereo image data reduction

Tube I x-ray results are merged with tube II x-ray results as if they are on a double exposure: the "central projection theorem" implies that on a double exposure, the slope of a line joining the tube I and tube II image of a target is constant for all targets.

$$\text{constant slope} = \frac{(Y_{II} - Y_I)}{(X_{II} - X_I)} = \tan\theta \qquad (2)$$

For a double exposure, X_I, Y_I are the tube I image coordinates of a target in the digitizer axis system. X_{II} and Y_{II} are the corresponding tube II image coordinates. θ is the stereobase angle with the y-axis of the inertial frame of reference.

For a stereo pair, tube I and tube II images are on different films.

$$\text{constant slope} = \frac{(Y_{II} - Y_I) + t_y}{(X_{II} - X_I) + t_x} = \tan\theta \qquad (3)$$

Where t_x and t_y are the same for all targets on the stereo pair, and the x and y quantities needed to subtract from the tube I image to merge the two films into the mathematical equivalent of a double exposure.

Rewriting equation (3) for the i^{th} target,

$$\tan\theta\,(\Delta X_i) + K = \Delta Y_i \qquad (3a)$$

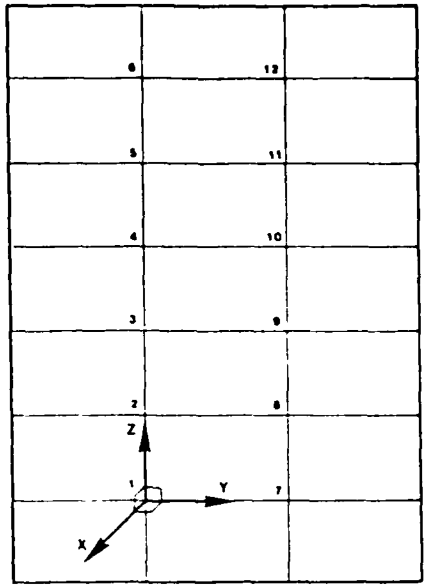

Figure 4.3. Inertial frame defined as shown on wire grid. Intersection points are numbered for computer identification.

where,

$$\Delta X_i = (X_{II} - X_I)_i$$
$$\Delta Y_i = (Y_{II} - Y_I)_i$$
$$K = t_x \tan\theta - t_y$$

Applying this to all wire, rod, chair and quartz cube targets,

$$\begin{bmatrix} \Delta X_1 & 1.0 \\ \Delta X_2 & 1.0 \\ \cdot & \cdot \\ \cdot & \cdot \\ \cdot & \cdot \\ \Delta X_N & 1.0 \end{bmatrix} \begin{bmatrix} \tan\theta \\ K \end{bmatrix} = \begin{bmatrix} \Delta Y_1 \\ \Delta Y_2 \\ \cdot \\ \cdot \\ \cdot \\ \Delta Y_N \end{bmatrix} \qquad (3b)$$

or,

$$[A][X] = [b] \qquad (4)$$

where [A] and [b] consists of known measurements from the film and [X] consists of the unknown t_x, t_y and θ . This equation can be solved by premultiplying equation (4) by the transpose of [A].

$$[A]^T [A] [X] = [A]^T [b] \qquad (5)$$

The solution for [X] then is given by,

$$[X] = [[A]^T [A]]^{-1} [A]^T [b] \qquad (6)$$

where A is an N x 2 matrix, and N is usually 25, depending upon the number of appropriate targets in the film. Thus, tube I and tube II data are known as if they are on a double exposure. When these calculations are completed, the data are in the film three-dimensional coordinate system.

The stereobase coordinate system is numerically defined for ease in calculating three-dimensional target locations. First, the origin of this coordinate system (as shown in Figure 4.2) is calculated. Since the stereobase angle θ is known from above, all image data are transformed into this coordinate system. Solving the equation for the origin of the stereobase coordinate system employs a 6 x 6 matrix. The linearity of the equation is obtained by assuming the glass rod is perpendicular to the film plane. This assumption is a source of error in the three-dimensional coordinates.

The three-dimensional coordinates are computed in the stereobase coordinate system using simple trigonometric ratios for similar triangles. The physical three-dimensional coordinates are also in the stereobase coordinate system. Therefore the three-dimensional coordinates must be transformed into the laboratory axis system.

Since the location of the wire target is known in the stereobase coordinate system, it is also known in the inertial frame. This geometry provides a numerical transformation for all anatomical targets into the inertial frame. With this step completed, the data are in the inertial frame. The seat reference point (SRP) is also digitized with the other anatomical targets and is reported in the inertial frame.

4.3 SYSTEM ACCURACY AND RESOLUTION

4.3.1 <u>Variation in a single film pair</u>

Variability of the data, from repeatedly *digitizing the same film*, indicates the error due to all sources. As an example, the Seat Reference Point of the Air Force chair (SRP) and the glass rod targets' distance are shown below for position LBAR 3.0 (Table 4.1):

Digitize attempt	SRP (cm) x	y	z	Glass Rod Targets' Distance (cm)
#1	30.27	13.21	10.31	35.56
#2	30.25	13.20	10.30	35.60
#3	30.22	13.21	10.30	35.58
#4	30.26	13.23	10.33	35.56
#5	30.19	13.22	10.29	35.58
#6	30.21	13.21	10.30	35.57
#7	30.22	13.21	10.31	35.55
Average	30.23	13.21	10.31	35.57
SD	± 0.02	± 0.01	± 0.01	± 0.02

Table 4.1. Results of repeated digitizing of same film pair.

The average target distance is 0.13 cm larger than the target distances (35.44 cm) used in this experiment. However, the variability in each coordinate is small when the range is examined. The range of variation for x is 0.08, y is 0.03, and z is 0.04.

4.3.2 Variation between different stereo pairs

Variation in three-dimensional coordinates from six different stereo pairs, each digitized seven times and averaged, is shown in Table 4.2. The average for the four positions (SEATERCT SEATEDP1, SEATEDP2 and SIDEBEND) are not used because these four films were the most difficult to digitize and the change in glass rod target orientation introduces an unknown error term.

	SRP (cm) x	y	z	Glass Rod Targets' Distance (cm)
LBARS3.0	30.23	13.21	10.31	35.56
LBARS3.5	30.21	13.20	10.31	35.55
LBARS4.0	30.18	13.21	10.30	35.55
LBARS4.5	30.19	13.22	10.30	35.57
LBARS5.0	30.18	13.22	10.30	35.53
LBARS5.5	30.19	13.21	10.30	35.57
Average	30.20	13.21	10.30	35.55
SD	$\pm$ 0.02	$\pm$ 0.01	$\pm$ 0.01	$\pm$ 0.02

Table 4.2. Results of averaged coordinates from different stereo pairs.

The SRP coordinates are very similar to those in Table 4.1 (one digitizing attempt only) except they fluctuate less because some random error from digitizing is minimized in the average value. The variation observed between these six pairs of LBAR 3.0 to LBAR 5.5 is reduced. The x-coordinate range is 0.05, y is 0.02, and z is 0.01. The glass rod target's distance is extremely close.

4.3.3 Reproducibility from different stereo pairs

The variation in 10 different stereo pairs, each digitized once, is shown in Table 4.3 for coordinates of two targets on the quartz cube (QUBE05 and QUBE06) and the glass rod targets' distance. The targets' distance on the glass rod has been independently measured to be 35.44 cm.

For all 10 positions, the glass rod targets' distance fluctuates around the measured value 35.44 cm. No pattern can be observed. This implies that the effect of various sources of experimental error in distances between targets is small.

There are two relatively homogeneous sets of film pairs in Table 4.3. The LBAR series of films (LBAR 3.0 - 5.5) represents a homogeneous set for both targets and the other four films (SEATERCT, SEATED P1, SEATED P2, and SIDEBEND) are also consistent. The difference in the two data sets is a movement of the glass rod targets which were inadvertently changed while repositioning Subject #18. The focal length and physical location of the quartz cube remained the same for all 10 film pairs. Thus, the difference is solely attributable to a change in orientation of the glass rod.

When the distances between quartz cube targets are compared, the effect of the glass rod is almost imperceptible. In addition, when the two data sets are examined separately, they are internally consistent with both, demonstrating similar ranges of variation. The variation present in

Film Pairs	QUBE05 (cm) x	y	z	QUBE06 (cm) x	y	z	Distance 5-6	Glass Rod Targets' Distance (cm)
LBAR 3.0	61.94	5.03	50.06	50.29	5.00	49.92	11.64	35.55
LBAR 3.5	61.91	5.01	50.06	50.28	4.99	49.91	11.63	35.55
LBAR 4.0	61.92	5.01	50.06	50.28	4.99	49.92	11.65	35.60
LBAR 4.5	61.93	5.03	50.05	50.29	5.00	49.90	11.64	35.59
LBAR 5.0	61.94	5.00	50.05	50.30	4.98	49.91	11.64	35.54
LBAR 5.5	61.95	5.00	50.04	50.30	4.99	49.90	11.66	35.56
SEATERCT	61.66	6.09	49.56	50.03	5.98	49.52	11.63	35.48
SEATEDP1	61.69	6.06	49.57	50.06	5.96	49.53	11.58	35.51
SEATEDP2	61.62	6.03	49.59	50.04	5.94	49.53	11.63	35.49
SIDEBEND	61.64	6.06	49.56	49.99	5.95	49.50	11.66	35.51

Table 4.3. Results of digitizing the same targets on different film pairs.

each set is due to random measurement error, and the difference between the two sets is a systematic error introduced by a change in orientation of the glass rod targets.

4.3.4 Accuracy of data

SAL's data accuracy for Subject # 18 is summarized in Table 4.4. The summary statistics, average and standard deviation, for five targets are presented to illustrate the range of variation in the data. The LBAR series describes the variation in the data when the location of glass rod, chair, quartz cube and x-ray tube were unchanged. The coordinates representing all of the cadaver positions describe the variation in the

Target		LBAR 3.0 - 5.5 (6 positions) x	y	z	All Cadaver Postions (10 positions) x	y	z
WIRE08	$\bar{x}$	0.07	30.51	30.41	0.09	30.50	30.41
	SD	± 0.04	± 0.01	± 0.01	± 0.06	± 0.02	± 0.01
STGT08	$\bar{x}$	17.71	28.94	56.44	Not Comparable		
	SD	± 0.04	± 0.01	± 0.01	(seat was moved)		
SRP	$\bar{x}$	30.20	13.21	10.30	Not Comparable		
	SD	± 0.02	± 0.01	± 0.01	(seat was moved)		
GLRD02	$\bar{x}$	46.635	8.67	50.51	46.99	8.89	50.34
	SD	± 0.01	± 0.01	± 0.01	± 0.46	± 0.28	± 0.22
QUBE05	$\bar{x}$	61.93	5.01	50.05	61.77	5.51	49.86
	SD	± 0.01	± 0.01	± 0.01	± 0.19	± 0.69	± 0.25

Table 4.4. Summary statistics representative of the variation in the coordinated data describing Subject #18's seated body positions.

data when the orientation of the glass rod was inadvertently changed. These raw data are in the inertial frame of reference and each statistic is based upon the coordinates obtained from film digitized seven times.

4.3.4.1. General considerations The farther a target is from the film, given a constant focal length and consistent glass rod location, the smaller the variation. That is, as the target-to-film distance increases, parallax increases, and a ratio between the measured quantity and the calculated quantity increases. The summary data in Table 4.4 for the LBAR 3.0 - 5.5 positions demonstrates a decreased standard deviation as the x coordinate increases. The cadaver is sitting in the 20-30 cm x-coordinate range, and the variation in the cadaver data is described by the STGT08 and SRP targets on the chair.

In contrast to the LBAR data, the SEATERCT, SEATEDP1, SEATEDP2, and SIDEBEND stereoradiographic film pairs have a different error term. These films were made on the same day as the LBAR series and digitized with the same procedure. However, the glass rod was inadvertently moved in the process of moving the cadaver into these positions. The data in Table 4.4 shows that the change in glass rod location affected the calculation of coordinate location of the wire grid (WIRE08) and quartz cube (QUBE05) despite the fact that their locations were not physically changed.

In this case, however, variation increases as the film-to-target distance increases. That is, the standard deviation of WIRE08 (the closest target to the film) was slightly affected where there was a change in order of magnitude for QUBE05 (the farthest target from the film).

4.3.4.2 Data in SRP frame of reference The data for each stereopair are consistent but the data from each stereopair has a different error term which arises from random measurement errors and glass rod orientation. Consequently, when the three-dimensional coordinates are transformed into the SRP axis system, some of the effect of the systematic error is reduced. That is, the data are considered to be more comparable between films when reported in the SRP frame of reference.

It is obvious in Table 4.2 that although the raw data have large systematic errors, the distances between the same two targets remain very stable. The maximum deviation between QUBE05 and QUBE06 for 10 film pairs is 0.18 cm. The effect of the nonperpendicular glass rod is compensating in y and z.

5.0 RESULTS OF THREE-DIMENSIONAL DATA ANALYSIS

5.1 DEFINITION OF TERMS USED IN ANALYSIS

Data analysis in the Systems Anthropometry Laboratory provides a description of the six degrees-of-freedom position and change of position of the pelvis and lumbar vertebrae with the use of anatomical pointmarks.

Laboratory axis system (inertial frame of reference): defined as shown in Figure 5.1. A more complete description of the laboratory axis system is provided in Section 3.1.1.1, Figure 3.1. The direction of the axes in this frame of reference is defined by the wire grid. The origin of the axis system is located at the intersection of vertical and horizontal wires previously described.

SRP axis system (Seat Reference Point frame of reference): defined with its origin at the Seat Reference Point of the wooden seat. The $\hat{X}$, $\hat{Y}$, and $\hat{Z}$ unit vectors are shown in Figure 5.1. The $\hat{Y}$ axis direction is defined by the intersection of the seat pan and seat back the $\hat{Z}$ axis by a vertical line parallel to the laboratory z axis and the $\hat{X}$ axis by a normal ($\hat{X}$) defined by the cross-product of the first two axes according to the right-hand rule. The SRP axis system is calculated for each position since the chair could have been moved between different cadaver positions.

Anatomical axis system (Anatomical frame of reference): defined by three anatomical pointmarks on the inferior surface of the vertebral body, e.g., IL4BLL, IL4BLR, and IL4APT (Figure 5.2). All of these position vectors are known in the SRP axis system. This bone frame is defined by passing a line from IL4BLR through IL4BLL, calculating a perpendicular line passing through IL4APT, and computing, according to the right-hand rule, the vector cross-product for the normal. Three unit vectors chosen along axes shown in Figure 5.2 are oriented in traditional anatomical directions where anterior is positive $\hat{i}$, left lateral is positive $\hat{j}$, and superior is positive $\hat{k}$.

Cadaver targets: small tungsten-carbide balls rigidly implanted in each bone in the cadaver. These balls are radiopaque and result in points which are digitized from stereoradiographic film pairs obtained from the cadaver seated in the wooden seat. There are a maximum of six cadaver targets on each bone and they are labeled with a six-letter acronym beginning with "C" (Appendix 7.0). Position vectors in the laboratory axis system of these cadaver targets are obtained from the digitizing program.

Anatomical pointmarks: a point on a boney surface that represents an anatomically homologous feature in the human skeleton. These points are identified visually on excised and cleaned bones and they are marked with small radiopaque tungsten-carbide balls. There are a maximum of 16 anatomical pointmarks identified on each vertebrae, 11 pointmarks on the sacrum and 8 pointmarks on the innominate bones (Appendix 7.0). The three-dimensional cartesian coordinates in the laboratory axis system for cadaver targets and anatomical pointmarks are reported in Section 7.3, Appendix B. It is important to understand that two types of data are collected. The

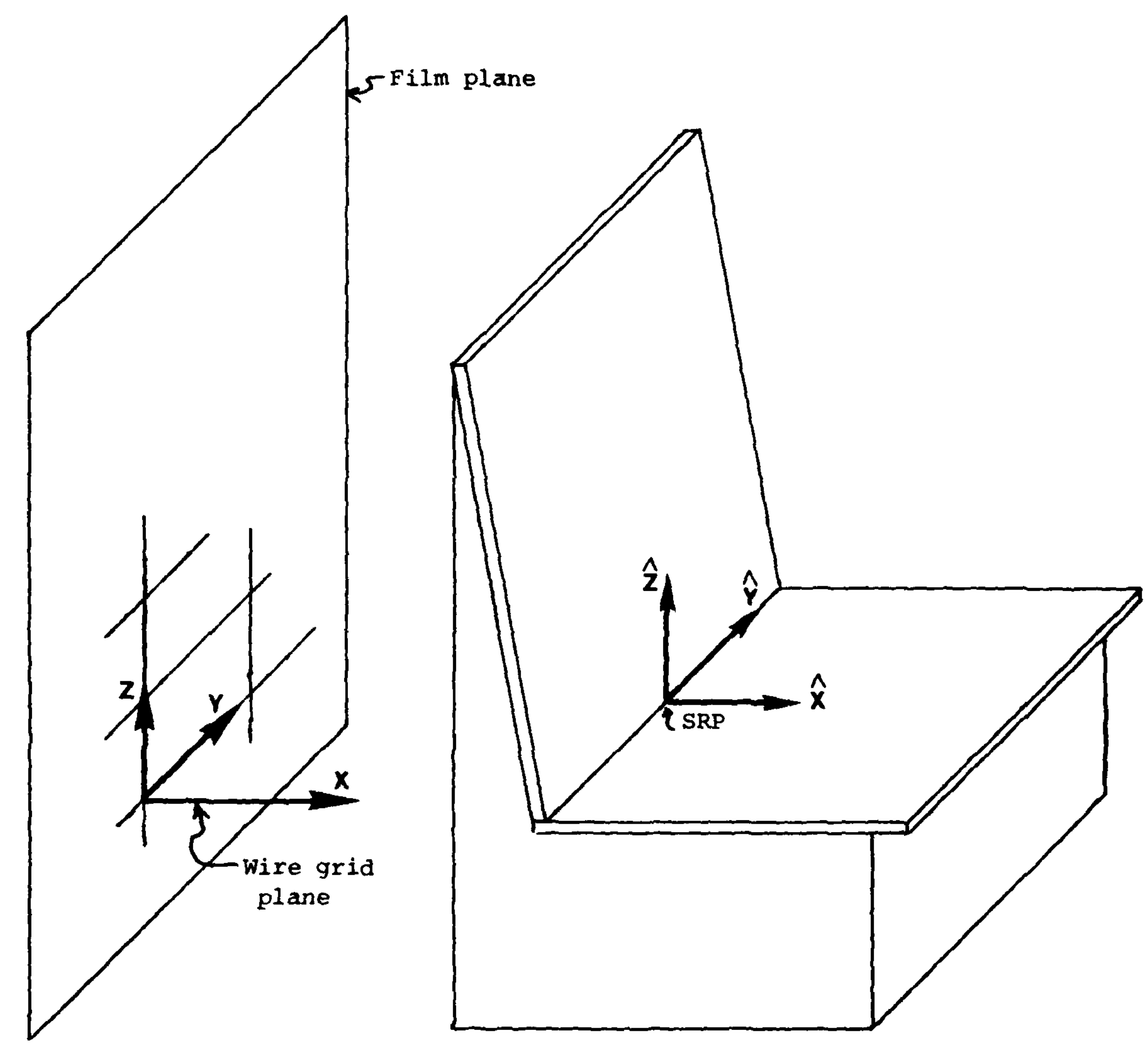

Figure 5.1. Seat axis system at SRP relative to the film plane and wire grid axis system.

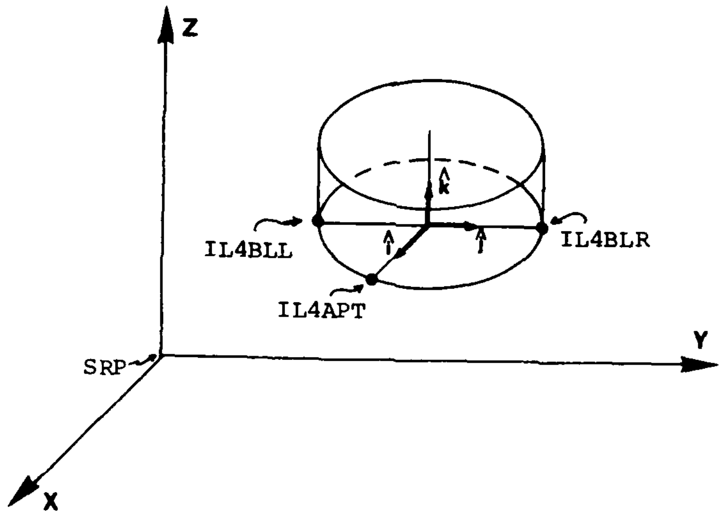

Figure 5.2. Bone frame (BF) of reference where $\hat{i}$, $\hat{j}$, $\hat{k}$, are 3 unit vectors defining the anatomical axis system.

first type is obtained from the cadaver in different seated positions and consists of the vector positions of the cadaver targets (e.g., SEATERCT film pair). The second type of data, consisting of the vector positions of both the cadaver targets and anatomical pointmarks, is taken from individual excised bones (e.g. BONES film pair) and is used to provide a transformation between the cadaver targets and anatomical pointmarks.

5.2 TRANSFORMATION OF ANATOMICAL POINTMARKS INTO SUBJECT BODY POSITION

The location of skeletal linkages in different body positions is measured with stereoradiographic images of small radiopaque balls rigidly implanted in each bone. After stereoradiographs of all body positions in the experiment have been made, the bones of the cadaver are excised, cleaned and targets are added at sites of comparable anatomical pointmarks. Stereoradiographs of the bones with both cadaver targets and anatomical pointmarks are made and digitized. Thus, the anatomical pointmarks are known as if they were measured in the cadaver. If comparable and homologous pointmarks identified by anatomical features are measured on different subjects and bones, the motion of anatomically and biomechanically important sketetal pointmarks can be studied with comparable displacements and instantaneous axes of rotation.

5.2.1 Step 0. Cadaver target data in the laboratory axis system

There are a maximum of six targets measured on each bone in the SEATERCT position data. For example, position vectors in the laboratory axis system for cadaver targets on L3 are reported in Table 5.1. These data are divided into two sets : a) BONES Data - five cadaver targets measured on the excised, cleaned L3 vertebra; and b) SEATERCT Data - the same five cadaver targets measured when the cadaver was in the SEATERCT position.

a) BONES DATA ON L3

Transformation Targets	x	y	z	Cadaver Targets
a	8.02	20.71	41.83	CL03TL
b	8.08	14.48	43.12	CL03R1
c	4.35	18.59	42.00	CL03S1
	4.33	18.61	42.22	CL03SM
	7.09	20.64	43.67	CL03L1

b) SEATERCT DATA ON L3

Transformation Targets	x	y	z	Cadaver Targets
a	31.81	15.24	31.56	CL03TL
b	31.55	9.66	34.90	CL03R1
c	27.98	13.36	32.17	CL03S1
	27.95	13.29	32.30	CL03SM
	30.98	14.96	33.13	CL03L1

Table 5.1. Three-dimensional coordinates (in centimeters) for five cadaver targets on L3 in the laboratory axis system.

When the geometric distances between cadaver targets are calculated for this set of data, CL03TL, CL03R1, and CL03S1 have the most comparable results (Table 5.2). These three targets, labeled a, b, and c, are separated by distances *ranging from* 4.24 cm to 6.50 cm with an average separation of 5.42 cm in the stereoradiographs of the excised bones compared to 5.54 cm in the SEATERCT stereoradiograph. Distances of this magnitude and differences in the location of these cadaver targets represent the best data for L3 to be used in calculating the displacement matrix between the SEATERCT data and bones data.

TARGET	BONES	SEATERCT	DIFFERENCE
DISTANCE			(%)
a-b	6.36	6.50	2.2%
b-c	5.66	5.82	2.8%
c-a	4.24	4.31	1.5%
average	5.42	5.54	2.2%

Table 5.2. Comparison of geometric distances between BONES and SEATERCT cadaver target pair distances (in centimeters).

5.2.2 <u>Step 1. Computation of displacement matrix between BONES position and SEATERCT data in the laboratory axis system</u>

Since the same cadaver targets on each bone are measured in two different positions (i.e., bones and SEATERCT data in Table 5.1), a displacement matrix is computed. Four targets, a, b, c, and a computed position vector (the origin of an axis system defined by these three

targets), are used in homogeneous coordinates (Marcus, 1980) to compute the displacement matrix (Suh and Radcliffe, 1978) in equation 7.

$$[D_{12}]\ [BP1] = [SP2] \qquad (7)$$

Or,

$$\left[D_{12}\right] \begin{bmatrix} A1_x & B1_x & C1_x & D1_x \\ A1_y & B1_y & C1_y & D1_y \\ A1_z & B1_z & C1_z & D1_z \\ 1.0 & 1.0 & 1.0 & 1.0 \end{bmatrix} = \begin{bmatrix} A2_x & B2_x & C2_x & D2_x \\ A2_y & B2_y & C2_y & D2_y \\ A2_z & B2_z & C2_z & D2_z \\ 1.0 & 1.0 & 1.0 & 1.0 \end{bmatrix} \qquad (8)$$

BP1 represents the position of the cadaver targets in the BONES position and SP2 represents the position of the same cadaver targets in the SEATERCT position, both of which are in the laboratory axis system. If equation 8 is solved by post multiplying both sides by the inverse of BP1, D_{12} can be calculated where the upper left 3 x 3 describes rotation, and the upper right 3 x 1 describes translation.

The resulting displacement matrix for the L3 example in Table 5.1 is given in Table 5.3.

$$\left[D_{12}\right] = \begin{bmatrix} 0.998 & 0.040 & -0.054 & 25.257 \\ -0.019 & 0.944 & 0.330 & -17.969 \\ 0.064 & -0.329 & 0.942 & -1.568 \\ 0.000 & 0.000 & 0.000 & 1.000 \end{bmatrix}$$

Table 5.3. Displacement matrix for L3.

The displacement matrix in Table 5.3 is subsequently applied to the L3 anatomical pointmarks so that they are expressed in the laboratory frame of reference with the cadaver in the SEATERCT position. The resulting data will be termed "displaced pointmarks in laboratory frame."

5.2.3 Step 2. Transformation to SRP axis system

The location of the wooden seat in the laboratory is measured in every cadaver position. Through the use of targets on the chair back, three unit vectors on the chair (as shown in Figure 5.1) are computed, to define the SRP frame. A transformation matrix (TM) from inertial frame to SRP is computed to transform the "displaced pointmarks in laboratory frame" (Step 1) into the SRP axis system. The result will be independent of any movement of the chair and will be called "transformed pointmarks in SRP axis system." These transformed coordinates represent the location of the anatomical pointmarks in the SRP frame of reference.

The origin of the SRP axis system measured in the inertial axis system, and the corresponding transformation matrix from the inertial axis system to the SRP axis system for L3 SEATERCT data are presented in Table 5.4. The upper 3 x 3 indicates that the chair is almost aligned parallel to the laboratory axis system so that the transformation is primarily a translation of the origin to a new location in the wooden seat.

	x	y	z
SRP origin:	30.368	12.288	9.981

$$[TM] = \begin{bmatrix} 1.000 & -0.016 & 0.000 & -30.168 \\ 0.016 & 1.000 & 0.000 & -12.771 \\ 0.000 & 0.000 & 1.000 & -9.981 \\ 0.000 & 0.000 & 0.000 & 1.000 \end{bmatrix}$$

Table 5.4. SRP origin in the laboratory axis system and the transformation matrix from laboratory axis system to SRP axis system.

5.2.4 Step 3. Transformation to an anatomical axis system in the inferior bone

An anatomical axis system is defined in the inferior bone for each bone with the exception of the innominate, in which case, the SRP axis system serves as the bone frame. For example, the inferior bone for L3 is L4; thus, data on L4, in the SEATERCT cadaver position, is first processed in the SRP axis system.

The three anatomical pointmarks (IL4BLL, IL4BLR, and IL4APT), origin of the L4 anatomical axis system, and position vectors PVX (on the $\hat{i}$ axis), PVY (on the $\hat{j}$), and PVZ (on the $\hat{k}$), that lie on the L4 BF axes with a magnitude equal to one, are reported in Table 5.5.

Pointmarks	Coordinates		
	x	y	z
IL4BLL	5.10	3.59	19.29
IL4BLR	4.93	-1.42	20.58
IL4APT	7.21	0.87	19.74
BF origin	5.01	1.00	19.96
PVX	6.01	0.94	19.86
PVY	5.04	1.97	19.71
PVZ	5.12	1.24	20.92

Table 5.5. L4 position vectors relative to the SRP axis system (in centimeters).

The BF origin, PVX, PVY, and PVZ position vectors in the SRP axis system are used to transform L3 body vectors given in the SRP axis system to the inferior bone frame in L4. The transformation matrix is given in Table 5.6.

$$[TM] = \begin{bmatrix} 0.994 & -0.059 & -0.097 & -2.981 \\ 0.033 & 0.968 & -0.249 & 3.835 \\ 0.109 & 0.244 & 0.964 & -20.019 \\ 0.000 & 0.000 & 0.000 & 1.000 \end{bmatrix}$$

Table 5.6. TM for L3 in SRP axis system to bone axis system.

Thus, all anatomical pointmark data on L3 are transformed from the laboratory axis system (Step 1) to the SRP axis system (Step 2) to the bone axis system (Step 3). An example of the results of these coordinate transformations is provided for L3 in Table 5.7. There are both cadaver targets and anatomical pointmarks in this table.

	Step 0 POINTMARKS BONES DATA (LABORATORY AXIS SYSTEM)			Step 1 DISPLACED POINTMARK (LABORATORY AXIS SYSTEM)			TARGET
	x	y	z	x	y	z	
1 C	8.02	20.71	41.83	31.81	15.24	31.56	CL03TL
2 C	8.08	14.48	43.12	31.56	9.79	34.83	CL03R1
3 C	4.35	18.59	42.00	28.06	13.36	32.18	CL03S1
4 C	4.33	18.61	42.22	28.03	13.46	32.38	CL03SM
5 C	7.09	20.64	43.67	30.78	15.80	33.25	CL03L1
6	8.30	20.72	40.98	32.14	14.97	30.77	IFML3L
7	8.18	17.26	41.04	31.87	11.72	31.96	IFML3R
8	13.48	18.74	40.58	37.25	12.86	31.38	IL3APT
9	11.66	21.29	40.85	35.52	15.39	30.67	IL3BLL
10	11.49	16.14	40.76	35.15	10.50	32.28	IL3BLR
11	8.33	20.37	44.23	31.98	15.71	33.95	SFML3L
12	8.09	17.12	43.88	31.63	12.53	34.67	SFML3R
13	8.02	23.62	44.01	31.81	18.71	32.65	TPL3LT
14	7.77	13.88	43.42	31.21	9.33	35.28	TPL3RT

	Step 2 TRANSFORMED POINTMARK (SRP AXIS SYSTEM)			Step 3 TRANSFORMED POINTMARK (BONE AXIS SYSTEM)			TARGET
	x	y	z	x	y	z	
1 C	1.40	2.98	21.58	-3.86	1.40	1.65	CL03TL
2 C	1.23	-2.48	24.85	-4.03	-4.71	3.45	CL03R1
3 C	-2.32	1.04	22.20	-7.51	-0.76	1.37	CL03S1
4 C	-2.36	1.13	22.40	-7.57	-0.72	1.58	CL03SM
5 C	0.36	3.52	23.27	-5.09	1.47	3.30	CL03L1
6	1.73	2.71	20.79	-3.28	1.71	0.84	IFML3L
7	1.52	-0.54	21.98	-3.50	-1.54	2.02	IFML3R
8	6.87	0.69	21.40	1.86	-0.31	1.44	IL3APT
9	5.11	3.19	20.69	0.09	2.19	0.74	IL3BLL
10	4.81	-1.71	22.30	-0.20	-2.70	2.34	IL3BLR
11	1.56	3.45	23.97	-3.45	2.45	4.01	SFML3L
12	1.26	0.26	24.69	-3.75	-0.74	4.73	SFML3R
13	1.34	6.45	22.67	-3.67	5.45	2.71	TPL3LT
14	0.89	-2.94	25.30	-4.12	-3.94	5.35	TPL3RT

Table 5.7. Summary of three-dimensional coordinates for L3.

5.3 SUBJECT POSITION IN THE MID-SAGITTAL PLANE

In the unembalmed cadaver, motion is simulated by a sequential change of body positions. Each position is measured with a pair of stereoradiographs. There are six positions simulating lumbar extension (LBAR 3.0 to LBAR 5.5), one seated-erect body position with no lumbar support (SEARERCT) and two positions simulating lumbar flexion (SEATEDP1 and SEATEDP2).

To illustrate Subject #18's body positions, two-dimensional plots of data representing the chair, lumbar support device, and subject have been prepared indicating the location of the dorsal spines of T12, L1-L4, sacrum, ASIS, and symphysion. Cadaver targets have been used since these data are the most accurate available on Subject #18.

Additional data on the locations of the iliac crest, ischium, sacral base, and H-point location have been derived from measurements of pelvic geometry by Reynolds, Snow, and Young (1981). The outline of the scaled pelvis is represented by anatomical pointmarks on the iliac crest, two on the sacral base, four on the ischium, and H-point. These pointmarks were measured on 30 male pelves selected from the skeletal collection at the Cleveland Museum of Natural History to represent the average United States male body size.

The average male pelvis data have been scaled to represent the pelvic geometry of Subject #18. A scale factor of 1.2117 was computed as the average ratio of average male pelvis size to the cadaver pelvis size. Table 5.8 reports the ratio for three distances computed between RASIS, LASIS, and SYMPH in both sets of data. This scale factor has been used to estimate the location of pointmarks not measured on the cadaver with pointmarks that were measured on the average male pelvis.

Distance	Ratio of Cadaver/ Published Data
RASIS - LASIS	1.1392
RASIS - SYMPH	1.2953
LASIS - SYMPH	1.2007
Average	1.2117

Table 5.8. Scale factor for adjusting population to cadaver data.

The three-dimensional coordinates for anatomical pointmarks presented in Table 5.9 were located for each of Subject #18's body positions by the method outlined in Step 1 of Section 5.2.2. That is, an anatomical axis system was established for the cadaver data that is comparable to the axis system used in the Reynolds, et al., (1981) pelvic data. A right-handed orthogonal anatomical axis system is based upon a line passing through the right and left anterior superior iliac spines (ASIS), a perpendicular passing through symphysion and a normal calculated according to the right-handed rule at the intersection of the first two axes. With both data sets in a comparable anatomical axis sytem, a displacement matrix is calculated as described in Step 1 and the three-dimensional coordinates are calculated. These data are scaled and then plotted to represent the cadaver's pelvic shape.

In Figure 5.3, the two polygons at the level of L2 and L3 dorsal spines represent the plexiglass plate at body positions LBAR 3.0 and LBAR 5.5. The polygon shapes are different because the plate rotated. The greatest rotation of the plate occurs at LBAR 5.5 when maximum lumbar extension produces the largest moment acting on the plate. The apparently smaller load required to extend the lumbar vertebrae in LBAR 3.0 results in an orientation of the plexiglass plate that is almost parallel to the seat back.

Figure 5.4 illustrates the change of position for slumped postures used to simulate lumbar flexion. The morphological outline of the pelvis

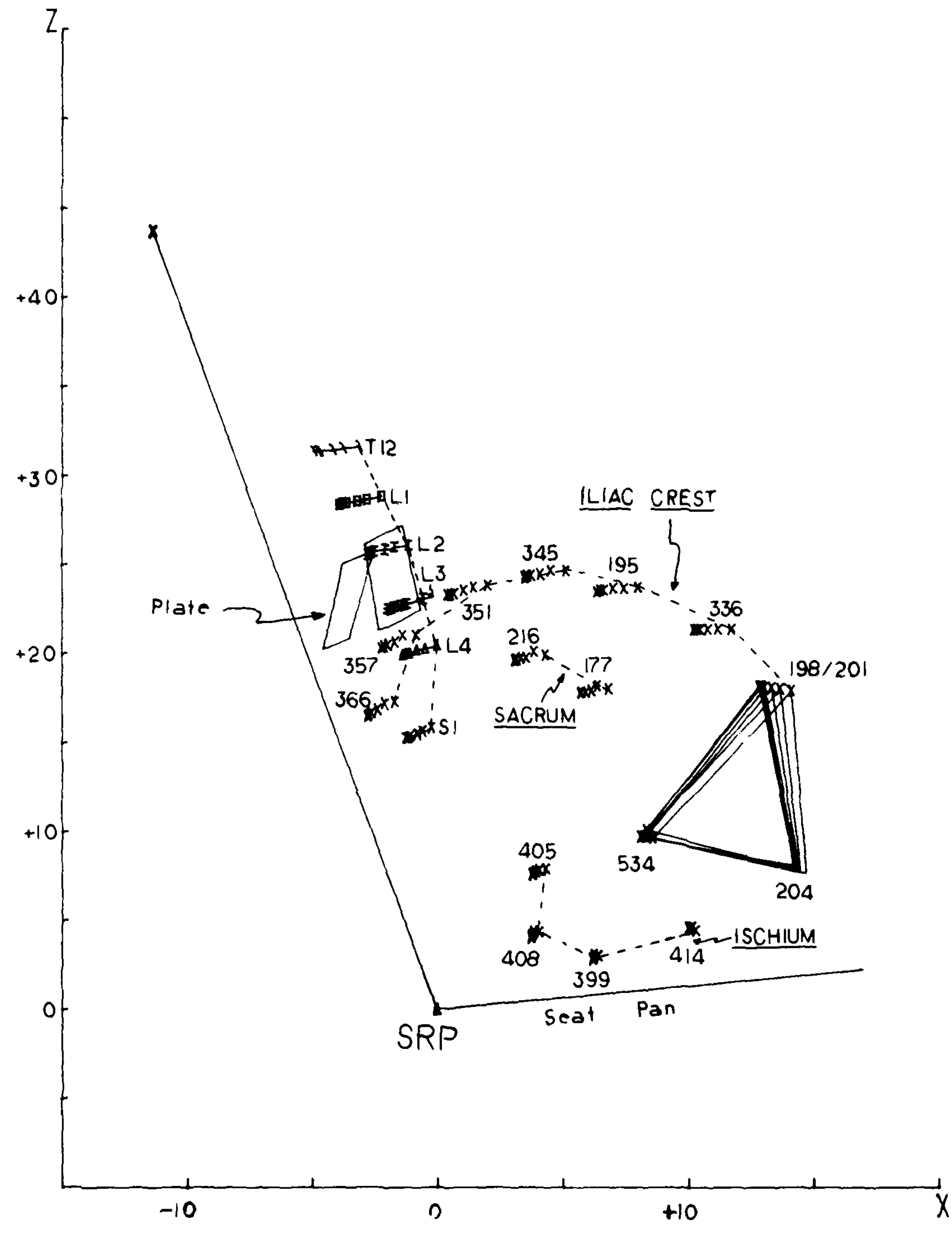

Figure 5.3. Plot of two-dimensional position of lumbar spine targets (T12, L1-L5) and pelvis pointmarks (177-414) for LBAR series.

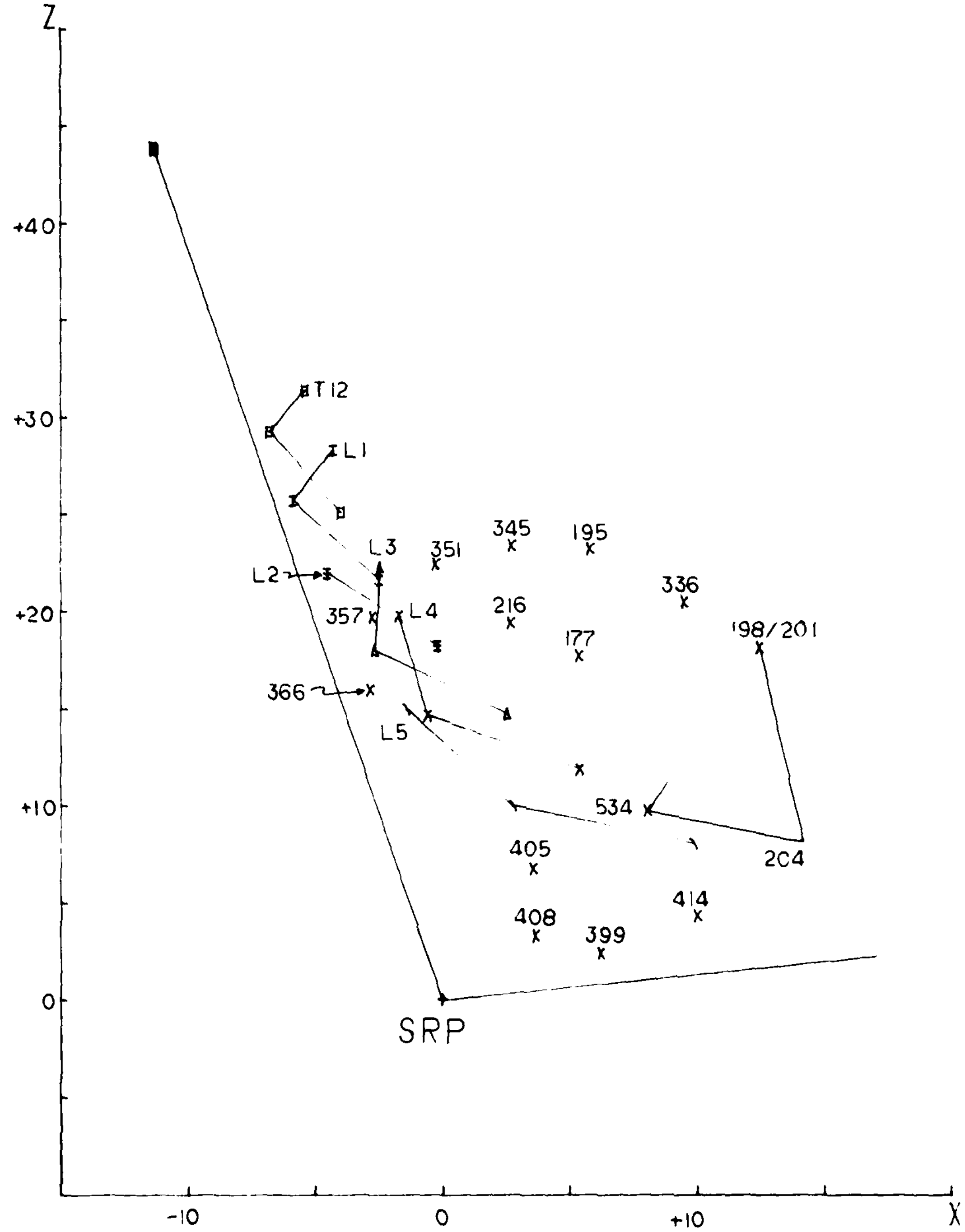

Figure 5.4. Plot of two-dimensional position of lumbar spine targets (T12, L1-L5) and pelvis pointmarks (177-414) for SEATERCT, SEATEDP1 and SEATEDP2.

	POINTMARK	COORDINATES		
		x	y	z
I				
L				
I	198 - 200 (RASIS)	0.0	-11.3	0.0
A	201 - 203 (LASIS)	0.0	+11.7	0.0
C	195 - 197	-4.8	-11.9	6.0
	336 - 338	-1.8	-12.3	3.4
C	345 - 347	-7.1	-9.5	7.3
R	351 - 353	-9.8	-6.6	6.9
E	357 - 359	-12.4	-4.6	4.6
S	366 - 368 (PSIS)	-13.1	-3.5	1.1
T				
I				
S				
C	405 - 407	-9.1	-7.2	-8.5
H	408 - 410 (ISCHIALE)	-9.6	-6.0	-11.8
I	399 - 401	-7.6	-3.9	-13.2
U	414 - 416	-4.1	-2.5	-12.1
M				
S				
A				
C	177 - 179 (PROMO)	-5.9	0.0	1.2
R	216 - 218	-7.9	0.0	3.3
U				
M				
	534 - 536 (H-Pt.)	-4.8	8.3	-6.5
	204 - 206 (SYMPH)	0.0	0.0	-7.8

Table 5.9. Selected pointmark position vectors used in Figures 5.3 and 5.4 obtained from Reynolds, et al., (1981).

is produced by the same pointmarks and scaling factor as in Figure 5.3. However, only the SEATERCT position is depicted since the other two lumbar flexion positions (SEATEDP1 and SEATEDP2) have incomplete data for pelvis anatomical pointmarks.

Right lateral sidebending is depicted in Figure 5.5, with the cadaver targets for T12, L1, L3, L4, and the sacrum. These are the same cadaver targets used in the two previous figures of lumbar extension and flexion. In this case, the motion occurs primarily in the yz plane from the SEATERCT to SIDEBEND body positions.

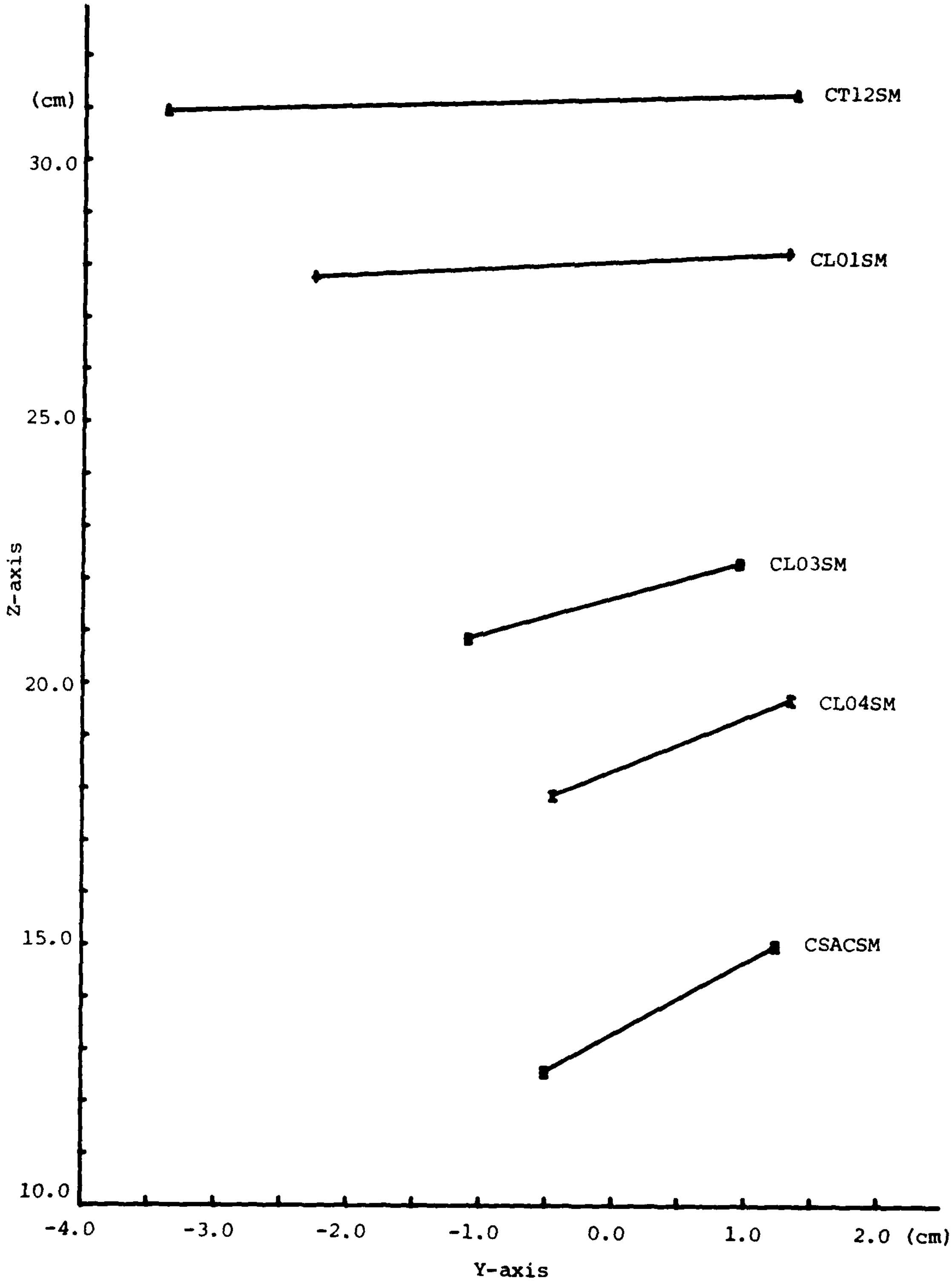

Figure 5.5. Motion of cadaver dorsal spine target for lumbar sidebending series (SEATERCT to SIDEBEND) in YZ plane of SRP frame of reference.

5.4 SCREW AXIS ANALYSIS: GENERAL DESCRIPTION OF ALGORITHM

The description of relative motion uses Chasles' theorem, *i.e.* the motion of one rigid body to another can be described by a rotation about and a translation along an axis. These parameters can be defined within laboratory or anatomical frames of reference that are external or internal to the bodies. In the present investigation, data in the SRP frame of reference are utilized since they provide for Subject #18 the most accurate data.

Rigid body motion, with six degrees of freedom, is generally described with the linear equation,

$$[D_{12}] \ [P1] = [P2] \tag{9}$$

where D_{12} is a 4 x 4 matrix describing the displacement of the rigid body P from position 1 (P1) to position 2 (P2). From this displacement matrix, six independent screw axis parameters are calculated (Figure 5.6). A translation S and rotation ϕ are calculated along and about on instantaneous screw axis (ISA) that is specified relative to a fixed axis system by direction cosines (U_x, U_y, U_z) and location (a position vector of the closest point on the ISA to the fixed axis system origin).

Relative motion between two bones in the present investigation is described by motion of the anatomically superior bone with respect to the anatomically inferior bone.

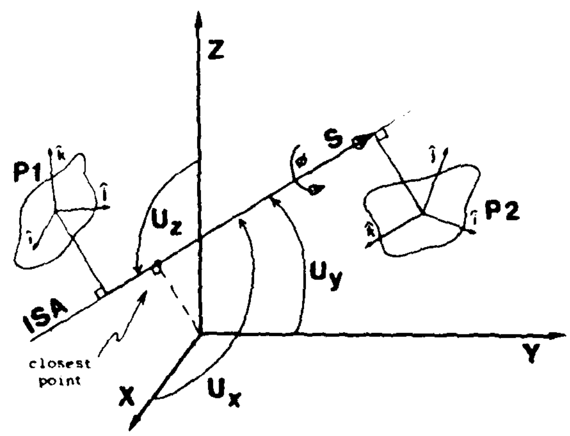

Figure 5.6. Screw axis analysis.

The computation in the screw axis program is done as follows:

- Raw data in the inertial frame for two bones are selected for position 1 and position 2 (three cadaver targets for each bone and each position).

- Three position vectors for each bone are then transformed into the SRP frame, and a "center of gravity" is calculated for each bone by vectorially summing each set of three position vectors.

- The displacement matrix for the inferior bone from position 1 to position 2 is calculated.

- Motions of the superior bone are calculated with respect to an inferior bone that has also changed position. Therefore, the effect of the reference frame change of position on the relative motion of the superior bone is subtracted vectorially for position 1. The new coordinates for the superior bone are termed "corrected position 1".

- The "corrected position 1" and "position 2" vector data of the superior bone are used to calculate the displacement matrix describing motion of the superior bone.

- Screw axis parameters (S, ϕ, U_x, U_y, U_z) are then calculated, and also a point on the screw axis closest to the origin of the inferior bone frame is calculated. This closest point is also displayed in the SRP frame.

5.5 SCREW AXIS RESULTS

5.5.1 Targets

Results of the screw axis analysis are based upon data in the SRP frame of reference. Each bone is represented by three cadaver targets located at least 0.5 cm apart. The cadaver targets are listed for each bone and position in Table 5.10. The same three targets are used for all 10 positions for the innominate, sacrum, and L4. There are two sets of targets used for T12, L1 - L3. The first set represents positions of lumbar extension (LBAR 3.0-5.5) and SEATERCT. The second set represents positions in lumbar flexion (SEATEDP1 and SEATEDP2) and right lateral side bending (SIDEBEND).

The different sets are selected to provide the most accurate data available. Targets are identified using two criteria:

1) targets separated by a distance greater than 0.5 cm;
2) distances between targets are stable.

As pointed out previously, errors exist in the experimental data for flexion and sidebending positions. In addition to experimental errors, different points were selected based upon ability to identify these targets on the film.

5.5.2 Screw axis description of anatomical motion

The parameters calculated in the screw axis analysis describe relative motion between two bones. In this report, motion segments have been analyzed using the bone in a motion segment pair closest to the seat as the fixed body and the bone in the motion segment furthest from the seat as the moving body (Table 5.11). For example, motion of the right innominate (moving body) is described relative to a fixed axis system in the seat.

Table 5.10. List of targets by position and bone used in the motion analysis.

	SEATERCT LBAR 3.0	LBAR 3.0 LBAR 4.0	LBAR 4.0 LBAR 4.5	LBAR 4.5 LBAR 5.0	LBAR 5.0 LBAR 5.5	LBAR 3.0 LBAR 5.5
RIGHT INNOMINATE	CINRAS CINRPS CINRPT	CINRAS CINRPS CINRPT	CINRAS CINRPS CINRPT	CINRAS CINRPS CINRPT	CINRAS CINRPS CINRPT	CINRAS CINRPS CINRPT
SACRUM	CSACLT CSACRT CSACSM	CSACLT CSACRT CSACSM	CSACLT CSACRT CSACSM	CSACLT CSACRT CSACSM	CSACLT CSACRT CSACSM	CSACLT CSACRT CSACSM
L4	CLO4R1 CLO4SM CLO4TL	CLO4R1 CLO4SM CLO4TL	CLO4R1 CLO4SM CLO4TL	CLO4R1 CLO4SM CLO4TL	CLO4R1 CLO4SM CLO4TL	CLO4R1 CLO4SM CLO4TL
L3	CLO3TL CLO3R1 CLO3S1	CLO3TL CLO3R1 CLO3S1	CLO3TL CLO3R1 CLO3S1	CLO3TL CLO3R1 CLO3S1	CLO3TL CLO3R1 CLO3S1	CLO3TL CLO3R1 CLO3S1
L2	-	CLO2L1 CLO2TL CLO2SM	CLO2L1 CLO2TL CLO2SM	CLO2L1 CLO2TL CLO2SM	CLO2L1 CLO2TL CLO2SM	CLO2L1 CLO2TL CLO2SM
L1	CLO1SM CLO1L1 CLO1R1	CLO1SM CLO1L1 CLO1R1	CLO1SM CLO1L1 CLO1R1	CLO1SM CLO1L1 CLO1R1	CLO1SM CLO1L1 CLO1R1	CLO1SM CLO1L1 CLO1R1
T12	CT12L1 CT12S1 CT12R1	CT12L1 CT12S1 CT12R1	CT12L1 CT12S1 CT12R1	CT12L1 CT12S1 CT12R1	CT12L1 CT12S1 CT12R1	CT12L1 CT12S1 CT12R1

Table 5.10 (continued)

	SEATERCT LBAR 5.5	SEATERCT SEATEDP1	SEATEDP1 SEATEDP2	SEATERCT SEATEDP2	SEATERCT SIDEBEND
RIGHT INNOMINATE	CINRAS CINRPS CINRPT	CINRAS CINRPS CINRPT	-	-	CINRAS CINRPS CINRPT
SACRUM	CSACLT CSACRT CSACSM	CSACLT CSACRT CSACSM	CSACLT CSACRT CSACSM	CSACLT CSACRT CSACSM	CSACLT CSACRT CSACSM
L4	CLO4R1 CLO4SM CLO4TL	CLO4R1 CLO4SM CLO4TL	CLO4R1 CLO4SM CLO4TL	CLO4R1 CLO4SM CLO4TL	CLO4R1 CLO4SM CLO4TL
L3	CLO3TL CLO3R1 CLO3S1	CLO3L1 CLO3R1 CLO3SM	CLO3L1 CLO3R1 CLO3SM	CLO3L1 CLO3R1 CLO3SM	CLO3L1 CLO3R1 CLO3SM
L2	-	-	CLO2S1 CLO2TL CLO2SM	-	-
L1	CLO1SM CLO1L1 CLO1R1	CLO1S1 CLO1TL CLO1TR	CLO1S1 CLO1L1 CLO1TR	CLO1S1 CLO1L1 CLO1TR	CLO1S1 CLO1TL CLO1SM
T12	CT12L1 CT12S1 CT12R1	CT12L1 CT12SM CT12TR	CT12L1 CT12SM CT12TR	CT12L1 CT12SM CT12TR	CT12L1 CT12SM CT12TR

Fixed Body	Moving Body
Seat	Rt. Innominate
Rt. Innominate	Sacrum
Sacrum	L4
L4	L3
L3	L2
L2	L1
L1	T12

Table 5.11. Motion segments.

For these motion segments, the screw axis parameters have been calculated and are presented in Table 5.12. The motions are described as a change of position along a path of positions. For example, the path for lumbar extension is described by seven screw axes beginning with the motion from SEATERCT position to LBAR 3.0. Data on L2 are missing in the SEATERCT position; consequently, the L1 screw axis parameters were calculated relative to L3. The paths of motion for lumbar flexion are represented by three screw axes beginning with the change of position from SEATERCT to SEATEDP1. Because only one lateral side bending position was measured, it is described relative to the SEATERCT position.

The following data are given in Table 5.12:

1) A positive or negative displacement (S) in centimeters,

2) A rotation (ϕ) in degrees around the screw axis with positive representing a clockwise rotation around the screw axis and negative, a counterclockwise rotation.

3) Direction cosines (U_x, U_y, U_z) describing the screw axis orientation relative to the Seat Reference Point axis system (see section 5.5.1).

The location of the screw axis, described by a position vector of the closest point to the inferior bone frame origin, is given in a later table following a description of the "center of gravity" data for each bone.

The stereoradiographic measurement system can resolve an angle of approximately 0.8 ° and a distance of approximately 0.03 cm. Motions described in Table 5.12 contain some rotations and displacements that are at or beyond the resolution limits of the measurement system. For example, the motion of L4 relative to the sacrum in the change of position from LBAR 3.0 to LBAR 4.0 is smaller than the system can measure. As a result, use of these data must be carefully evaluated in terms of the resolution of the system.

For the small extension displacements, the direction cosines defining the orientation of each screw axis would be expected to reflect maximal rotations about the y-axis with a cosine value approaching one, similar to results seen for flexion (SEATERCT to SEATEDP1 or SEATEDP2). Relatively few axes are approximately perpendicular to the xz plane, which would indicate rotary motion primarily in the sagittal plane. The direction cosines are given relative to an axis system that approximates the cardinal anatomical planes, and the seat axis system is approximately parallel to the inertial axis system. The cadaver was positioned with as much anatomical symmetry as possible with respect to the xz plane, but there are obvious discrepancies to a symmetrical position visible on the radiographic

Table 5.12. Screw axis results for all motion segments.

	SEATERCT - LBAR 3.0					LBAR 3.0 - LBAR 4.0				
	S	ϕ	Direction Cosines			S	ϕ	Direction Cosines		
	(cm)	(Deg)	U_x	U_y	U_z	(cm)	(Deg)	U_x	U_y	U_z
INNR	-0.26	1.7	-0.239	0.796	-0.555	0.01	0.8	-0.226	0.938	0.254
SAC	-0.04	1.0	0.325	0.205	0.923	0.00	0.5	1.000	0.000	0.000
L4	0.03	0.7	-0.026	-0.611	-0.797	0.12	0.6	1.000	0.000	0.000
L3	0.02	2.4	0.157	-0.645	-0.748	-0.06	1.7	-0.541	0.254	0.802
L2	-	-	-	-	-	0.05	1.9	-0.180	-0.444	-0.878
L1	-0.07	3.2	-0.482	-0.297	0.824	-0.02	1.2	0.539	0.523	-0.661
T12	0.02	1.8	-0.238	-0.194	-0.952	0.00	2.4	-0.028	-0.891	0.453

	LBAR 4.0 - LBAR 4.5					LBAR 4.5 - LBAR 5.0				
	S	ϕ	Direction Cosines			S	ϕ	Direction Cosines		
	(cm)	(Deg)	U_x	U_y	U_z	(cm)	(Deg)	U_x	U_y	U_z
INNR	0.08	1.0	-0.054	0.992	0.119	0.06	1.2	-0.069	0.989	0.131
SAC	0.03	0.4	1.000	0.000	0.000	0.05	0.6	1.000	0.000	0.000
L4	0.02	0.6	0.092	-0.625	-0.771	-0.04	0.4	1.000	0.000	0.000
L3	-0.26	0.5	1.000	0.000	0.000	-0.05	1.8	-0.673	0.057	0.737
L2	-0.02	1.0	0.970	-0.082	0.231	0.00	2.0	0.218	-0.291	-0.932
L1	0.02	1.2	-0.396	-0.202	-0.897	-0.01	0.9	0.115	-0.447	0.871
T12	-0.24	0.5	1.000	0.000	0.000	0.02	1.1	0.139	-0.982	-0.129

[1]Since L2 data are missing, L1 analyzed relative to L3.

Table 5.12 (continued)

	LBAR 5.0 - LBAR 5.5					LBAR 3.0 - LBAR 5.5				
	S (cm)	ϕ (Deg)	Direction Cosines U_x	U_y	U_z	S (cm)	ϕ (Deg)	Direction Cosines U_x	U_y	U_z
INNR	0.05	1.2	-0.063	0.978	0.197	0.20	4.1	-0.095	0.981	0.172
SAC	-0.05	0.5	1.000	0.000	0.000	-0.04	0.7	-0.407	-0.816	0.407
L4	-0.02	0.8	0.118	-0.659	-0.740	0.04	1.6	-0.714	-0.667	0.213
L3	-0.03	1.9	0.549	-0.129	-0.826	-0.09	2.1	-0.649	0.315	0.693
L2	0.04	1.8	-0.015	0.292	0.957	0.03	2.1	0.491	-0.459	-0.741
L1	-0.00	2.3	-0.801	-0.451	0.396	0.02	2.0	-0.816	-0.573	-0.076
T12	0.05	0.9	0.537	0.052	-0.842	0.08	3.3	0.051	-0.999	0.023

	SEATERCT - LBAR 5.5					SEATERCT - SEATEDP1				
	S (cm)	ϕ (Deg)	Direction Cosines U_x	U_y	U_z	S (cm)	ϕ (Deg)	Direction Cosines U_x	U_y	U_z
INNR	-0.02	5.4	-0.152	0.988	-0.036	-0.86	33.2	-0.020	-0.999	-0.023
SAC	-0.14	1.2	0.085	-0.275	0.957	0.16	0.8	-0.150	-0.919	-0.366
L4	0.08	1.5	0.151	-0.856	-0.495	-0.22	10.4	0.122	0.988	-0.100
L3	0.01	1.4	-0.729	-0.644	-0.236	0.25	9.0	0.058	0.975	0.216
L2	-	-	-	-	-	-	-	-	-	-
L1	-0.12	3.7	-0.533	-0.799	0.280	0.13	16.2	0.085	0.993	0.082
T12	0.14	4.0	-0.059	-0.917	-0.395	0.04	4.1	-0.031	0.998	0.054

Table 5.12 (continued)

	SEATEDP1 - SEATEDP2					SEATERCT - SEATEDP2				
	S (cm)	ϕ (Deg)	Direction Cosines U_x	U_y	U_z	S (cm)	ϕ (Deg)	Direction Cosines U_x	U_y	U_z
INNR	-	-	-	-	-	-	-	-	-	-
SAC	-	-	-	-	-	-	-	-	-	-
L4	0.03	1.3	-0.289	-0.903	0.320	-0.21	9.2	0.105	0.993	-0.063
L3	-0.01	0.6	0.356	0.933	0.078	0.25	9.6	0.017	0.981	0.194
L2	-0.09	7.7	0.194	0.133	-0.972	-	-	-	-	-
L1	-0.02	5.8	-0.330	0.554	0.764	-0.13	20.4	0.030	0.995	-0.097
T12	-0.05	1.7	0.198	-0.295	0.935	0.09	3.9	0.066	0.907	0.417

SEATERCT - SIDEBEND

	S (cm)	ϕ (Deg)	Direction Cosines U_x	U_y	U_z
INNR	1.13	17.9	0.073	-0.964	0.255
SAC	-0.02	1.6	-0.137	0.914	-0.383
L4	-0.03	7.8	0.211	0.970	0.124
L3	-0.13	6.8	0.747	0.652	0.132
L2	-	-	-	-	-
L1	0.18	13.0	0.683	0.653	0.328
T12	0.03	4.1	0.619	0.657	0.431

films. To clearly demonstrate the relative motions between two bones, comparable pointmarks must be used and an axis system based on these pointmarks. If this procedure is not followed then the interpretation of the relative motion becomes very difficult.

In conclusion, these screw axis parameters are presented primarily to demonstrate the feasibility of obtaining a description of spinal kinematics with respect to seated position. They describe measured positions of the lumbar spine, sacrum, and innominate with anatomical landmarks important to an understanding of the relationship between position and mobility of the seated position.

5.5.3 Position vectors for screw axis location

For each measured position and subsequent motion analysis, many position vectors can be utilized to locate the screw axis and bones relative to an external reference system. In the present investigation, two basic position vectors were calculated.

First, the origin of an axis system describing each bone is defined (Table 5.13) by vectorially summing the target coordinates and calculating the average position vector, i.e., "center of gravity" of each bone. The orientation of the axes is kept parallel to the SRP frame of reference previously described.

Second, a point on the screw axis closest to the inferior bone "center of gravity" is calculated (Table 5.14). That is, a position vector in the inferior bone frame of reference defines a point on the screw axis for comparison with anatomical pointmarks on both bones. In this instance, the inferior bone refers to the fixed bone closest to the seat; e.g., L4 is the inferior bone for motion of L3. Therefore, when data are analyzed in comparable anatomical frames of reference and joint surfaces are defined by three-dimensional pointmarks, location of the closest point on the screw axis provides a basis for anatomical evaluation of the movements. The data presented in Table 5.14, however, were calculated using cadaver targets reported in Table 5.10. These pointmarks are not, strictly speaking, anatomically comparable between bones. Consequently, the results have some differences due to imprecise location of the targets used in defining the inferior bone frame.

As in the screw axis parameter results, considerable variation appears to exist in the location of the closest point on the screw axis. These data, however, are only as comparable as the definition of each axis system; and the use of imprecisely located cadaver pointmarks has already been noted. In order to reduce the effect of the anatomical axes systems for these data, the position vector in Table 5.14 was vectorially summed with the position vector (Table 5.13) of the bone frame origin in the SRP axis system. The resulting set of position vectors of the closest point on the screw axis to the inferior bone frame origin in the SRP axis system is presented in Table 5.15.

Each motion segment screw axis has two position vectors. A position vector that describes the closest point for the first position and a corresponding position vector for the second position. For example, the first position in Table 5.15 is SEATERCT. There are position vectors for each bone in the SEATERCT position. Since a screw axis describes the change of position from SEATERCT to LBAR 3.0 (which is the initial lumbar extension

Table 5.13. Center of gravity defined by average of each coordinate set

	Bone Origin in SRP for SEATERCT			Bone Origin in SRP for LBAR 3.0			Bone Origin in SRP for LBAR 4.0		
	x	y	z	x	y	z	x	y	z
SRP	0.00	0.00	0.00	0.00	0.00	0.00	0.00	0.00	0.00
INNR	10.39	-7.70	16.29	10.69	-7.67	16.38	10.85	-7.64	16.37
SAC	-0.63	1.10	13.31	-0.49	1.25	13.58	-0.37	1.33	13.69
L4	0.68	1.01	20.37	1.04	1.21	20.59	1.25	1.30	20.69
L3	0.08	0.47	22.89	0.31	0.69	23.06	0.71	0.79	23.20
L2	-	-	-	-0.60	2.08	25.86	-0.31	2.19	25.95
L1	-2.38	1.20	28.80	-1.98	1.59	28.98	-1.70	1.73	29.06
T12	-3.93	1.04	31.99	-3.39	1.54	32.11	-3.07	1.70	32.17

	Bone Origin in SRP for LBAR 4.5			Bone Origin in SRP for LBAR 5.0			Bone Origin in SRP for LBAR 5.5		
	x	y	z	x	y	z	x	y	z
SRP	0.00	0.00	0.00	0.00	0.00	0.00	0.00	0.00	0.00
INNR	11.11	-7.50	16.35	11.41	-7.41	16.31	11.83	-7.32	16.29
SAC	-0.12	1.39	13.82	0.07	1.42	13.97	0.43	1.43	14.13
L4	1.60	1.38	20.79	1.93	1.44	20.90	2.40	1.49	21.02
L3	1.06	0.81	23.31	1.49	0.98	23.45	1.94	0.99	23.56
L2	0.06	2.29	26.05	0.43	2.37	26.18	1.01	2.43	26.31
L1	-1.25	1.83	29.15	-0.87	1.92	29.25	-0.27	2.00	29.37
T12	-2.61	1.79	32.23	-2.24	1.90	32.32	-1.59	2.12	32.42

	Bone Origin in SRP for SEATEDP1			Bone Origin in SRP for SEATEDP2			Bone Origin in SRP for SIDEBEND		
	x	y	z	x	y	z	x	y	z
SRP	0.00	0.00	0.00	0.00	0.00	0.00	0.00	0.00	0.00
INNR	12.30	-6.95	17.63	-	-	-	10.75	-8.55	17.26
SAC	4.44	1.89	9.00	11.66	1.01	7.46	0.38	-0.55	11.18
L4	1.45	1.98	16.35	7.02	1.18	13.94	-0.51	-0.64	18.93
L3	-0.83	1.33	19.64	3.99	0.54	16.70	-1.87	-1.66	22.08
L2	-3.52	2.58	22.38	0.69	1.80	18.83	-	-	-
L1	-2.97	2.15	26.38	0.36	1.48	22.89	-4.90	-1.88	27.95
T12	-4.76	1.88	30.13	-2.07	1.32	26.33	-4.71	-3.61	31.78

Table 5.14. Closest point on screw axis by position pairs: Movement relative to Bone frame.

	SEATERCT - LBAR 3.0			LBAR 3.0 - LBAR 4.0			LBAR 4.0 - LBAR 4.5		
	x	y	z	x	y	z	x	y	z
INNR	8.31	5.41	4.18	5.68	0.86	1.88	9.37	0.17	2.83
SAC	-15.55	8.03	3.69	-7.25	10.55	1.46	-9.43	17.44	-1.47
L4	-4.41	-7.89	6.20	-3.59	0.28	1.24	0.83	-2.08	1.79
L3	1.66	2.38	-1.70	1.49	5.96	-0.88	4.18	-0.13	5.50
L2	-	-	-	-1.70	4.06	-1.71	-0.92	3.20	5.01
L1	-1.84	5.81	1.02	-4.15	3.03	-0.99	-0.77	-2.62	0.93
T12	-1.71	-3.41	1.12	-0.83	0.95	1.82	-0.27	3.57	2.69

	LBAR 4.5 - LBAR 5.0			LBAR 5.0 - LBAR 5.5			LBAR 3.0 - LBAR 5.5		
	x	y	z	x	y	z	x	y	z
INNR	7.49	0.22	2.24	9.29	1.16	-2.79	8.13	0.65	0.77
SAC	-9.78	1.42	-6.76	-8.33	8.80	-2.21	-8.24	4.42	0.64
L4	1.67	5.05	-3.92	2.32	-1.64	1.83	1.93	0.03	6.55
L3	-0.01	1.77	-0.15	0.27	2.19	-0.16	1.90	4.08	-0.08
L2	-2.13	4.28	-1.83	-1.83	6.02	-1.86	0.88	2.81	-1.16
L1	-0.62	1.85	1.09	-0.14	-0.07	-0.36	1.69	-2.71	2.21
T12	-0.11	-0.32	2.34	-2.73	-1.25	-1.82	0.92	0.11	2.88

[1] Data presented in previous bone frame represents the SRP.
[2] Data presented relative to L3 since no data on L2.

Table 5.14 (continued)

	SEATERCT - LBAR 5.5			SEATERCT - SEATEDP1			SEATEDP1 - SEATEDP2		
	x	y	z	x	y	z	x	y	z
INNR	10.32	1.66	1.91	9.26	-0.67	20.61	-	-	-
SAC	-14.00	6.21	3.02	-1.71	21.48	-53.28	-	-	-
L4	3.52	-3.51	7.13	2.67	0.41	7.31	2.11	-2.13	-4.11
L3	-0.16	-0.69	2.37	1.26	-1.18	5.00	0.31	-0.89	9.26
L2	-	-	-	-	-	-	-1.05	1.37	-0.02
L1	0.00	1.38	3.94	2.80	-0.60	4.38	1.77	-2.52	2.59
T12	0.35	-1.60	3.66	2.73	-0.07	2.99	-0.60	-3.36	-0.93

	SEATERCT - SEATEDP2			SEATERCT - SIDEBEND		
	x	y	z	x	y	z
INNR	-	-	-	7.34	4.34	14.35
SAC	-	-	-	-10.73	-1.68	-0.17
L4	0.84	0.50	9.36	4.83	-2.08	7.98
L3	0.11	-1.08	5.47	-0.07	-0.93	4.96
L2	-	-	-	-	-	-
L1	1.10	0.48	5.24	0.59	-2.47	3.69
T12	1.57	-2.27	4.68	1.12	-2.38	2.02

Table 5.15. Position vectors of the closest point on the screw axis to the center of gravity in the SRP frame of reference.

	SEATERCT				LBAR 3.0			
	x	y	z	D[1]	x	y	z	D
INNR	8.31	5.41	4.18	10.76	8.31	5.41	4.18	10.76
SAC	-5.16	0.33	19.98	20.64	-4.86	0.36	20.07	20.65
L4	-5.04	-6.79	19.51	21.26	-4.90	-6.64	19.78	21.43
L3	2.32	3.39	18.67	19.12	2.70	3.59	18.89	19.42
L2	-	-	-	-	-	-	-	-
L1[2]	-1.76	6.28	23.91	24.78	-1.53	6.50	24.08	24.99
T12	-4.09	-2.21	29.92	30.28	-3.68	-1.82	30.10	30.38

	LBAR 3.0				LBAR 4.0			
	x	y	z	D	x	y	z	D
INNR	5.68	0.86	1.88	6.04	5.68	0.86	1.88	6.04
SAC	3.44	2.88	17.84	18.40	3.60	2.91	17.83	18.42
L4	-1.45	-2.04	10.55	10.84	-1.33	-1.96	13.66	13.86
L3	2.53	7.17	19.71	21.13	2.74	7.26	19.81	21.28
L2	-1.39	4.75	21.35	21.92	-0.99	4.85	21.49	22.05
L1	-4.75	5.11	24.87	25.83	-4.46	5.22	24.96	25.89
T12	-2.81	2.54	30.80	31.03	2.53	2.68	30.88	31.10

	LBAR 4.0				LBAR 4.5			
	x	y	z	D	x	y	z	D
INNR	9.37	0.17	2.83	9.79	9.37	0.17	2.83	9.79
SAC	1.42	9.80	14.90	17.89	1.68	9.94	14.88	17.91
L4	-1.93	-0.94	19.41	19.53	-1.68	-0.88	19.54	19.63
L3	5.43	1.17	26.19	26.77	5.78	1.25	26.29	26.95
L2	-0.21	3.99	28.21	28.49	0.14	4.01	28.32	28.60
L1	-1.08	-0.43	26.88	26.91	-0.71	-0.33	26.98	26.99
T12	-L.97	5.30	31.75	32.25	-1.52	5.40	31.84	32.33

	LBAR 4.5				LBAR 5.0			
	x	y	z	D	x	y	z	D
INNR	7.49	0.22	2.24	7.82	7.49	0.22	2.24	7.82
SAC	1.33	-6.08	9.59	10.24	1.63	-5.99	9.55	11.39
L4	1.96	3.32	19.67	20.04	2.15	3.35	19.82	20.22
L3	1.59	3.15	20.64	20.94	1.92	3.21	20.75	21.08
L2	-1.02	5.09	21.48	22.10	-0.64	5.26	21.62	22.26
L1	-0.56	4.14	27.14	27.46	-0.19	4.22	27.27	27.60
T12	-1.36	1.51	31.49	31.56	-0.98	1.60	31.59	31.65

[1] D is the distance between the closest point and the center of gravity.

[2] Since L2 bone frame data are missing for SEATERCT positions, the L3 bone frame was used for these L1 screw axis point position vectors.

Table 5.15 (continued)

	LBAR 5.0 x	y	z	D	LBAR 5.5 x	y	z	D
INNR	9.29	1.16	-2.79	9.77	9.29	1.16	-2.79	9.77
SAC	3.08	1.30	14.10	14.50	3.50	1.48	14.08	14.58
L4	2.39	-0.22	15.80	15.98	2.75	-0.21	15.96	16.20
L3	2.20	3.63	20.74	21.17	2.67	3.68	20.86	21.35
L2	-0.34	7.00	21.59	22.70	0.11	7.01	21.70	22.80
L1	0.29	2.30	25.82	25.92	0.87	2.36	25.95	26.07
T12	-3.60	0.67	27.43	27.67	-3.00	0.75	27.55	27.72

	LBAR 3.0 x	y	z	D	LBAR 5.5 x	y	z	D
INNR	8.13	0.65	0.77	8.19	8.13	0.65	0.77	8.19
SAC	2.45	-3.25	17.02	17.50	3.59	-2.90	16.93	17.55
L4	1.44	1.25	20.13	20.22	2.36	1.46	20.68	20.86
L3	2.94	5.29	20.51	21.38	4.30	5.57	20.96	22.11
L2	1.19	3.50	21.90	22.21	2.82	3.80	22.40	22.89
L1	1.09	-0.63	28.07	28.10	2.70	-0.28	28.52	28.65
T12	-1.06	1.70	31.86	331.92	0.65	2.11	32.25	32.33

	SEATERCT x	y	z	D	LBAR 5.5 x	y	z	D
INNR	10.32	1.66	1.91	10.63	10.32	1.66	1.91	10.63
SAC	-3.61	-1.49	-36.99	37.20	-2.27	-1.11	19.31	19.46
L4	2.89	-2.41	20.44	20.78	3.95	-2.08	21.26	21.72
L3	0.52	0.32	22.74	22.75	2.24	0.80	23.39	23.51
L2	-	-	-	-	-	-	-	-
L1	0.08	1.85	26.83	26.89	1.84	2.37	27.50	27.67
T12	-2.03	-0.40	32.46	32.53	0.08	0.40	33.03	33.03

	SEATERCT x	y	z	D	SEATEDP1 x	y	z	D
INNR	9.26	-0.67	20.61	22.60	9.26	-0.67	20.61	22.60
SAC	8.68	13.78	-36.99	40.42	10.59	14.53	-35.65	39.93
L4	2.04	1.51	20.62	20.78	8.11	2.30	16.31	18.36
L3	1.94	-0.17	25.37	25.44	2.71	0.80	21.35	21.54
L2	-	-	-	-	-	-	-	
L1	2.51	-0.25	27.84	27.95	1.97	0.73	24.02	24.11
T12	1.33	1.22	32.13	32.18	0.24	2.08	29.37	29.44

Table 5.15 (continued)

	SEATEDP1				SEATEDP2			
	x	y	z	D	x	y	z	D
INNR	-	-	-	-	-	-	-	-
SAC	-	-	-	-	-	-	-	-
L4	6.55	-0.24	4.89	8.18	13.77	-1.12	3.35	14.22
L3	1.75	1.09	25.61	25.69	7.33	0.29	23.20	24.33
L2	-1.88	2.70	19.62	19.89	2.94	1.91	16.68	17.04
L1	-1.75	0.06	24.97	25.03	2.46	-0.72	21.42	21.57
T12	-3.57	-1.21	25.45	25.73	-0.24	-1.88	21.96	22.04

	SEATERCT				SEATEDP2			
	x	y	z	D	x	y	z	D
INNR	-	-	-	-	-	-	-	-
SAC	-	-	-	-	-	-	-	-
L4	0.21	1.60	22.67	22.73	12.50	1.51	16.82	21.01
L3	0.79	-0.07	25.84	25.85	7.13	0.10	19.41	20.68
L2	-	-	-	-	-	-	-	-
L1	0.89	0.83	28.70	28.73	5.09	1.02	21.94	22.55
T12	0.17	-0.98	33.82	33.83	1.93	-0.79	27.57	27.65

	SEATERCT				SIDEBEND			
	x	y	z	D	x	y	z	D
INNR	7.34	4.34	14.35	16.69	7.34	4.34	14.35	16.69
SAC	-0.34	-9.38	16.12	18.65	0.02	-10.23	17.09	19.92
L4	4.20	-0.98	21.29	21.72	5.21	-2.63	19.16	20.03
L3	0.61	0.08	25.33	25.34	-0.58	-1.57	23.89	23.95
L2	-	-	-	-	-	-	-	-
L1	0.38	-2.12	27.15	27.24	-1.28	-4.13	25.77	26.13
T12	-1.88	0.79	30.47	30.54	-3.78	-4.35	29.97	30.52

position), a second position vector is calculated for LBAR 3.0. Thus, two position vectors describe the relative location of the closest point on the screw axis to the change of position in each motion segment.

5.6 RIGID BODY MODEL

Data presented herein assume that each bone is a rigid body; i.e., distances between any two targets (target pair) on the same bone remain unchanged during all cadaver positions and after the bone is excised and cleaned. Transformations calculated to describe the relative displacement assume stable, accurate three-dimensional coordinates, yet the measured data have errors associated with the experiment, instrumentation and human operator. As a result, various analytical methods have been developed to use these data within a rigid body analysis framework.

5.6.1. Errors in empirical data

5.6.1.1. Loss of cadaver target Cadaver targets are implanted with a spring-loaded syringe and are, therefore, dependent upon being wedged in the bone so that they stay fixed relative to the bone and one another. Due to incomplete wedging, a target can move slightly inside the bone; or, with incomplete penetration, the target can be located on the bone surface and fall off during cleaning. In the latter instances, the bone is examined closely; and a target is glued on if an impression remains at the site of the original cadaver target, or the probable location can be measured as the intersection of two radii from two targets that remained in the bone.

5.6.1.2. Digitizing algorithm The digitizing algorithm, discussed in Sections 4.2 and 4.3, can be a source of error on the resulting three-dimensional data in the inertial frame.

5.6.1.3. Film quality Occasionally, the six targets representing one bone cannot be correctly identified on the tube I and tube II film images. This type of error was eliminated for most cases; but if the film quality was poor, errors in the data are still present.

5.6.1.4. Random measurement error Random error by the technician digitizing the films, and from limitations of the digitizer board itself, are also present. However, these errors are negligible compared to the above three types of errors.

5.6.2 Minimizing effect of error in the data analysis

Confronted with different sources of error in the empirical data, SAL has used various methods to reduce their effect. The following procedures have been used or are being developed for use.

5.6.2.1. Repeated digitizing Random error is reduced by repeatedly digitizing every film pair several times. In most cases, seven sets of data are averaged. The sample size to obtain maximum statistical efficiency will be investigated.

5.6.2.2. Rigidized displacement matrix All displacement matrices are calculated from orthogonal unit vectors on a bone derived from the measured targets of the bone. Using orthogonalized unit vectors imposes a "rigid body" model on the bone; the displacement matrix is referred to as the "rigidized" displacement matrix.

5.6.2.3. Overdetermined displacement matrix In cases where more than three targets on a bone were measured accurately, the displacement matrix can be calculated from all targets available. Thus the displacement matrix is overdetermined. Rather than obtaining the result from three targets which is the minimum for a rigid body, the position is described by six targets. Mathematically, this methodology is expected to produce more stable data less affected by random errors.

For one point in position 1 displaced to position 2:

$$\underset{\substack{4\times4\\\text{matrix}}}{[D_{12}]}\ \underset{\substack{4\times1\\\text{matrix}}}{[V_1]} = \underset{\substack{4\times1\\\text{matrix}}}{[V_2]} \tag{10}$$

For m points, we have:

$$[D_{12}]\ [V_1^i] = [V_2^i] \quad i = 1,\ldots,m \tag{11}$$

Putting all m position vectors in matrix form,

$$[D_{12}]\ [P1] = [P2] \tag{12}$$

where

$$[P1] = (V_1^1, V_1^2, \ldots, V_1^m) \tag{13}$$

$$[P2] = (V_2^1, V_2^2, \ldots, V_2^m) \tag{14}$$

$$[D_{12}]\ [P1][P1]^T = [P2][P1]^T \tag{15}$$

$$[D_{12}] = [P2][P1]^T\ [[P1][P1]^T]^{-1} \tag{16}$$

5.6.2.4. Statistical axis system definition Preliminary results from this approach have shown some numerical problems in solving the matrix equation. Points on the bone are used, and this provides the most insensitive linearly solved coordinate system. A method has been developed by Menashe Brosh, not yet published, and will be investigated further.

6.0 DISCUSSION AND CONCLUSIONS

6.1 VARIATIONS IN MOTION PARAMETERS FOR SUBJECT #18

The current data reported for subject #18 reflect considerable variation when examined with respect to the orientation of the screw axis and the position vector of a point on the screw axis. Some of the motions reported by the displacements (S) and rotations (ϕ) in Table 5.12 are at the current resolution limits of the stereoradiographic measurement system in SAL. Orientations of the screw axes reported in Table 5.12 indicate for some motion segments that the axis of rotation is primarily about the z-axis (a rotation in the horizontal plane); and for other motion segments, the axis of rotation is primarily about the x-axis (rotation in the frontal plane). There appear to be multiple explanations for this variation.

a) Subject position. The cadaver was not placed symmetrically with the laboratory axis system. In addition, the spinal column is not aligned in the sagittal plane.

b) Anatomical axis system definition. Since the bones pointmarks were not used in the screw axis analysis and the cadaver targets were not located at anatomical pointmarks, there is variation due to use of non-comparable axis systems.

c) Loading to produce motion. The device built to establish positions in lumbar extension produced a moment acting on the spinal column producing a rotation in the XY plane in addition to extension in the XZ plane.

d) Erroneous data. The position and orientation of the glass rod were inadvertently changed for SEATERCT, SEATEDP1, SEATEDP2, and SIDEBEND positions. Consequently, these positions are not strictly comparable to the better data in the LBAR series for lumbar extension. Thus, there are errors in the data attributable to the experiment, i.e. misalignment of the glass rod.

e) Unknown nature of soft tissue. The biomechanical properties of the cadaver's soft tissue, i.e. ligaments and disc, are unknown. As discussed in the literature review, the soft tissues are extremely important in spinal kinematics.

In conclusion, variation in the motion data appears to be primarily attributable to experimental and analytical parameters that can be improved and better controlled. Thus, with succeeding subjects, these sources of error will either be eliminated or minimized.

6.2 IMPROVEMENTS IN SYSTEMS ANTHROPOMETRY LABORATORY

Projected improvements for SAL, discussed in detail in previous sections of this report, may be summarized as follows:

6.2.1 Use of quartz cube

As pointed out in Section 4.0, the digitizing algorithm is dependent on the perpendicularity of glass rod to film plane. Either improved alignment procedures for the glass rod or a new calibration device, a 3-D quartz cube with targets on each corner, will replace the current

laboratory procedure. Since the geometry of the quartz cube is known in three dimensions, it may prove a better device for use in merging the film pair.

6.2.2 Digitizing error detection

One digitizing difficulty has been identification of the same target in a stereo pair. Analytical detection of this type of error will be built into the digitizing program. A computer upgrade from the GA16-460 to a GA16-480 with 128K memory will allow greater development of the digitizing program.

6.2.3 Increase of accuracy in axis system definition

Six targets per bone have been used in the present experiment. However, the targets could not be utilized in calculations because of numerical problems in solving matrix equations. Future study will address the reduction or elimination of this difficulty. Details have been discussed in Section 5.6.

6.2.4 Targeting technique

The success of the anthropometric investigation depends to a large degree upon implanting targets in the skeletal system in such a manner that they remain in the same relative location through the cadaver motion study, skeletal preparation, and bone targeting procedure. An improved system for target implantation has been developed.

6.2.5 Redigitize previous films

Data from three subjects were not presented in this final report because the digitizing algorithm has continually been improved; only the most recent subject's data have been considered here. The films from Subjects 15, 16, and 17 will be measured as part of the ongoing research in SAL; they will be digitized and the data submitted to the Air Force Aerospace Medical Research Laboratory.

6.3 UNIQUE THREE-DIMENSIONAL DATA

Data presented in this report are unique to Systems Anthropometry Laboratory. A major objective of research in SAL has been to develop a three-dimensional anthropometric methodology that can describe position and mobility of the human body from measured data. Data are measured to describe the body as an anthropomechanical system; i.e., a dynamic linkage system with mass properties that must be defined by independent but comparable axes systems. The laboratory has emphasized development of three-dimensional axes systems for each link in the body with which joint kinematics and/or mass distribution can be defined. Position and mobility of the body linkage system has therefore been defined by anatomical frames of reference relative to a laboratory axis system.

Rigid body assumptions have been used to investigate joint kinematics. The traditional linkage system for a set of rigid bodies is defined as the functional straight-line distance between opposing joints. This is an appropriate model of the human body's appendages, in which there is one functional joint at the ends of each link. Structurally and functionally, the torso presents a different set of conditions.

Each vertebra (i.e., link) joint has complementary surfaces determining the position and mobility of the vertebra. That is, a superior articular facet is complemented by an inferior articular facet. On each vertebra there are a pair of superior articular facets and a pair of inferior articular facets. A complex separation of two vertebrae bodies complete the mechanical joint (vertebral body - disc - vertebral body). As a result of this complicated anatomical structure, i.e. soft tissue connections, articular facets and disc, motions are coupled in the vertebral column. The vertebrae, therefore, require a more complicated simulation than do the appendage joints, which are generally modeled as mechanical joints such as a ball-and-socket or hinge.

In summary, the research investigation in SAL studies kinematics in the torso to describe the anthropomechanical linkage system from hip to shoulder joints. To measure representative positions of the living body in a physiologically passive state, the kinematic system is studied in unembalmed cadavers. With the use of anatomical frames of reference defined by comparable pointmarks in the skeletal system, position and mobility data between subjects can be measured and compared.

In conclusion, the unique data collected in SAL can provide a complete anatomical geometry for current simulations. It provides the basis for a kinematic description of the human body previously unavailable. With these three-dimensional data, improvements in models can be made that will simulate the ergonomic performance or dynamic response of the human body with greater biofidelity.

7.0 APPENDICES

7.1 APPENDIX A: GLOSSARY OF ANATOMIC LANDMARKS

*Note: Following is a list of terms which specify anatomic landmarks which are identified by the Systems Anthropometry Laboratory on the spinal column, pelvic girdle, and femur of cadaveric research subjects. The acronym by which each pointmark is known and a description of the point is provided.

SACRUM

PROMO — Promontorion: The midpoint of the anterior-superior margin on the base of the first sacral segment (excluding exostoses).

SIBDYP — Posterior Point on First Sacral Vertebral Body: The midpoint of the postero-superior margin on the base of the first sacral segment. This point is posterior to Promontorion.

SACBLL — Left Lateral Point on First Sacral Vertebral Body: The most lateral point on the left articular surface of the first sacral body. In cases with "lipping" present, the point was estimated as the most lateral point on the superior surface that would be found in the general contour without any lipping.

SACBLR — Right Lateral Point on First Sacral Vertebral Body: Same as description above, except on the right articular surface.

SAFLSL — Superior Articular Facet: Lateral Superior, Left: The point is the most superior point on the lateral side of the left superior articular facet of the sacrum.

SAFMSL — Superior Articular Facet: Medial Superior, Left: The point is the most superior point on the medial side of the left superior articular facet of the sacrum.

SAFLIL — Superior Articular Facet: Lateral Inferior, Left: The point is the most inferior point on the medial side of the left superior articular facet of the sacrum.

SAFLSR — Superior Articular Facet: Lateral Superior, Right: The point is the most superior point on the lateral side of the right superior articular facet of the sacrum.

SAFMSR — Superior Articular Facet, Medial Superior, Right: The point is the most superior point on the medial side of the right superior articular facet of the sacrum.

SAFLIR — Superior Articular Facet, Lateral Inferior, Right: The point is the most inferior point on the lateral side of the right superior articular facet of the sacrum.

SAFMIR — Superior Articular Facet, Medial Inferior, Right: The point is the most inferior point on the medial side of the right superior articular facet of the sacrum.

SPOLLS — Superior Pole, Left Sacrum: A point on the posterior margin of the sacroiliac joint surface that lies on a line bisecting the superior pole of the joint surface.

SLSMLS — Superior Lobe, Superior Margin Midpoint, Left Sacrum: A point along the superior margin of the superior pole of the left sacroiliac joint surface that lies on a perpendicular line that bisects the line passing between the sacroiliac midpoint and superior pole.

SLIMLS — Superior Lobe, Inferior Margin Midpoint: A point along the inferior margin of the superior pole of the sacroiliac joint surface that lies on a perpendicular line that bisects the line passing between sacroiliac midpoint and the superior pole.

SACMPL — Sacroiliac Midpoint, Left Sacrum: The point that lies at the intersect of the lines which bisect the superior and inferior poles of the left sacroiliac joint.

IFPMLS — Inferior Lobe, Posterior Margin, Left Sacrum: A point along the posterior margin of the left inferior lobe that lies on a perpendicular line bisecting the line between the sacroiliac midpoint and the inferior pole.

ILAMLS — Inferior Lobe, Anterior Margin, Left Sacrum: A point along the anterior margin of the inferior lobe of the left sacroiliac joint surface that lies on a perpendicular line bisecting the line between the sacroiliac midpoint and the inferior pole.

IPOLLS — Inferior Pole, Left Sacrum: A point of the inferior margin which lies on a line bisecting the inferior pole of the left sacroiliac joint.

SPOLRS — Superior Pole, Right Sacrum: A point on the posterior margin of the sacroiliac joint surface that lies on a line bisecting the superior pole of the joint surface.

SLSMRS — Superior Lobe, Superior Margin Midpoint, Right Sacrum: A point along the superior margin of the superior pole of the sacroiliac joint surface that lies on a perpendicular line that bisects the line passing between the sacroiliac midpoint and superior pole.

SLIMRS — Superior Lobe, Inferior Margin Midpoint, Right Sacrum: A point along the inferior margin of the superior pole of the right sacroiliac joint surface that lies on a perpendicular line that bisects the line passing between sacroiliac midpoint and the superior pole.

SACMPR — Sacroiliac Midpoint, Right Sacrum: The point that lies at the intersect of the lines which bisect the superior and inferior poles of the sacroiliac.

IFPMRS — Inferior Lobe, Posterior Margin, Right Sacrum: A point along the posterior margin of the right inferior lobe that lies on a perpendicular line bisecting the line between the sacroiliac midpoint and the inferior pole.

ILAMRS — Inferior Lobe, Anterior Margin, Right Sacrum: A point along the anterior margin of the inferior lobe of the right sacroiliac joint surface that lies on a perpendicular line bisecting the line between the sacroiliac midpoint and the inferior pole.

IPOLRS — Inferior Pole, Right Sacrum: A point on the inferior margin which lies on a line bisecting the inferior pole of the right sacroiliac joint.

CSACSM — Dorsal Spine of the First Sacral Vertebra in Cadaver: The most superior point on the dorsal spine of the first sacral segment.

CSACLT — Sacrum Left Point, in Cadaver: Point targeted in cadaver on the left side of the sacrum at S2-S3.

CSACRT — Sacrum Right Point, in Cadaver: Point targeted in cadaver on the right side of the sacrum at S2-S3.

P-CAUD — Caudion, Posterior: The midpoint of the posterior-inferior margin of the last sacral segment. Morphological observations should be examined to determine the exact sacral or coccygeal vertebra upon which Caudion was located.

CSACS1 — Dorsal Spine of the First Sacral Vertebrae in Cadaver: The most inferior point on the dorsal spine of the first sacral segment.

CSACL1 — Sacrum Left Point, in Cadaver: 2nd point targeted in cadaver on the left side of the sacrum at S4.

CSACR1 — Sacrum Right Point, in Cadaver: 2nd point targeted in cadaver on the right side of the sacrum at S4.

SAFMPL — Superior Articular Facet, Midpoint, Left: The midpoint of the left articular facet of the sacrum.

SAFMPR — Superior Articular Facet, Midpoint, Right: The midpoint of the right articular facet of the sacrum.

VERTEBRAE

(L5 will be used as an example.)

SLSL5L — Superior Articular Facet, Lateral Superior L5, Left Side: The point is the most superior point on the lateral side of the left superior articular facet of L5.

SMSL5L — Superior Articular Facet, Medial Sueprior L5, Left Side: The point is the most superior point on the medial side of the left superior articular facet of L5.

SLIL5L — Superior Articular Facet, Lateral Inferior L5, Left Side: The point is the most inferior point on the medial side of the left superior articular facet of L5.

SL5PPT — Superior Body Surface L5, Posterior Point: The midpoint of the postero-superior margin of the L5 superior body surface.

SL5APT — Superior Body Surface L5, Anterior Point: The midpoint of anterior-superior margin of the L5 superior body surface.

SL5BLL — Superior Body Surface L5, Lateral Point Left: The most lateral point on the left side of the articular surface on the L5 superior body surface. In cases with "lipping" present, the point was estimated as the most lateral point on the superior surface that would be found in the general contour with no lipping present.

SL5BLR — Superior Body Surface L5, Lateral Point Right: Same as description above, except on the right side of the articular surface.

ILSL5L — Inferior Articular Facet, Lateral Superior L5, Left Side: The point is the most superior point on the lateral side of the left inferior articular facet of L5.

IMSL5L — Inferior Articular Facet, Medial Superior L5, Left Side: The point is the most superior point on the medial side of the left inferior articular facet of L5.

ILIL5L Inferior Articular Facet, Lateral Inferior L5, Left Side: The point is the most inferior point on the lateral side of the left inferior articular facet of L5.

IMIL5L Inferior Articular Facet, Medial Inferior L5, Left Side: The point is the most inferior point on the medial side of the left inferior articular facet of L5.

ILSL5R Inferior Articular Facet, Lateral Superior L5, Right Side: The point is the most superior point on the lteral side of the right inferior articular facet of L5.

IMSL5R Inferior Articular Facet, Medial Superior L5, Right Side: The point is the most superior point on the medial side of the right inferior articular facet of L5.

ILIL5R Inferior Articular Facet, Lateral Inferior L5, Right Side: The point is the most inferior point on the lateral side of the right inferior articular facet of L5.

IMIL5R Inferior Articular Facet, Medial Inferior L5, Right Side: The point is the most inferior point on the medial side of the right inferior articular facet of L5.

IL5PPT Inferior Body Surface L5, Posterior Point: The midpoint of the posterior margin of the L5 inferior body surface.

IL5APT Inferior Body Surface L5, Anterior Point: The midpoint of the anterior margin of the L5 inferior body surface.

IL5BLL Inferior Body Surface L5, Lateral Point Left: The most lateral point on the left side of the articular surface of the L5 superior body surface.

TPL5LT Transverse Process L5, Left Side: The most projecting point on the left transverse process of L5. In the case of a large contact area, the midpoint of the contact area is targeted.

CL05TL Transverse Process L5, Left Side, in Cadaver: Same as description above, target implanted in bone while cadaver is intact.

CL05L1 Left Point in Cadaver: 2nd left point, more medial than CL05TL.

TPL5RT Transverse Process L5, Right Side: The most projecting point on the right transverse process of L5.

CL05TR Transverse Process L5, Right Side, in Cadaver: Same as preceding description, target implanted in bone while cadaver is intact.

CLO5R1 — L5 Right Point in Cadaver: 2nd right point more medial than CLO5TR.

SPMTL5 — L5 Spinous Midpoint: The most projecting point on the spinous process. In case of a large surface area, the midpoint is used.

CLO5SM — L5 Spinous Point, in Cadaver: The most superior target on L5 spinous process.

CLO5S1 — L5 Spinous Point, in Cadaver: The most inferior target on L5 spinous process.

SFML5L — Superior Articular Facet, Midpoint, L5 Left: The midpoint of the left superior articular facet of L5.

SFML5R — Superior Articular Facet, Midpoint, L5 Right: The midpoint of the right superior articular facet of L5.

IFML5L — Inferior Articular Facet, Midpoint, L5 Left: The midpoint of the left inferior articular facet of L5.

IFML5R — Inferior Articular Facet, Midpoint, L5 Right: The midpoint of the right inferior articular facet of L5.

FEMUR

(Left femur used as an example.)

HFEMRL — Head of Femur, Left: The most superior point on head measured by obtaining total morphological length.

TROCHL — Trochanterion, Left: The most superior point of the trochanter along the medial lip border.

CFMLTL — Trochanterion, Left, in Cadaver: Same as preceding description, marked in cadaver.

CFEMML — Femur, Midpoint Left, in Cadaver: A point targeted in the cadaver at the approximate midpoint of the femur.

ADTUBL — Adductor Tubercle Point, Left Femur: The point is the most projecting point of the adductor tubercle found on the superior region of the medial epicondyle, the insertion for adductor magnus.

CFMLME — Medial Epicondyle, Left Femur in Cadaver: Point marked at the medial epicondyle in cadaver.

LEPICL — Lateral Epicondyle, Left Femur: Found by placing the medial and laterial condyle in contact with the horizontal

surface of ostometric board. Move bone so that the lateral aspect of trochanter and the lateral epicondyle are in contact with one vertical plate. The lateral epicondyle is the point which is in contact with the vertical plate.

CFMLLE — Lateral Epicondyle, Left Femur in Cadaver: Point marked at the lateral epicondyle in cadaver.

INNOMINATE

(Left innominate used as an example. Insert "R" for Right innominate.)

ASNOTL — Anterior Sciatic Notch Point, Left Innominate: The point on the inferior margin of the sciatic notch midway between ischial spinale and apex of the sciatic notch.

ACETIL — Acetabulion, Inferior, Left Innominate: Position the hemisphere (Reynolds, Snow and Young, 1981) within the acetabulum so that the anterior extremity of one of the hemisphere diameter lines is opposite acetabulion anterior. Mark the point on the acetabular rim closest to the inferior diameter line when the innominate is held in the anatomical position.

ACETPL — Acetabulion, Posterior, Left Innominate: Position the hemisphere within the acetabulum so that the anterior extremity of one of the hemisphere diameter lines is opposite acetabulion anterior. Mark the point on the acetabular rim closest to the posterior diameter line when the innominate is held in the anatomical position.

ACETAL — Acetabulion, Anterior, Left Innominate: The most anteriorly projecting point defined on the pubic portion of the acetabular rim. It is found by rotating the innominate in the osteometric board from position 1 to position 2 (Reynolds, Snow, and Young, 1981).

ACETSL — Acetabulion, Superior, Left Innominate: Position the hemisphere within the acetabulum so that the anterior extremity of one of the diameter lines is opposite acetabulion anterior. Mark the point on the acetabular rim closest to the superior diameter line when the innominate is held in the antomical position.

ACETCL — Acetabulion, Center Point, Left Innominate: Position the hemisphere within the acetabulum so that the anterior extremity of one of the hemisphere diameter lines is opposite acetabulion anterior. Insert marker through H-point hole in the hemisphere and mark the contact point of the interior surface of the acetabulum.

ACETHL H-Point, Left Innominate: Choose a plexiglass hemisphere which best fits the acetabulum of the right innominate. Position the hemisphere so that the anterior extremity of one of the perpendicular diameter lines is opposite acetabulion anterior. H-point is the center point of the hemispheric surface.

ISHALL Ischiale, Left Innominate: The right innominate rests on its medial surface with the iliac blade and pubic symphysis in contact with the horizontal surface of an osteometric board. Move the bone into the right angle corner of the board in such a way that the superior border of the iliac crest is in contact with one of the vertical plates, and the anterior border of the iliac crest and the pubic bone are in contact with the second vertical plate of the osteometric board. Ischiale is defined as the highest point on the ischial tuberosity from the surface of the osteometric board.

PUBISL Inferior Symphyseal Pole, Left Innominate: This point is found at the most inferior point on the margin of the symphyseal surface.

PUBSSL Superior Symphyseal Point, Left Innominate: This point is found at the most superior point on the margin of the symphyseal surface.

PUBTBL Pubotubercle, Left Innominate: This point is found at the anterior most projecting point of the summit of the pubic tubercle when the innominate is held in the anatomical position.

CINLPT Pubic Tubercle in Cadaver, Left Innominate: Same as description above, target implanted while cadaver is intact.

SCNOTL Apex of Sciatic Notch, Left Innominate: The point on the sciatic notch border at the greatest perpendicular distance from an imaginary line between posterior-inferior iliospinale and ischial spinale (left innominate).

BOTUBL Bouisson Tubercle, Left Innominate: The most prominent point on the tubercle of Bouisson found at the apex of the tubercle formed by the origin of m. piriformis (left innominate).

IPOLLI Inferior Pole: A point on the inferior margin which lies on a line bisecting the inferior pole of the left sacroiliac joint.

ILAMLI Inferior Lobe, Anterior Margin, Left Innominate: A point along the anterior margin of the inferior lobe of the sacroiliac joint surface that lies on a perpendicular line

bisecting the line between the sacroiliac midpoint and the inferior pole.

ILPMLT Inferior Lobe, Posterior Margin, Left Innominate: A point along the posterior margin of the inferior lobe that lies on a perpendicular line bisecting the line between the sacroiliac midpoint and the inferior pole.

SLSMLI Superior Lobe, Superior Margin Midpoint, Left Innominate: A point along the superior margin of the superior pole of the left sacroiliac joint surface that lies on a perpendicular line that bisects the line passing between the sacroiliac midpoint and superior pole.

SPOLLI Superior Pole, Left Innominate: A point on the posterior margin of the sacroiliac joint surface that lies on a line bisecting the superior pole of the joint surface (left innominate).

PIISL Posterior Inferior Iliospinale, Left Innominate: The most projecting point on the posterior auricular margin, left innominate.

PSISL Posterior Superior Iliospinale, Left Innominte: The right innominate rests on its medial surface with the iliac blade and pubic symphysis in contact with the horizontal surface of an osteometric board. Move the bone into the right angle corner of the board in such a way that the superior border of the iliac crest is in contact with one of the vertical plates and the anterior border of the iliac crest and the pubic bone are in contact with the second vertical plate of the osteometric board. Posterior superior iliospinale, the posterior superior iliac spine, is defined as the point along the posterior border of the iliac crest in contact with a moveable vertical plate oriented at right angles to the vertical plates of the osteometric board. In cases where a considerable area is in contact, the landmark is taken as the midpoint of the contact area.

CINLPS Posterior Superior Iliospinale in Cadaver: Same as description above, target implanted while cadaver is intact.

ILCRSL Iliocristale, Summum, Left Innominate: The left innominate rests on its medial surface with the iliac blade and pubic symphysis in contact with the horizontal surface of an osteometric board. Move the bone into the right angle corner of the board in such a way that the superior border of the iliac crest is in contact with one of the vertical plates and the anterior border of the iliac crest and the pubic bone are in contact with the second vertical plate of the osteometric board. Iliocristale summum is defined as the point along the superior border of the iliac crest in contact with the vertical plate. In cases where a consider-

able area is in contact, the landmark is taken as the midpoint of the contact area.

ASISL — Left Iliospinale, Summum: The left innominate rests on its medial surface with the iliac blade and pubic symphysis in contact with the horizontal surface of an osteometric board. Move the bone into the right angle corner of the board in such a way that the superior border of the iliac crest is in contact with one of the vertical plates and the anterior border of the iliac crest and the pubic bone are in contact wit the second vertical plate of the osteometric board. Iliospinale summum, the anterior superior iliac spine, is defined as the point along the anterior border of the iliac crest in contact with the vertical plate. In cases where a considerable area is in contact, the landmark is taken as the midpoint of the contact area.

CINLAS — Anterior Superior Iliospinale in Cadaver: Same as description above, target implanted while cadaver is intact.

ILSCML — Sacroiliac Midpoint, Left Innominate: The point that lies at the intersect of the lines which bisect the superior and inferior poles of the left innominate's sacroiliac joint.

SYMPTL — Symphyseal Midpoint, Left Innominate: This point is the midpoint of the margin of the symphyseal surface of the left innominate.

7.2 APPENDIX B: COORDINATE DATA FOR SUBJECT #18 IN INERTIAL FRAME

The complete data for subject #18 are presented in the laboratory frame of reference described in Section 3.1.1.1. The following list includes both Bones and Motion data. The format by columns is as follows.

Column	Content
1-4	Subject ID
5-12	Position of Cadaver or Bones
13-16	Ignore (Internal Laboratory Code)
17-22	Target Name (See Appendix A)
23-29	X-coordinate (cm) in Inertial Frame
30-36	Y-coordinate (cm) in Inertial Frame
37-43	Z-coordinate (cm) in Inertial Frame
44-53	Film ID
54-56	Initials of person digitizing film

0018BONES	9401CL01L1	9.313	14.830	27.1380403820102LJB
0018BONES	9401CL01R1	8.195	13.101	25.9970403820102LJB
0018BONES	9401CL01SM	6.202	14.702	27.9540403820102LJB
0018BONES	9401CL01TR	10.359	13.017	26.1610403820102LJB
0018BONES	9401CL02L1	8.536	5.658	25.5020403820102LJB
0018BONES	9401CL02SM	5.915	4.986	28.1670403820102LJB
0018BONES	9401CL02TL	8.754	5.922	26.8290403820102LJB
0018BONES	9401CL03L1	7.093	20.641	43.6660403820102LJB
0018BONES	9401CL03R1	8.083	14.480	43.1240403820102LJB
0018BONES	9401CL03S1	4.354	18.587	42.0000403820102LJB
0018BONES	9401CL03SM	4.333	18.606	42.2190403820102LJB
0018BONES	9401CL03TL	8.023	20.711	41.8320403820102LJB
0018BONES	9401CL04R1	7.973	3.771	42.7510403820102LJB
0018BONES	9401CL04SM	4.228	6.474	40.8610403820102LJB
0018BONES	9401CL04TL	7.598	8.515	40.3310403820102LJB
0018BONES	9401CL04TR	7.010	4.122	43.0400403820102LJB
0018BONES	9401CT12L1	9.203	23.040	27.1110403820102LJB
0018BONES	9401CT12S1	9.155	22.849	26.9960403820102LJB
0018BONES	9401CT12SM	9.322	22.359	27.1540403820102LJB
0018BONES	9401CT12TL	6.653	21.895	27.6410403820102LJB
0018BONES	9401GLROD1	81.101	8.909	49.4460403820102LJB
0018BONES	9401GLROD2	45.800	8.877	49.4460403820102LJB
0018BONES	9401IFML1L	9.083	15.719	25.5470403820102LJB
0018BONES	9401IFML1R	9.136	13.020	25.5630403820102LJB
0018BONES	9401IFML2L	8.764	6.648	26.1930403820102LJB
0018BONES	9401IFML2R	8.868	3.452	25.9600403820102LJB
0018BONES	9401IFML3L	8.300	20.722	40.9840403820102LJB
0018BONES	9401IFML3R	8.175	17.255	41.0430403820102LJB
0018BONES	9401IFML4L	7.945	8.724	41.3550403820102LJB
0018BONES	9401IFML4R	7.825	3.544	41.1470403820102LJB
0018BONES	9401IFT12L	8.619	23.324	25.4880403820102LJB
0018BONES	9401IFT12R	8.748	20.962	25.5180403820102LJB
0018BONES	9401IL1APT	14.157	13.382	24.5370403820102LJB
0018BONES	9401IL1BLL	12.899	16.105	25.2710403820102LJB
0018BONES	9401IL1BLR	11.682	11.522	25.3210403820102LJB
0018BONES	9401IL2APT	14.012	4.560	24.6840403820102LJB
0018BONES	9401IL2BLL	12.221	7.065	25.1580403820102LJB
0018BONES	9401IL2BLR	12.204	2.300	25.4490403820102LJB
0018BONES	9401IL3APT	13.478	18.738	40.5840403820102LJB
0018BONES	9401IL3BLL	11.661	21.288	40.8460403820102LJB
0018BONES	9401IL3BLR	11.487	16.136	40.7630403820102LJB
0018BONES	9401IL4APT	12.871	6.436	40.5390403820102LJB
0018BONES	9401IL4BLL	10.680	9.124	40.7170403820102LJB
0018BONES	9401IL4BLR	10.669	3.955	40.8950403820102LJB
0018BONES	9401IT12AP	14.091	22.334	24.4440403820102LJB
0018BONES	9401IT12LL	12.038	24.432	25.0080403820102LJB
0018BONES	9401IT12LR	11.875	20.000	25.1940403820102LJB
0018BONES	9401QUBE01	61.878	6.133	57.9050403820102LJB
0018BONES	9401QUBE02	50.186	6.199	57.9730403820102LJB
0018BONES	9401QUBE03	61.844	21.351	57.9860403820102LJB
0018BONES	9401QUBE04	50.065	21.341	58.1980403820102LJB
0018BONES	9401QUBE05	62.089	6.258	48.5860403820102LJB
0018BONES	9401QUBE06	50.326	6.289	48.6260403820102LJB

0018BONES	9401QUBE06	50.336	6.292	48.6240403820102LJB
0018BONES	9401QUBE07	62.044	21.413	48.7170403820102LJB
0018BONES	9401QUBE08	50.398	21.429	48.8600403820102LJB
0018BONES	9401SFML1L	10.066	15.458	28.8230403820102LJB
0018BONES	9401SFML1R	9.571	13.080	28.7640403820102LJB
0018BONES	9401SFML2L	9.699	6.623	28.7120403820102LJB
0018BONES	9401SFML2R	9.420	3.665	29.0900403820102LJB
0018BONES	9401SFML3L	8.334	20.372	44.2300403820102LJB
0018BONES	9401SFML3R	8.090	17.118	43.8770403820102LJB
0018BONES	9401SFML4L	7.640	8.442	43.4660403820102LJB
0018BONES	9401SFML4R	7.956	4.931	43.3460403820102LJB
0018BONES	9401SFT12L	9.935	23.453	28.7360403820102LJB
0018BONES	9401SFT12R	10.269	20.863	28.9890403820102LJB
0018BONES	9401TPL1LT	10.002	18.189	28.0910403820102LJB
0018BONES	9401TPL1RT	8.865	10.291	28.4570403820102LJB
0018BONES	9401TPL2LT	9.223	9.495	27.9380403820102LJB
0018BONES	9401TPL2RT	9.106	0.801	28.4920403820102LJB
0018BONES	9401TPL3LT	8.024	23.622	44.0070403820102LJB
0018BONES	9401TPL3RT	7.771	13.884	43.4230403820102LJB
0018BONES	9401TPL4LT	8.479	10.974	43.4730403820102LJB
0018BONES	9401TPL4RT	8.380	2.017	43.2430403820102LJB
0018BONES	9401TPT12L	9.076	24.687	27.5910403820102LJB
0018BONES	9401TPT12R	9.484	19.785	27.7070403820102LJB
0018BONES	9401WIRE02	0.046	-0.002	30.4580403820102LJB
0018BONES	9401WIRE03	0.036	0.006	60.9800403820102LJB
0018BONES	9401WIRE08	0.016	30.533	30.4160403820102LJB
0018BONES	9401WIRE09	0.035	30.518	60.9460403820102LJB
0018BONES	9702CINRAS	16.954	8.082	24.7340203820304LJB
0018BONES	9702CINRPS	10.559	3.059	28.2190203820304LJB
0018BONES	9702CINRPT	17.322	22.122	29.1020203820304LJB
0018BONES	9702CSACLT	8.898	9.702	49.1440203820304LJB
0018BONES	9702CSACRT	9.509	14.982	49.3560203820304LJB
0018BONES	9702CSACS1	9.672	12.756	51.7330203820304LJB
0018BONES	9702CSACSM	8.891	12.137	52.0230203820304LJB
0018BONES	9702GLROD1	81.076	8.880	49.4230203820304LJB
0018BONES	9702GLROD2	45.792	8.853	49.4230203820304LJB
0018BONES	9702ILSCMR	9.749	12.024	31.6120203820304LJB
0018BONES	9702ISHALR	6.340	23.505	25.0110203820304LJB
0018BONES	9702PROMO	3.833	12.884	52.7260203820304LJB
0018BONES	9702PSISR	4.994	12.656	34.8990203820304LJB
0018BONES	9702PUBTBR	17.682	21.956	28.2150203820304LJB
0018BONES	9702QUBE01	61.851	6.113	57.8840203820304LJB
0018BONES	9702QUBE02	50.143	6.172	57.9830203820304LJB
0018BONES	9702QUBE03	61.834	21.319	57.9540203820304LJB
0018BONES	9702QUBE04	50.177	21.297	58.0570203820304LJB
0018BONES	9702QUBE05	62.075	6.232	48.5560203820304LJB
0018BONES	9702QUBE06	50.304	6.265	48.6020203820304LJB
0018BONES	9702QUBE07	62.023	21.384	48.6840203820304LJB
0018BONES	9702QUBE08	50.383	21.400	48.8190203820304LJB
0018BONES	9702SACBLL	5.850	9.781	53.2380203820304LJB
0018BONES	9702SACBLR	5.789	15.550	53.4610203820304LJB
0018BONES	9702SACMPL	5.800	7.660	49.0230203820304LJB
0018BONES	9702SACMPR	6.078	18.139	48.8490203820304LJB
0018BONES	9702SAFMPL	8.420	10.508	53.4280203820304LJB

```
0018BONES     9702SAFMPR  8.504 15.501 53.5240203820304LJB
0018BONES     9702SYMPTR 15.807 23.433 30.3960203820304LJB
0018BONES     9702WIRE02  0.055  0.003 30.4530203820304LJB
0018BONES     9702WIRE03  0.058  0.011 60.9710203820304LJB
0018BONES     9702WIRE08  0.045 30.524 30.4140203820304LJB
0018BONES     9702WIRE09  0.070 30.523 60.9330203820304LJB
0018LBARS3.09601CC07L1 25.195 12.947 76.0100110811213LJB
0018LBARS3.09601CC07R1 26.292 11.234 76.0970110811213LJB
0018LBARS3.09601CC07S1 23.710 12.756 75.4370110811213LJB
0018LBARS3.09601CC07SM 24.204 12.506 75.9710110811213LJB
0018LBARS3.09601CC07TL 26.318 13.518 77.9950110811213LJB
0018LBARS3.09601CC07TR 26.723 11.491 76.2870110811213LJB
0018LBARS3.09601CINLAS 42.157 28.157 28.1240110811213LJB
0018LBARS3.09601CINLPS 34.005 25.852 30.8950110811213LJB
0018LBARS3.09601CINLPT 44.559 16.850 18.5540110811213LJB
0018LBARS3.09601CINRAS 43.505  2.430 28.5040110811213LJB
0018LBARS3.09601CINRPS 35.754  2.279 33.2920110811213LJB
0018LBARS3.09601CINRPT 44.347 13.170 18.2790110811213LJB
0018LBARS3.09601CL01L1 28.852 15.752 40.2280110811213LJB
0018LBARS3.09601CL01R1 29.441 13.661 38.8810110811213LJB
0018LBARS3.09601CL01S1 27.449 14.717 37.5880110811213LJB
0018LBARS3.09601CL01SM 26.286 14.819 38.7440110811213LJB
0018LBARS3.09601CL01TL 28.989 15.740 40.4360110811213LJB
0018LBARS3.09601CL01TR 31.111 14.133 40.8930110811213LJB
0018LBARS3.09601CL02L1 30.968 15.539 35.8150110811213LJB
0018LBARS3.09601CL02S1 27.340 14.780 35.9740110811213LJB
0018LBARS3.09601CL02SM 27.415 14.245 35.9130110811213LJB
0018LBARS3.09601CL02TL 30.296 16.070 36.7650110811213LJB
0018LBARS3.09601CL03L1 31.092 16.161 33.6240110811213LJB
0018LBARS3.09601CL03R1 31.621 10.911 35.3750110811213LJB
0018LBARS3.09601CL03S1 28.087 14.454 32.6730110811213LJB
0018LBARS3.09601CL03SM 28.192 14.357 32.8430110811213LJB
0018LBARS3.09601CL03TL 31.838 16.438 32.0610110811213LJB
0018LBARS3.09601CL04L1 31.913 15.560 30.0010110811213LJB
0018LBARS3.09601CL04R1 32.677 12.504 32.7770110811213LJB
0018LBARS3.09601CL04S1 28.323 14.676 29.8470110811213LJB
0018LBARS3.09601CL04SM 28.802 14.754 30.2440110811213LJB
0018LBARS3.09601CL04TL 32.196 16.167 29.6810110811213LJB
0018LBARS3.09601CL05R1 32.869 12.540 30.1100110811213LJB
0018LBARS3.09601CL05TR 33.150 13.114 31.3930110811213LJB
0018LBARS3.09601CSACL1 29.453 16.399 19.8740110811213LJB
0018LBARS3.09601CSACLT 29.870 17.013 22.6970110811213LJB
0018LBARS3.09601CSACR1 30.730 13.607 18.8630110811213LJB
0018LBARS3.09601CSACRT 30.297 11.747 23.3750110811213LJB
0018LBARS3.09601CSACS1 29.052 13.910 24.8150110811213LJB
0018LBARS3.09601CSACSM 28.941 14.614 25.5740110811213LJB
0018LBARS3.09601CT01L1 23.963 13.636 74.0440110811213LJB
0018LBARS3.09601CT01R1 26.616 10.695 74.1520110811213LJB
0018LBARS3.09601CT01S1 22.346 13.203 74.1020110811213LJB
0018LBARS3.09601CT01SM 23.092 12.738 74.2710110811213LJB
0018LBARS3.09601CT01TL 25.698 13.993 74.7270110811213LJB
0018LBARS3.09601CT01TR 25.916 10.847 74.2320110811213LJB
0018LBARS3.09601CT04L1 23.215 15.286 67.9050110811213LJB
0018LBARS3.09601CT04R1 23.819 10.387 68.2500110811213LJB
```

0018LBARS3.09601CT04S1	20.905	13.785	67.7740110811213LJB
0018LBARS3.09601CT04SM	20.874	13.885	68.0940110811213LJB
0018LBARS3.09601CT04TL	24.091	14.924	70.2110110811213LJB
0018LBARS3.09601CT04TR	23.549	10.300	68.7340110811213LJB
0018LBARS3.09601CT08L1	22.357	15.278	55.2590110811213LJB
0018LBARS3.09601CT08R1	21.634	11.266	55.8590110811213LJB
0018LBARS3.09601CT08S1	20.121	14.715	55.0830110811213LJB
0018LBARS3.09601CT08SM	20.196	14.402	55.5240110811213LJB
0018LBARS3.09601CT08TL	21.851	16.470	56.0830110811213LJB
0018LBARS3.09601CT08TR	22.646	13.566	55.7690110811213LJB
0018LBARS3.09601CT11L1	24.985	16.484	46.2580110811213LJB
0018LBARS3.09601CT11R1	25.851	13.608	45.1760110811213LJB
0018LBARS3.09601CT11S1	24.147	15.014	44.8230110811213LJB
0018LBARS3.09601CT11SM	23.745	15.015	44.9300110811213LJB
0018LBARS3.09601CT11TL	26.126	16.706	46.5130110811213LJB
0018LBARS3.09601CT11TR	26.360	13.847	45.1570110811213LJB
0018LBARS3.09601CT12L1	27.126	15.499	43.4490110811213LJB
0018LBARS3.09601CT12R1	27.800	13.804	42.5050110811213LJB
0018LBARS3.09601CT12S1	25.424	14.631	41.2930110811213LJB
0018LBARS3.09601CT12SM	25.247	14.950	41.7230110811213LJB
0018LBARS3.09601CT12TL	27.250	15.871	43.4620110811213LJB
0018LBARS3.09601CT12TR	29.323	13.866	43.6080110811213LJB
0018LBARS3.09601GLROD1	82.207	8.711	50.5180110811213LJB
0018LBARS3.09601GLROD2	46.640	8.673	50.5180110811213LJB
0018LBARS3.09601PLXSLB	25.579	16.338	30.6120110811213LJB
0018LBARS3.09601PLXSLT	26.341	16.829	35.4000110811213LJB
0018LBARS3.09601PLXSRB	26.818	10.397	31.1680110811213LJB
0018LBARS3.09601PLXSRT	27.752	10.848	36.0190110811213LJB
0018LBARS3.09601QUBE01	61.949	5.107	59.2640110811213LJB
0018LBARS3.09601QUBE02	50.236	5.032	59.1710110811213LJB
0018LBARS3.09601QUBE03	61.599	20.229	59.2260110811213LJB
0018LBARS3.09601QUBE04	49.855	20.255	59.1550110811213LJB
0018LBARS3.09601QUBE05	61.938	5.027	50.0610110811213LJB
0018LBARS3.09601QUBE06	50.295	5.004	49.9170110811213LJB
0018LBARS3.09601QUBE07	61.659	20.184	49.8770110811213LJB
0018LBARS3.09601QUBE08	49.847	20.172	49.8400110811213LJB
0018LBARS3.09601STGSRP	30.228	13.215	10.3070110811213LJB
0018LBARS3.09601STGT02	22.163	2.095	42.8440110811213LJB
0018LBARS3.09601STGT03	19.180	5.927	53.7580110811213LJB
0018LBARS3.09601STGT06	26.306	27.939	24.2050110811213LJB
0018LBARS3.09601STGT07	20.854	25.334	44.8770110811213LJB
0018LBARS3.09601STGT08	17.781	28.941	56.4360110811213LJB
0018LBARS3.09601STGT13	19.192	4.897	54.0500110811213LJB
0018LBARS3.09601STGT16	26.307	27.293	24.0940110811213LJB
0018LBARS3.09601STGT17	20.740	24.702	45.5270110811213LJB
0018LBARS3.09601STGT18	17.748	28.392	56.8160110811213LJB
0018LBARS3.09601WIRE02	0.138	0.011	30.4600110811213LJB
0018LBARS3.09601WIRE03	0.070	0.007	60.9770110811213LJB
0018LBARS3.09601WIRE08	0.126	30.504	30.4130110811213LJB
0018LBARS3.09601WIRE09	0.093	30.516	60.9300110811213LJB
0018LBARS3.59701CC07L1	25.119	12.995	76.0220110811011LJB
0018LBARS3.59701CC07R1	26.223	11.294	76.1040110811011LJB
0018LBARS3.59701CC07S1	23.645	12.804	75.4540110811011LJB
0018LBARS3.59701CC07SM	24.093	12.552	75.9790110811011LJB

0018LBARS3.59701CC07TL	26.258	13.566	78.0070110811011LJB
0018LBARS3.59701CC07TR	26.679	11.552	76.2910110811011LJB
0018LBARS3.59701CINLAS	42.143	28.201	28.0780110811011LJB
0018LBARS3.59701CINLPS	34.081	25.884	30.9090110811011LJB
0018LBARS3.59701CINLPT	44.528	16.874	18.5030110811011LJB
0018LBARS3.59701CINRAS	43.573	2.472	28.4910110811011LJB
0018LBARS3.59701CINRPS	35.872	2.313	33.3290110811011LJB
0018LBARS3.59701CINRPT	44.333	13.195	18.2360110811011LJB
0018LBARS3.59701CL01L1	29.024	15.802	40.2710110811011LJB
0018LBARS3.59701CL01R1	29.555	13.712	38.9200110811011LJB
0018LBARS3.59701CL01S1	27.569	14.756	37.6320110811011LJB
0018LBARS3.59701CL01SM	26.392	14.858	38.7780110811011LJB
0018LBARS3.59701CL01TL	29.091	15.798	40.4550110811011LJB
0018LBARS3.59701CL01TR	31.234	14.187	40.9260110811011LJB
0018LBARS3.59701CL02L1	31.067	15.583	35.8590110811011LJB
0018LBARS3.59701CL02S1	27.517	14.806	36.0330110811011LJB
0018LBARS3.59701CL02SM	27.550	14.288	35.9740110811011LJB
0018LBARS3.59701CL02TL	30.390	16.107	36.7910110811011LJB
0018LBARS3.59701CL03L1	31.252	16.189	33.6590110811011LJB
0018LBARS3.59701CL03R1	32.088	10.962	35.5320110811011LJB
0018LBARS3.59701CL03S1	28.317	14.504	32.7510110811011LJB
0018LBARS3.59701CL03SM	28.322	14.398	32.8930110811011LJB
0018LBARS3.59701CL03TL	31.990	16.460	32.0940110811011LJB
0018LBARS3.59701CL04L1	32.066	15.590	30.0500110811011LJB
0018LBARS3.59701CL04S1	28.407	14.705	29.9160110811011LJB
0018LBARS3.59701CL04SM	28.939	14.790	30.3040110811011LJB
0018LBARS3.59701CL04TL	32.218	16.196	29.7090110811011LJB
0018LBARS3.59701CL05R1	32.929	12.556	30.1290110811011LJB
0018LBARS3.59701CL05TR	33.280	13.149	31.4310110811011LJB
0018LBARS3.59701CSACL1	29.516	16.425	19.9390110811011LJB
0018LBARS3.59701CSACLT	29.931	17.037	22.7510110811011LJB
0018LBARS3.59701CSACR1	30.764	13.626	18.9140110811011LJB
0018LBARS3.59701CSACRT	30.347	11.775	23.4270110811011LJB
0018LBARS3.59701CSACS1	29.163	13.933	24.8700110811011LJB
0018LBARS3.59701CSACSM	29.003	14.639	25.6280110811011LJB
0018LBARS3.59701CT01L1	23.902	13.682	74.0410110811011LJB
0018LBARS3.59701CT01R1	26.559	10.750	74.1570110811011LJB
0018LBARS3.59701CT01S1	22.252	13.254	74.1100110811011LJB
0018LBARS3.59701CT01SM	23.007	12.792	74.2830110811011LJB
0018LBARS3.59701CT01TL	25.662	14.049	74.7320110811011LJB
0018LBARS3.59701CT01TR	25.866	10.897	74.2350110811011LJB
0018LBARS3.59701CT04L1	23.121	15.333	67.8900110811011LJB
0018LBARS3.59701CT04R1	23.721	10.438	68.2450110811011LJB
0018LBARS3.59701CT04S1	20.836	13.833	67.7500110811011LJB
0018LBARS3.59701CT04SM	20.782	13.937	68.0610110811011LJB
0018LBARS3.59701CT04TL	24.002	14.970	70.2010110811011LJB
0018LBARS3.59701CT04TR	23.487	10.349	68.7260110811011LJB
0018LBARS3.59701CT08L1	22.348	15.331	55.2100110811011LJB
0018LBARS3.59701CT08R1	21.618	11.314	55.8020110811011LJB
0018LBARS3.59701CT08S1	20.073	14.759	55.0330110811011LJB
0018LBARS3.59701CT08SM	20.167	14.460	55.4810110811011LJB
0018LBARS3.59701CT08TL	21.823	16.514	56.0340110811011LJB
0018LBARS3.59701CT08TR	22.624	13.629	55.7230110811011LJB
0018LBARS3.59701CT11L1	25.063	16.539	46.2560110811011LJB

0018LBARS3.59701CT11R1	26.037	13.658	45.1940110811011LJB
0018LBARS3.59701CT11S1	24.258	15.066	44.8120110811011LJB
0018LBARS3.59701CT11SM	23.817	15.071	44.9190110811011LJB
0018LBARS3.59701CT11TL	26.211	16.760	46.5210110811011LJB
0018LBARS3.59701CT11TR	26.464	13.903	45.1530110811011LJB
0018LBARS3.59701CT12L1	27.285	15.552	43.4740110811011LJB
0018LBARS3.59701CT12R1	27.880	13.835	42.5240110811011LJB
0018LBARS3.59701CT12S1	25.595	14.674	41.3150110811011LJB
0018LBARS3.59701CT12SM	25.370	14.997	41.7330110811011LJB
0018LBARS3.59701CT12TL	27.345	15.923	43.4720110811011LJB
0018LBARS3.59701CT12TR	29.434	13.917	43.6320110811011LJB
0018LBARS3.59701GLROD1	82.184	8.698	50.5070110811011LJB
0018LBARS3.59701GLROD2	46.632	8.664	50.5070110811011LJB
0018LBARS3.59701PLXSLB	25.740	16.114	30.9810110811011LJB
0018LBARS3.59701PLXSLT	26.072	16.740	35.7830110811011LJB
0018LBARS3.59701PLXSRB	27.424	10.298	31.6950110811011LJB
0018LBARS3.59701PLXSRT	27.621	10.846	36.4590110811011LJB
0018LBARS3.59701QUBE01	61.929	5.088	59.2580110811011LJB
0018LBARS3.59701QUBE02	50.241	5.024	59.1690110811011LJB
0018LBARS3.59701QUBE03	61.547	20.222	59.2250110811011LJB
0018LBARS3.59701QUBE04	49.820	20.249	59.1450110811011LJB
0018LBARS3.59701QUBE05	61.914	5.013	50.0560110811011LJB
0018LBARS3.59701QUBE06	50.283	4.993	49.9110110811011LJB
0018LBARS3.59701QUBE07	61.642	20.173	49.8680110811011LJB
0018LBARS3.59701QUBE08	49.825	20.169	49.8370110811011LJB
0018LBARS3.59701STGSRP	30.207	13.204	10.3060110811011LJB
0018LBARS3.59701STGT02	22.108	2.096	42.8430110811011LJB
0018LBARS3.59701STGT03	19.123	5.921	53.7580110811011LJB
0018LBARS3.59701STGT06	26.240	27.936	24.1970110811011LJB
0018LBARS3.59701STGT07	20.762	25.333	44.8650110811011LJB
0018LBARS3.59701STGT08	17.704	28.941	56.4280110811011LJB
0018LBARS3.59701STGT13	19.143	4.888	54.0450110811011LJB
0018LBARS3.59701STGT16	26.272	27.292	24.0830110811011LJB
0018LBARS3.59701STGT17	20.678	24.710	45.5220110811011LJB
0018LBARS3.59701STGT18	17.641	28.390	56.8070110811011LJB
0018LBARS3.59701WIRE02	0.087	0.006	30.4610110811011LJB
0018LBARS3.59701WIRE03	0.049	0.005	60.9780110811011LJB
0018LBARS3.59701WIRE08	0.082	30.508	30.3990110811011LJB
0018LBARS3.59701WIRE09	-0.049	30.528	60.9250110811011LJB
0018LBARS4.09701CC07L1	25.001	13.061	76.0640110810809LJB
0018LBARS4.09701CC07R1	26.016	11.357	76.1440110810809LJB
0018LBARS4.09701CC07S1	23.480	12.878	75.4920110810809LJB
0018LBARS4.09701CC07SM	24.021	12.618	76.0210110810809LJB
0018LBARS4.09701CC07TL	26.119	13.637	78.0540110810809LJB
0018LBARS4.09701CC07TR	26.539	11.615	76.3330110810809LJB
0018LBARS4.09701CINLAS	42.253	28.248	28.0430110810809LJB
0018LBARS4.09701CINLPS	34.152	25.941	30.9290110810809LJB
0018LBARS4.09701CINLPT	44.565	16.921	18.4630110810809LJB
0018LBARS4.09701CINRAS	43.703	2.520	28.4690110810809LJB
0018LBARS4.09701CINRPS	36.004	2.360	33.3580110810809LJB
0018LBARS4.09701CINRPT	44.351	13.237	18.2010110810809LJB
0018LBARS4.09701CL01L1	29.091	15.885	40.2970110810809LJB
0018LBARS4.09701CL01R1	29.630	13.776	38.9640110810809LJB
0018LBARS4.09701CL01S1	27.681	14.815	37.6760110810809LJB

0018LBARS4.09701CL01SM	26.497	14.924	38.8260110810809LJB
0018LBARS4.09701CL01TL	29.190	15.872	40.5170110810809LJB
0018LBARS4.09701CL01TR	31.335	14.267	40.9670110810809LJB
0018LBARS4.09701CL02L1	31.179	15.637	35.9050110810809LJB
0018LBARS4.09701CL02S1	27.582	14.867	36.0940110810809LJB
0018LBARS4.09701CL02SM	27.611	14.343	36.0420110810809LJB
0018LBARS4.09701CL02TL	30.525	16.173	36.8230110810809LJB
0018LBARS4.09701CL03L1	31.309	16.247	33.7120110810809LJB
0018LBARS4.09701CL03R1	32.176	11.020	35.5820110810809LJB
0018LBARS4.09701CL03S1	28.363	14.547	32.7920110810809LJB
0018LBARS4.09701CL03SM	28.396	14.432	32.9570110810809LJB
0018LBARS4.09701CL03TL	32.032	16.516	32.1480110810809LJB
0018LBARS4.09701CL04L1	32.099	15.637	30.0850110810809LJB
0018LBARS4.09701CL04R1	32.901	12.587	32.8590110810809LJB
0018LBARS4.09701CL04S1	28.463	14.742	29.9850110810809LJB
0018LBARS4.09701CL04SM	28.977	14.835	30.3620110810809LJB
0018LBARS4.09701CL04TL	32.231	16.243	29.7580110810809LJB
0018LBARS4.09701CL05R1	32.976	12.607	30.1640110810809LJB
0018LBARS4.09701CL05TR	33.341	13.264	31.4670110810809LJB
0018LBARS4.09701CSACL1	29.459	16.461	19.9790110810809LJB
0018LBARS4.09701CSACLT	29.916	17.074	22.8050110810809LJB
0018LBARS4.09701CSACR1	30.753	13.662	18.9650110810809LJB
0018LBARS4.09701CSACRT	30.328	11.809	23.4820110810809LJB
0018LBARS4.09701CSACS1	29.153	13.972	24.9280110810809LJB
0018LBARS4.09701CSACSM	29.021	14.684	25.6960110810809LJB
0018LBARS4.09701CT01L1	23.775	13.751	74.0700110810809LJB
0018LBARS4.09701CT01R1	26.433	10.814	74.1980110810809LJB
0018LBARS4.09701CT01S1	22.136	13.315	74.1450110810809LJB
0018LBARS4.09701CT01SM	22.867	12.858	74.3120110810809LJB
0018LBARS4.09701CT01TL	25.529	14.116	74.7760110810809LJB
0018LBARS4.09701CT01TR	25.704	10.967	74.2730110810809LJB
0018LBARS4.09701CT04L1	23.082	15.398	67.8890110810809LJB
0018LBARS4.09701CT04R1	23.667	10.500	68.2470110810809LJB
0018LBARS4.09701CT04S1	20.775	13.903	67.7330110810809LJB
0018LBARS4.09701CT04SM	20.734	14.003	68.0440110810809LJB
0018LBARS4.09701CT04TL	23.904	15.039	70.2170110810809LJB
0018LBARS4.09701CT04TR	23.409	10.414	68.7250110810809LJB
0018LBARS4.09701CT08L1	22.432	15.411	55.1620110810809LJB
0018LBARS4.09701CT08R1	21.668	11.377	55.7480110810809LJB
0018LBARS4.09701CT08S1	20.129	14.820	54.9860110810809LJB
0018LBARS4.09701CT08SM	20.232	14.533	55.4370110810809LJB
0018LBARS4.09701CT08TL	21.907	16.587	55.9850110810809LJB
0018LBARS4.09701CT08TR	22.671	13.705	55.6860110810809LJB
0018LBARS4.09701CT11L1	25.196	16.615	46.2750110810809LJB
0013LBARS4.09701CT11R1	26.131	13.738	45.2180110810809LJB
0018LBARS4.09701CT11S1	24.377	15.140	44.8120110810809LJB
0018LBARS4.09701CT11SM	23.949	15.148	44.9130110810809LJB
0018LBARS4.09701CT11TL	26.353	16.839	46.5400110810809LJB
0018LBARS4.09701CT11TR	26.573	13.990	45.1740110810809LJB
0018LBARS4.09701CT12L1	27.342	15.629	43.4990110810809LJB
0018LBARS4.09701CT12R1	28.045	13.930	42.5870110810809LJB
0018LBARS4.09701CT12S1	25.726	14.743	41.3480110810809LJB
0018LBARS4.09701CT12SM	25.403	15.062	41.7520110810809LJB
0018LBARS4.09701CT12TL	27.459	16.001	43.5090110810809LJB

0018LBARS4.09701CT12TR	29.518	14.003	43.6720110810809LJB
0018LBARS4.09701GLROD1	82.180	8.697	50.5200110810809LJB
0018LBARS4.09701GLROD2	46.626	8.666	50.5200110810809LJB
0018LBARS4.09701PLXSLB	26.192	16.150	31.0680110810809LJB
0018LBARS4.09701PLXSLT	26.110	16.741	35.9170110810809LJB
0018LBARS4.09701PLXSRB	27.869	10.323	31.9230110810809LJB
0018LBARS4.09701PLXSRT	27.647	10.857	36.6930110810809LJB
0018LBARS4.09701QUBE01	61.946	5.085	59.2640110810809LJB
0018LBARS4.09701QUBE02	50.237	5.020	59.1760110810809LJB
0018LBARS4.09701QUBE03	61.534	20.220	59.2410110810809LJB
0018LBARS4.09701QUBE04	49.817	20.246	59.1660110810809LJB
0018LBARS4.09701QUBE05	61.923	5.014	50.0630110810809LJB
0018LBARS4.09701QUBE06	50.278	4.992	49.9190110810809LJB
0018LBARS4.09701QUBE07	61.609	20.174	49.8830110810809LJB
0018LBARS4.09701QUBE08	49.808	20.165	49.8510110810809LJB
0018LBARS4.09701STGSRF	30.176	13.207	10.3030110810809LJB
0018LBARS4.09701STGT02	22.131	2.092	42.8480110810809LJB
0018LBARS4.09701STGT03	19.106	5.920	53.7660110810809LJB
0018LBARS4.09701STGT06	26.196	27.936	24.2030110810809LJB
0018LBARS4.09701STGT07	20.746	25.335	44.8830110810809LJB
0018LBARS4.09701STGT08	17.703	28.934	56.4560110810809LJB
0018LBARS4.09701STGT13	19.126	4.884	54.0550110810809LJB
0018LBARS4.09701STGT16	26.215	27.302	24.0900110810809LJB
0018LBARS4.09701STGT17	20.654	24.710	45.5390110810809LJB
0018LBARS4.09701STGT18	17.614	28.390	56.8270110810809LJB
0018LBARS4.09701WIRE02	0.071	0.003	30.4600110810809LJB
0018LBARS4.09701WIRE03	0.038	0.006	60.9810110810809LJB
0018LBARS4.09701WIRE08	0.017	30.515	30.4170110810809LJB
0018LBARS4.09701WIRE09	-0.042	30.521	60.9440110810809LJB
0018LBARS4.59701CC07L1	24.960	13.200	76.0580110810607LJB
0018LBARS4.59701CC07R1	26.130	11.489	76.1330110810607LJB
0018LBARS4.59701CC07S1	23.506	13.003	75.4380110810607LJB
0018LBARS4.59701CC07SM	23.997	12.751	76.0240110810607LJB
0018LBARS4.59701CC07TL	26.107	13.761	78.0620110810607LJB
0018LBARS4.59701CC07TR	26.592	11.747	76.3150110810607LJB
0018LBARS4.59701CINLAS	42.473	28.365	27.9330110810607LJB
0018LBARS4.59701CINLPS	34.461	26.040	30.9500110810607LJB
0018LBARS4.59701CINLPT	44.654	17.016	18.3570110810607LJB
0018LBARS4.59701CINRAS	43.958	2.636	28.4180110810607LJB
0018LBARS4.59701CINRPS	36.361	2.468	33.4260110810607LJB
0018LBARS4.59701CINRPT	44.454	13.336	18.1050110810607LJB
0018LBARS4.59701CL01L1	29.587	16.011	40.3890110810607LJB
0018LBARS4.59701CL01R1	30.090	13.903	39.0490110810607LJB
0018LBARS4.59701CL01S1	28.127	14.933	37.7690110810607LJB
0018LBARS4.59701CL01SM	26.946	15.048	38.9120110810607LJB
0018LBARS4.59701CL01TL	29.642	15.990	40.5800110810607LJB
0018LBARS4.59701CL01TR	31.800	14.400	41.0520110810607LJB
0018LBARS4.59701CL02L1	31.537	15.756	35.9890110810607LJB
0018LBARS4.59701CL02S1	27.977	14.980	36.2060110810607LJB
0018LBARS4.59701CL02SM	28.042	14.453	36.1610110810607LJB
0018LBARS4.59701CL02TL	30.941	16.287	36.9090110810607LJB
0018LBARS4.59701CL03L1	31.644	16.356	33.7960110810607LJB
0018LBARS4.59701CL03R1	32.565	11.137	35.6870110810607LJB
0018LBARS4.59701CL03S1	28.692	14.631	32.9270110810607LJB

```
0018LBARS4.59701CL03SM 28.716 14.545 33.0710110810607_JB
0018LBARS4.59701CL03TL 32.429 16.613 32.2230110810607_JB
0018LBARS4.59701CL04L1 32.472 15.734 30.1780110810607_JB
0018LBARS4.59701CL04R1 33.282 12.691 32.9450110810607_JB
0018LBARS4.59701CL04S1 28.801 14.829 30.1310110810607_JB
0018LBARS4.59701CL04SM 29.342 14.926 30.4850110810607_JB
0018LBARS4.59701CL04TL 32.596 16.349 29.8350110810607_JB
0018LBARS4.59701CL05R1 33.288 12.701 30.2490110810607_JB
0018LBARS4.59701CL05TR 33.736 13.304 31.5480110810607_JB
0018LBARS4.59701CSACL1 29.639 16.530 20.1060110810607_JB
0018LBARS4.59701CSACLT 30.143 17.149 22.9220110810607_JB
0018LBARS4.59701CSACR1 30.913 13.726 19.0760110810607_JB
0018LBARS4.59701CSACRT 30.612 11.887 23.6130110810607_JB
0018LBARS4.59701CSACS1 29.435 14.049 25.0590110810607_JB
0018LBARS4.59701CSACSM 29.318 14.762 25.8300110810607_JB
0018LBARS4.59701CT01L1 23.781 13.873 74.0410110810607_JB
0018LBARS4.59701CT01R1 26.453 10.944 74.1760110810607_JB
0018LBARS4.59701CT01S1 22.146 13.432 74.1270110810607_JB
0018LBARS4.59701CT01SM 22.881 12.984 74.2960110810607_JB
0018LBARS4.59701CT01TL 25.487 14.245 74.7560110810607_JB
0018LBARS4.59701CT01TR 25.743 11.097 74.2420110810607_JB
0018LBARS4.59701CT04L1 23.064 15.517 67.8290110810607_JB
0018LBARS4.59701CT04R1 23.679 10.622 68.1970110810607_JB
0018LBARS4.59701CT04S1 20.749 14.019 67.6450110810607_JB
0018LBARS4.59701CT04SM 20.688 14.123 67.9530110810607_JB
0018LBARS4.59701CT04TL 23.868 15.162 70.1780110810607_JB
0018LBARS4.59701CT04TR 23.428 10.534 68.6690110810607_JB
0018LBARS4.59701CT08L1 22.636 15.545 55.0560110810607_JB
0018LBARS4.59701CT08R1 21.908 11.502 55.6510110810607_JB
0018LBARS4.59701CT08S1 20.358 14.932 54.8680110810607_JB
0018LBARS4.59701CT08SM 20.466 14.649 55.3170110810607_JB
0018LBARS4.59701CT08TL 22.111 16.703 55.8820110810607_JB
0018LBARS4.59701CT08TR 22.933 13.838 55.5790110810607_JB
0018LBARS4.59701CT11L1 25.630 16.752 46.2540110810607_JB
0018LBARS4.59701CT11R1 26.599 13.872 45.2400110810607_JB
0018LBARS4.59701CT11S1 24.854 15.280 44.7930110810607_JB
0018LBARS4.59701CT11SM 24.439 15.276 44.8830110810607_JB
0018LBARS4.59701CT11TL 26.794 16.984 46.5520110810607_JB
0018LBARS4.59701CT11TR 27.073 14.135 45.1940110810607_JB
0018LBARS4.59701CT12L1 27.844 15.769 43.5530110810607_JB
0018LBARS4.59701CT12R1 28.510 14.071 42.6540110810607_JB
0018LBARS4.59701CT12S1 26.193 14.865 41.3880110810607_JB
0018LBARS4.59701CT12SM 25.933 15.195 41.7930110810607_JB
0018LBARS4.59701CT12TL 27.920 16.142 43.5570110810607_JB
0018LBARS4.59701CT12TR 29.985 14.149 43.7410110810607_JB
0018LBARS4.59701GLROD1 82.197  8.709 50.5080110810607_JB
0018LBARS4.59701GLROD2 46.633  8.676 50.5080110810607_JB
0018LBARS4.59701PLXSLB 26.789 16.139 31.3690110810607_JB
0018LBARS4.59701PLXSLT 26.250 16.720 36.1790110810607_JB
0018LBARS4.59701PLXSRB 28.479 10.351 32.3380110810607_JB
0018LBARS4.59701PLXSRT 27.835 10.875 37.0700110810607_JB
0018LBARS4.59701QUBE01 61.939  5.104 59.2570110810607_JB
0018LBARS4.59701QUBE02 50.243  5.032 59.1660110810607_JB
0018LBARS4.59701QUBE03 61.583 20.234 59.2260110810607_JB
```

0018LBARS4.59701QUBE04	49.846	20.262	59.1510110810607LJB
0018LBARS4.59701QUBE05	61.933	5.031	50.0500110810607LJB
0018LBARS4.59701QUBE06	50.295	5.005	49.9050110810607LJB
0018LBARS4.59701QUBE07	61.655	20.185	49.8780110810607LJB
0018LBARS4.59701QUBE08	49.864	20.177	49.8390110810607LJB
0018LBARS4.59701STGSRP	30.188	13.218	10.2980110810607LJB
0018LBARS4.59701STGT02	22.140	2.105	42.8380110810607LJB
0018LBARS4.59701STGT03	19.141	5.919	53.7630110810607LJB
0018LBARS4.59701STGT06	26.296	27.942	24.2040110810607LJB
0018LBARS4.59701STGT07	20.793	25.341	44.8770110810607LJB
0018LBARS4.59701STGT08	17.744	28.948	56.4460110810607LJB
0018LBARS4.59701STGT13	19.147	4.889	54.0540110810607LJB
0018LBARS4.59701STGT16	26.291	27.308	24.0880110810607LJB
0018LBARS4.59701STGT17	20.716	24.710	45.5330110810607LJB
0018LBARS4.59701STGT18	17.702	28.392	56.8220110810607LJB
0018LBARS4.59701WIRE02	0.089	0.001	30.4500110810607LJB
0018LBARS4.59701WIRE03	0.048	0.005	60.9780110810607LJB
0018LBARS4.59701WIRE08	0.116	30.513	30.4100110810607LJB
0018LBARS4.59701WIRE09	0.009	30.523	60.9440110810607LJB
0018LBARS5.09701CC07L1	24.677	13.419	76.1390110810405LJB
0018LBARS5.09701CC07R1	25.763	11.714	76.2220110810405LJB
0018LBARS5.09701CC07S1	23.178	13.227	75.5670110810405LJB
0018LBARS5.09701CC07SM	23.728	12.981	76.1050110810405LJB
0018LBARS5.09701CC07TL	25.788	14.003	78.1490110810405LJB
0018LBARS5.09701CC07TR	26.235	11.981	76.4110110810405LJB
0018LBARS5.09701CINLAS	42.669	28.493	27.7980110810405LJB
0018LBARS5.09701CINLFS	34.708	26.144	30.9760110810405LJB
0018LBARS5.09701CINLPT	44.731	17.124	18.2230110810405LJB
0018LBARS5.09701CINRAS	44.290	2.767	28.3520110810405LJB
0018LBARS5.09701CINRPS	36.801	2.583	33.5050110810405LJB
0018LBARS5.09701CINRPT	44.548	13.444	17.9950110810405LJB
0018LBARS5.09701CL01L1	29.938	16.155	40.4730110810405LJB
0018LBARS5.09701CL01R1	30.474	14.028	39.1640110810405LJB
0018LBARS5.09701CL01S1	28.510	15.040	37.8930110810405LJB
0018LBARS5.09701CL01SM	27.308	15.159	39.0270110810405LJB
0018LBARS5.09701CL01TL	30.046	16.139	40.6850110810405LJB
0018LBARS5.09701CL01TR	32.182	14.554	41.1520110810405LJB
0018LBARS5.09701CL02L1	31.902	15.864	36.0940110810405LJB
0018LBARS5.09701CL02S1	28.338	15.068	36.3590110810405LJB
0018LBARS5.09701CL02SM	28.417	14.566	36.3120110810405LJB
0018LBARS5.09701CL02TL	31.263	16.413	37.0340110810405LJB
0018LBARS5.09701CL03L1	31.977	16.459	33.9010110810405LJB
0018LBARS5.09701CL03R1	33.118	11.404	35.8640110810405LJB
0018LBARS5.09701CL03S1	29.074	14.710	33.0680110810405LJB
0018LBARS5.09701CL03SM	28.932	14.624	33.1730110810405LJB
0018LBARS5.09701CL03TL	32.724	16.695	32.3150110810405LJB
0018LBARS5.09701CL04L1	32.757	15.831	30.2880110810405LJB
0018LBARS5.09701CL04R1	33.654	12.796	33.0500110810405LJB
0018LBARS5.09701CL04S1	29.086	14.892	30.3030110810405LJB
0018LBARS5.09701CL04SM	29.637	14.996	30.6280110810405LJB
0018LBARS5.09701CL04TL	32.901	16.440	29.9330110810405LJB
0018LBARS5.09701CL05R1	33.607	12.790	30.3400110810405LJB
0018LBARS5.09701CL05TR	33.995	13.389	31.6290110810405LJB
0018LBARS5.09701CSACL1	29.763	16.570	20.2590110810405LJB

```
0018LBARS5.09701CSACLT 30.298 17.196 23.0630110810405LJB
0018LBARS5.09701CSACR1 30.999 13.763 19.2100110810405LJB
0018LBARS5.09701CSACRT 30.789 11.948 23.7640110810405LJB
0018LBARS5.09701CSACS1 29.613 14.112 25.2130110810405LJB
0018LBARS5.09701CSACSM 29.507 14.816 25.9930110810405LJB
0018LBARS5.09701CT01L1 23.488 14.094 74.0760110810405LJB
0018LBARS5.09701CT01R1 26.127 11.180 74.2580110810405LJB
0018LBARS5.09701CT01S1 21.861 13.647 74.1760110810405LJB
0018LBARS5.09701CT01SM 22.594 13.213 74.3390110810405LJB
0018LBARS5.09701CT01TL 25.231 14.473 74.8170110810405LJB
0018LBARS5.09701CT01TR 25.409 11.329 74.3110110810405LJB
0018LBARS5.09701CT04L1 22.909 15.730 67.7890110810405LJB
0018LBARS5.09701CT04R1 23.493 10.835 68.1830110810405LJB
0018LBARS5.09701CT04S1 20.604 14.228 67.5440110810405LJB
0018LBARS5.09701CT04SM 20.561 14.328 67.8490110810405LJB
0018LBARS5.09701CT04TL 23.648 15.391 70.1680110810405LJB
0018LBARS5.09701CT04TR 23.207 10.742 68.6560110810405LJB
0018LBARS5.09701CT08L1 22.809 15.727 54.9740110810405LJB
0018LBARS5.09701CT08R1 22.068 11.639 55.5630110810405LJB
0018LBARS5.09701CT08S1 20.588 15.114 54.7350110810405LJB
0018LBARS5.09701CT08SM 20.613 14.834 55.1830110810405LJB
0018LBARS5.09701CT08TL 22.273 16.882 55.7860110810405LJB
0018LBARS5.09701CT08TR 23.074 14.027 55.5160110810405LJB
0018LBARS5.09701CT11L1 25.955 16.926 46.2760110810405LJB
0018LBARS5.09701CT11R1 26.954 14.029 45.3010110810405LJB
0018LBARS5.09701CT11S1 25.246 15.436 44.8040110810405LJB
0018LBARS5.09701CT11SM 24.827 15.435 44.8930110810405LJB
0018LBARS5.09701CT11TL 27.169 17.157 46.5890110810405LJB
0018LBARS5.09701CT11TR 27.435 14.302 45.2410110810405LJB
0018LBARS5.09701CT12L1 28.172 15.921 43.6280110810405LJB
0018LBARS5.09701CT12R1 28.874 14.222 42.7650110810405LJB
0018LBARS5.09701CT12S1 26.585 14.993 41.4730110810405LJB
0018LBARS5.09701CT12SM 26.319 15.318 41.8780110810405LJB
0018LBARS5.09701CT12TL 28.307 16.302 43.6340110810405LJB
0018LBARS5.09701CT12TR 30.402 14.310 43.8420110810405LJB
0018LBARS5.09701GLROD1 82.172  8.690 50.5040110810405LJB
0018LBARS5.09701GLROD2 46.638  8.657 50.5040110810405LJB
0018LBARS5.09701PLXSLB 27.227 16.086 31.4940110810405LJB
0018LBARS5.09701PLXSLT 26.642 16.745 36.2900110810405LJB
0018LBARS5.09701PLXSRB 29.071 10.337 32.5760110810405LJB
0018LBARS5.09701PLXSRT 28.329 10.934 37.2900110810405LJB
0018LBARS5.09701QUBE01 61.935  5.073 59.2490110810405LJB
0018LBARS5.09701QUBE02 50.241  5.008 59.1660110810405LJB
0018LBARS5.09701QUBE03 61.545 20.211 59.2190110810405LJB
0018LBARS5.09701QUBE04 49.830 20.233 59.1440110810405LJB
0018LBARS5.09701QUBE05 61.937  5.001 50.0480110810405LJB
0018LBARS5.09701QUBE06 50.296  4.985 49.9130110810405LJB
0018LBARS5.09701QUBE07 61.620 20.166 49.8660110810405LJB
0018LBARS5.09701QUBE08 49.788 20.160 49.8310110810405LJB
0018LBARS5.09701STGSRP 30.183 13.217 10.3030110810405LJB
0018LBARS5.09701STGT02 22.121  2.097 42.8430110810405LJB
0018LBARS5.09701STGT03 19.123  5.925 53.7620110810405LJB
0018LBARS5.09701STGT06 26.230 27.946 24.1980110810405LJB
0018LBARS5.09701STGT07 20.725 25.340 44.8720110810405LJB
```

```
0018LBARS5.09701STGT08 17.694 28.939 56.4450110810405LJB
0018LBARS5.09701STGT13 19.135  4.886 54.0530110810405LJB
0018LBARS5.09701STGT16 26.224 27.306 24.0830110810405LJB
0018LBARS5.09701STGT17 20.660 24.708 45.5290110810405LJB
0018LBARS5.09701STGT18 17.630 28.391 56.8210110810405LJB
0018LBARS5.09701WIRE02  0.070  0.006 30.4520110810405LJB
0018LBARS5.09701WIRE03  0.062  0.003 60.9760110810405LJB
0018LBARS5.09701WIRE08  0.032 30.520 30.4080110810405LJB
0018LBARS5.09701WIRE09 -0.062 30.528 60.9310110810405LJB
0018LBARS5.59701CC07L1 24.678 13.616 76.1290110810203LJB
0018LBARS5.59701CC07R1 25.699 11.911 76.2060110810203LJB
0018LBARS5.59701CC07S1 23.199 13.412 75.5580110810203LJB
0018LBARS5.59701CC07SM 23.714 13.162 76.1070110810203LJB
0018LBARS5.59701CC07TL 25.786 14.212 78.1490110810203LJB
0018LBARS5.59701CC07TR 26.226 12.179 76.3940110810203LJB
0018LBARS5.59701CINLAS 42.979 28.618 27.6810110810203LJB
0018LBARS5.59701CINLPS 35.077 26.242 31.0070110810203LJB
0018LBARS5.59701CINLPT 44.933 17.233 18.1150110810203LJB
0018LBARS5.59701CINRAS 44.765  2.900 28.2940110810203LJB
0018LBARS5.59701CINRPS 37.394  2.692 33.5910110810203LJB
0018LBARS5.59701CINRPT 44.773 13.552 17.8990110810203LJB
0018LBARS5.59701CL01L1 30.539 16.276 40.5650110810203LJB
0018LBARS5.59701CL01R1 31.125 14.130 39.2930110810203LJB
0018LBARS5.59701CL01S1 29.102 15.124 38.0130110810203LJB
0018LBARS5.59701CL01SM 27.887 15.249 39.1470110810203LJB
0018LBARS5.59701CL01TL 30.569 16.261 40.7850110810203LJB
0018LBARS5.59701CL01TR 32.816 14.679 41.2630110810203LJB
0018LBARS5.59701CL02L1 32.481 15.959 36.2140110810203LJB
0018LBARS5.59701CL02S1 28.896 15.138 36.5150110810203LJB
0018LBARS5.59701CL02SM 28.953 14.622 36.4720110810203LJB
0018LBARS5.59701CL02TL 31.894 16.490 37.1470110810203LJB
0018LBARS5.59701CL03L1 32.493 16.555 34.0130110810203LJB
0018LBARS5.59701CL03R1 33.513 11.348 35.9380110810203LJB
0018LBARS5.59701CL03S1 29.574 14.763 33.2390110810203LJB
0018LBARS5.59701CL03SM 29.571 14.688 33.3960110810203LJB
0018LBARS5.59701CL03TL 33.192 16.768 32.4160110810203LJB
0018LBARS5.59701CL04L1 33.163 15.909 30.3830110810203LJB
0018LBARS5.59701CL04R1 34.139 12.890 33.1460110810203LJB
0018LBARS5.59701CL04S1 29.581 14.932 30.4720110810203LJB
0018LBARS5.59701CL04SM 30.132 15.053 30.7750110810203LJB
0018LBARS5.59701CL04TL 33.339 16.505 30.0320110810203LJB
0018LBARS5.59701CL05R1 34.098 12.865 30.4470110810203LJB
0018LBARS5.59701CL05TR 34.440 13.480 31.7020110810203LJB
0018LBARS5.59701CSACL1 30.055 16.590 20.4270110810203LJB
0018LBARS5.59701CSACLT 30.609 17.237 23.2040110810203LJB
0018LBARS5.59701CSACR1 31.262 13.790 19.3580110810203LJB
0018LBARS5.59701CSACRT 31.177 11.988 23.9290110810203LJB
0018LBARS5.59701CSACS1 30.016 14.149 25.3820110810203LJB
0018LBARS5.59701CSACSM 29.903 14.857 26.1600110810203LJB
0018LBARS5.59701CT01L1 23.456 14.270 74.0290110810203LJB
0018LBARS5.59701CT01R1 26.157 11.369 74.2470110810203LJB
0018LBARS5.59701CT01S1 21.868 13.816 74.1410110810203LJB
0018LBARS5.59701CT01SM 22.584 13.396 74.3050110810203LJB
0018LBARS5.59701CT01TL 25.211 14.667 74.7940110810203LJB
```

0018LBARS5.59701CT01TR	25.440	11.533	74.2930110810203LJB
0018LBARS5.59701CT04L1	22.953	15.894	67.6860110810203LJB
0018LBARS5.59701CT04R1	23.574	11.004	68.1100110810203LJB
0018LBARS5.59701CT04S1	20.658	14.384	67.3910110810203LJB
0018LBARS5.59701CT04SM	20.595	14.492	67.7010110810203LJB
0018LBARS5.59701CT04TL	23.672	15.567	70.0900110810203LJB
0018LBARS5.59701CT04TR	23.301	10.908	68.5740110810203LJB
0018LBARS5.59701CT08L1	23.254	15.861	54.8740110810203LJB
0018LBARS5.59701CT08R1	22.517	11.777	55.4500110810203LJB
0018LBARS5.59701CT08S1	20.996	15.259	54.5670110810203LJB
0018LBARS5.59701CT08SM	21.030	14.955	55.0090110810203LJB
0018LBARS5.59701CT08TL	22.644	17.024	55.6700110810203LJB
0018LBARS5.59701CT08TR	23.505	14.163	55.4230110810203LJB
0018LBARS5.59701CT11L1	26.594	17.050	46.2970110810203LJB
0018LBARS5.59701CT11R1	27.640	14.168	45.3750110810203LJB
0018LBARS5.59701CT11S1	25.866	15.550	44.8150110810203LJB
0018LBARS5.59701CT11SM	25.499	15.553	44.9030110810203LJB
0018LBARS5.59701CT11TL	27.716	17.300	46.6270110810203LJB
0018LBARS5.59701CT11TR	28.127	14.437	45.2980110810203LJB
0018LBARS5.59701CT12L1	28.817	16.047	43.7180110810203LJB
0018LBARS5.59701CT12R1	29.530	14.353	42.8780110810203LJB
0018LBARS5.59701CT12S1	27.220	15.088	41.5510110810203LJB
0018LBARS5.59701CT12SM	26.966	15.417	41.9670110810203LJB
0018LBARS5.59701CT12TL	28.927	16.421	43.7170110810203LJB
0018LBARS5.59701CT12TR	31.015	14.443	43.9440110810203LJB
0018LBARS5.59701GLROD1	82.210	8.697	50.4970110810203LJB
0018LBARS5.59701GLROD2	46.642	8.662	50.4970110810203LJB
0018LBARS5.59701PLXSLB	27.754	16.028	31.6410110810203LJB
0018LBARS5.59701PLXSLT	27.144	16.733	36.4170110810203LJB
0018LBARS5.59701PLXSRB	29.627	10.321	32.7730110810203LJB
0018LBARS5.59701PLXSRT	28.874	10.951	37.4910110810203LJB
0018LBARS5.59701QUBE01	61.957	5.080	59.2450110810203LJB
0018LBARS5.59701QUBE02	50.255	5.023	59.1630110810203LJB
0018LBARS5.59701QUBE03	61.574	20.213	59.2080110810203LJB
0018LBARS5.59701QUBE04	49.805	20.243	59.1420110810203LJB
0018LBARS5.59701QUBE05	61.955	5.009	50.0390110810203LJB
0018LBARS5.59701QUBE06	50.296	4.986	49.8980110810203LJB
0018LBARS5.59701QUBE07	61.631	20.173	49.8530110810203LJB
0018LBARS5.59701QUBE08	49.818	20.160	49.8240110810203LJB
0018LBARS5.59701STGSRP	30.194	13.215	10.3010110810203LJB
0018LBARS5.59701STGT02	22.128	2.106	42.8380110810203LJB
0018LBARS5.59701STGT03	19.120	5.925	53.7610110810203LJB
0018LBARS5.59701STGT06	26.287	27.956	24.1810110810203LJB
0018LBARS5.59701STGT07	20.754	25.340	44.8690110810203LJB
0018LBARS5.59701STGT08	17.674	28.945	56.4290110810203LJB
0018LBARS5.59701STGT13	19.148	4.895	54.0480110810203LJB
0018LBARS5.59701STGT16	26.307	27.304	24.0850110810203LJB
0018LBARS5.59701STGT17	20.714	24.714	45.5210110810203LJB
0018LBARS5.59701STGT18	17.627	28.399	56.8160110810203LJB
0018LBARS5.59701WIRE02	0.098	0.004	30.4460110810203LJB
0018LBARS5.59701WIRE03	0.063	0.003	60.9710110810203LJB
0018LBARS5.59701WIRE08	0.060	30.519	30.4010110810203LJB
0018LBARS5.59701WIRE09	-0.038	30.524	60.9230110810203LJB
0018SEATEDP10201CC07L1	26.780	10.912	73.1090110812021LJB

0018SEATEDP10201CC07R1	27.844	9.152	73.1350110812021LJB
0018SEATEDP10201CC07S1	25.258	10.789	72.5450110812021LJB
0018SEATEDP10201CC07SM	25.729	10.502	73.0590110812021LJB
0018SEATEDP10201CC07TL	27.874	11.373	75.0760110812021LJB
0018SEATEDP10201CC07TR	28.274	9.394	73.3100110812021LJB
0018SEATEDP10201CINLIS	48.757	17.633	15.1570110812021LJB
0018SEATEDP10201CINLPS	35.655	25.455	27.4570110812021LJB
0018SEATEDP10201CINLPT	51.318	15.572	23.1610110812021LJB
0018SEATEDP10201CINRAS	43.499	1.487	30.3630110812021LJB
0018SEATEDP10201CINRPS	34.013	1.879	29.9230110812021LJB
0018SEATEDP10201CINRPT	51.001	11.914	22.7150110812021LJB
0018SEATEDP10201CL01L1	27.610	15.457	37.1070110812021LJB
0018SEATEDP10201CL01S1	26.053	14.677	34.4660110812021LJB
0018SEATEDP10201CL01SM	24.956	14.777	35.6970110812021LJB
0018SEATEDP10201CL01TL	27.695	15.459	37.2780110812021LJB
0018SEATEDP10201CL01TR	29.743	13.708	37.5170110812021LJB
0018SEATEDP10201CL02S1	26.320	14.845	32.0930110812021LJB
0018SEATEDP10201CL02SM	26.320	14.381	32.0090110812021LJB
0018SEATEDP10201CL02TL	29.235	15.943	33.1390110812021LJB
0018SEATEDP10201CL03L1	30.855	16.041	29.6050110812021LJB
0018SEATEDP10201CL03R1	30.869	10.736	31.3930110812021LJB
0018SEATEDP10201CL03S1	28.137	14.526	27.8790110812021LJB
0018SEATEDP10201CL03SM	28.136	14.433	28.0400110812021LJB
0018SEATEDP10201CL04L1	33.615	15.270	25.4710110812021LJB
0018SEATEDP10201CL04R1	32.480	12.285	28.5090110812021LJB
0018SEATEDP10201CL04S1	30.608	14.745	24.0410110812021LJB
0018SEATEDP10201CL04SM	30.263	14.849	24.7180110812021LJB
0018SEATEDP10201CL04TL	34.002	15.828	25.9230110812021LJB
0018SEATEDP10201CL05R1	33.722	12.309	26.1040110812021LJB
0018SEATEDP10201CL05TR	33.620	12.861	27.4740110812021LJB
0018SEATEDP10201CSACL1	37.570	16.008	15.6590110812021LJB
0018SEATEDP10201CSACLT	36.271	16.661	18.2100110812021LJB
0018SEATEDP10201CSACR1	39.035	13.143	15.5270110812021LJB
0018SEATEDP10201CSACRT	35.822	11.398	18.8770110812021LJB
0018SEATEDP10201CSACS1	34.022	13.660	19.8800110812021LJB
0018SEATEDP10201CSACSM	33.586	14.388	20.0180110812021LJB
0018SEATEDP10201CT01L1	25.623	11.706	71.2740110812021LJB
0018SEATEDP10201CT01R1	28.101	8.665	71.1810110812021LJB
0018SEATEDP10201CT01S1	23.947	11.325	71.2800110812021LJB
0018SEATEDP10201CT01SM	24.662	10.812	71.4620110812021LJB
0018SEATEDP10201CT01TL	27.303	11.974	71.8840110812021LJB
0018SEATEDP10201CT01TR	27.434	8.831	71.2960110812021LJB
0018SEATEDP10201CT04L1	24.770	13.565	65.3160110812021LJB
0018SEATEDP10201CT04R1	25.117	8.643	65.4770110812021LJB
0018SEATEDP10201CT04S1	22.392	12.142	65.3020110812021LJB
0018SEATEDP10201CT04SM	22.332	12.230	65.6220110812021LJB
0018SEATEDP10201CT04TL	25.639	13.101	67.5250110812021LJB
0018SEATEDP10201CT04TR	24.845	8.546	65.9780110812021LJB
0018SEATEDP10201CT08L1	23.055	14.253	53.0830110812021LJB
0018SEATEDP10201CT08R1	22.210	10.197	53.7930110812021LJB
0018SEATEDP10201CT08S1	20.785	13.730	53.1500110812021LJB
0018SEATEDP10201CT08SM	20.926	13.386	53.3250110812021LJB
0018SEATEDP10201CT08TL	22.680	15.440	54.0830110812021LJB
0018SEATEDP10201CT08TR	23.283	12.483	53.4470110812021LJB

0018SEATEDP10201CT11R1	24.897	13.086	42.5120110812021LJB
0018SEATEDP10201CT11S1	23.195	14.642	42.6100110812021LJB
0018SEATEDP10201CT11SM	22.900	14.653	42.8050110812021LJB
0018SEATEDP10201CT11TL	25.354	16.043	44.1330110812021LJB
0018SEATEDP10201CT11TR	25.349	13.379	42.5260110812021LJB
0018SEATEDP10201CT12L1	26.052	15.091	40.7450110812021LJB
0018SEATEDP10201CT12R1	26.508	13.428	39.4490110812021LJB
0018SEATEDP10201CT12S1	24.134	14.421	38.8030110812021LJB
0018SEATEDP10201CT12SM	24.012	14.721	39.2750110812021LJB
0018SEATEDP10201CT12TL	26.177	15.459	40.7310110812021LJB
0018SEATEDP10201CT12TR	28.045	13.363	40.4780110812021LJB
0018SEATEDP10201GLROD1	83.052	9.243	50.0900110812021LJB
0018SEATEDP10201GLROD2	47.540	9.219	50.0900110812021LJB
0018SEATEDP10201QUBE02	50.041	5.986	58.7670110812021LJB
0018SEATEDP10201QUBE03	61.585	21.236	58.7530110812021LJB
0018SEATEDP10201QUBE04	49.821	21.190	58.7680110812021LJB
0018SEATEDP10201QUBE05	61.691	6.059	49.5690110812021LJB
0018SEATEDP10201QUBE06	50.060	5.957	49.5260110812021LJB
0018SEATEDP10201QUBE07	61.601	21.191	49.4030110812021LJB
0018SEATEDP10201QUBE08	49.786	21.111	49.4570110812021LJB
0018SEATEDP10201STGSRP	30.755	12.384	10.0360110812021LJB
0018SEATEDP10201STGT02	22.024	1.549	42.5710110812021LJB
0018SEATEDP10201STGT03	19.300	5.456	53.5140110812021LJB
0018SEATEDP10201STGT06	27.675	27.222	23.9540110812021LJB
0018SEATEDP10201STGT07	22.107	24.789	44.6730110812021LJB
0018SEATEDP10201STGT08	19.284	28.449	56.2800110812021LJB
0018SEATEDP10201STGT13	19.196	4.435	53.8030110812021LJB
0018SEATEDP10201STGT16	27.655	26.573	23.8490110812021LJB
0018SEATEDP10201STGT17	21.976	24.160	45.3270110812021LJB
0018SEATEDP10201STGT18	19.183	27.927	56.6480110812021LJB
0018SEATEDP10201WIRE02	0.061	0.000	30.4610110812021LJB
0018SEATEDP10201WIRE03	0.074	0.012	60.9840110812021LJB
0018SEATEDP10201WIRE08	0.089	30.494	30.4300110812021LJB
0018SEATEDP10201WIRE09	0.058	30.487	60.9670110812021LJB
0018SEATEDP20201CC07L1	27.437	10.926	69.4630110812425LJB
0018SEATEDP20201CC07R1	28.489	9.163	69.4690110812425LJB
0018SEATEDP20201CC07S1	25.908	10.817	68.9050110812425LJB
0018SEATEDP20201CC07SM	26.439	10.511	69.4260110812425LJB
0018SEATEDP20201CC07TL	28.571	11.372	71.4360110812425LJB
0018SEATEDP20201CC07TR	28.918	9.418	69.6340110812425LJB
0018SEATEDP20201CINLIS	55.997	16.657	16.4470110812425LJB
0018SEATEDP20201CINLPS	40.791	24.457	25.4790110812425LJB
0018SEATEDP20201CINLPT	55.265	15.106	24.3040110812425LJB
0018SEATEDP20201CINRPS	39.030	1.011	28.1520110812425LJB
0018SEATEDP20201CINRPT	56.394	11.167	24.4410110812425LJB
0018SEATEDP20201CL01S1	29.780	13.809	30.7050110812425LJB
0018SEATEDP20201CL01SM	28.470	13.971	31.6940110812425LJB
0018SEATEDP20201CL01TL	31.083	14.679	33.7640110812425LJB
0018SEATEDP20201CL01TR	32.979	12.959	34.4040110812425LJB
0018SEATEDP20201CL02L1	33.667	14.458	28.9280110812425LJB
0018SEATEDP20201CL02S1	30.762	13.917	28.4050110812425LJB
0018SEATEDP20201CL02SM	30.724	13.447	28.3220110812425LJB
0018SEATEDP20201CL02TL	33.378	15.040	29.9530110812425LJB
0018SEATEDP20201CL03L1	35.730	15.081	26.8180110812425LJB

0018SEATEDP20201CL03R1	35.448	9.828	28.7100110812425LJB
0018SEATEDP20201CL03S1	33.469	13.494	24.6430110812425LJB
0018SEATEDP20201CL03SM	33.459	13.416	24.7870110812425LJB
0018SEATEDP20201CL03TL	37.488	15.632	25.7940110812425LJB
0018SEATEDP20201CL04L1	39.531	14.279	23.3960110812425LJB
0018SEATEDP20201CL04R1	37.689	11.325	26.2070110812425LJB
0018SEATEDP20201CL04S1	36.883	13.629	21.3850110812425LJB
0018SEATEDP20201CL04SM	36.321	13.744	21.9310110812425LJB
0018SEATEDP20201CL04TL	39.756	14.892	23.8890110812425LJB
0018SEATEDP20201CL05R1	39.424	11.307	24.1200110812425LJB
0018SEATEDP20201CL05TR	38.942	11.878	25.3870110812425LJB
0018SEATEDP20201CSACL1	45.440	14.831	14.7020110812425LJB
0018SEATEDP20201CSACLT	43.693	15.517	16.8740110812425LJB
0018SEATEDP20201CSACR1	46.872	11.998	14.9860110812425LJB
0018SEATEDP20201CSACRT	43.159	10.268	17.5650110812425LJB
0018SEATEDP20201CSACS1	41.125	12.491	18.1440110812425LJB
0018SEATEDP20201CSACSM	40.801	13.243	18.1320110812425LJB
0018SEATEDP20201CT01L1	26.300	11.748	67.5630110812425LJB
0018SEATEDP20201CT01R1	28.728	8.702	67.4720110812425LJB
0018SEATEDP20201CT01S1	24.620	11.360	67.6020110812425LJB
0018SEATEDP20201CT01SM	25.375	10.862	67.7490110812425LJB
0018SEATEDP20201CT01TL	27.999	12.011	68.2110110812425LJB
0018SEATEDP20201CT01TR	28.030	8.870	67.5970110812425LJB
0018SEATEDP20201CT04L1	25.466	13.651	61.5160110812425LJB
0018SEATEDP20201CT04R1	25.817	8.734	61.6880110812425LJB
0018SEATEDP20201CT04S1	23.071	12.270	61.4100110812425LJB
0018SEATEDP20201CT04SM	23.026	12.364	61.7300110812425LJB
0018SEATEDP20201CT04TL	26.315	13.184	63.7930110812425LJB
0018SEATEDP20201CT04TR	25.507	8.649	62.1620110812425LJB
0018SEATEDP20201CT08L1	24.307	14.205	49.1020110812425LJB
0018SEATEDP20201CT08R1	23.250	10.045	49.7320110812425LJB
0018SEATEDP20201CT08S1	21.854	13.636	49.3200110812425LJB
0018SEATEDP20201CT08SM	22.105	13.407	49.3540110812425LJB
0018SEATEDP20201CT08TL	23.753	15.481	49.9780110812425LJB
0018SEATEDP20201CT08TR	24.465	12.453	49.5530110812425LJB
0018SEATEDP20201CT11R1	27.324	12.574	38.6610110812425LJB
0018SEATEDP20201CT11S1	25.616	14.063	38.4610110812425LJB
0018SEATEDP20201CT11SM	25.142	14.077	38.5550110812425LJB
0018SEATEDP20201CT11TL	27.714	15.513	40.1870110812425LJB
0018SEATEDP20201CT11TR	27.743	12.783	38.7180110812425LJB
0018SEATEDP20201CT12L1	28.777	14.452	36.9490110812425LJB
0018SEATEDP20201CT12SM	26.938	14.037	35.1760110812425LJB
0018SEATEDP20201CT12TL	28.957	14.819	36.9550110812425LJB
0018SEATEDP20201CT12TR	30.830	12.703	37.0760110812425LJB
0018SEATEDP20201GLROD1	83.026	9.219	50.1020110812425LJB
0018SEATEDP20201GLROD2	47.545	9.186	50.1020110812425LJB
0018SEATEDP20201QUBE04	49.853	21.172	58.7760110812425LJB
0018SEATEDP20201QUBE05	61.623	6.029	49.5890110812425LJB
0018SEATEDP20201QUBE06	50.045	5.945	49.5290110812425LJB
0018SEATEDP20201QUBE07	61.558	21.174	49.4250110812425LJB
0018SEATEDP20201QUBE08	49.837	21.090	49.4840110812425LJB
0018SEATEDP20201STGSRP	30.884	12.372	10.0680110812425LJB
0018SEATEDP20201STGT02	22.177	1.546	42.5910110812425LJB
0018SEATEDP20201STGT03	19.471	5.456	53.5320110812425LJB

0018SEATEDP20201STGT06	27.786	27.198	23.9720110812425LJB
0018SEATEDP20201STGT07	22.193	24.773	44.6970110812425LJB
0018SEATEDP20201STGT08	19.402	28.439	56.2910110812425LJB
0018SEATEDP20201STGT13	19.348	4.411	53.8230110812425LJB
0018SEATEDP20201STGT16	27.722	26.560	23.8540110812425LJB
0018SEATEDP20201STGT17	22.042	24.151	45.3420110812425LJB
0018SEATEDP20201STGT18	19.291	27.926	56.6570110812425LJB
0018SEATEDP20201WIRE02	0.126	0.013	30.4770110812425LJB
0018SEATEDP20201WIRE03	0.105	-0.016	60.9710110812425LJB
0018SEATEDP20201WIRE08	0.118	30.500	30.4290110812425LJB
0018SEATEDP20201WIRE09	0.076	30.483	60.9480110812425LJB
0018SEATERCT9701CC07L1	25.883	11.161	75.4580110811819LJB
0018SEATERCT9701CC07R1	26.895	9.403	75.5210110811819LJB
0018SEATERCT9701CC07S1	24.407	11.044	74.8800110811819LJB
0018SEATERCT9701CC07SM	24.842	10.762	75.4130110811819LJB
0018SEATERCT9701CC07TL	27.020	11.664	77.4120110811819LJB
0018SEATERCT9701CC07TR	27.383	9.656	75.6930110811819LJB
0018SEATERCT9701CINLAS	42.774	26.537	27.9010110811819LJB
0018SEATERCT9701CINLIS	38.431	17.334	13.0140110811819LJB
0018SEATERCT9701CINLPS	34.496	24.544	30.4840110811819LJB
0018SEATERCT9701CINLPT	44.818	15.221	18.2840110811819LJB
0018SEATERCT9701CINRAS	42.670	0.794	28.1010110811819LJB
0018SEATERCT9701CINRPS	34.806	0.918	32.7230110811819LJB
0018SEATERCT9701CINRPT	44.418	11.553	17.9790110811819LJB
0018SEATERCT9701CL01L1	28.739	14.479	39.7500110811819LJB
0018SEATERCT9701CL01R1	29.156	12.408	38.3420110811819LJB
0018SEATERCT9701CL01S1	27.246	13.559	37.0970110811819LJB
0018SEATERCT9701CL01SM	26.109	13.680	38.2610110811819LJB
0018SEATERCT9701CL01TL	28.831	14.470	39.9390110811819LJB
0018SEATERCT9701CL01TR	30.871	12.763	40.3300110811819LJB
0018SEATERCT9701CL02L1	30.826	14.304	35.3010110811819LJB
0018SEATERCT9701CL02TL	30.181	14.831	36.2390110811819LJB
0018SEATERCT9701CL03L1	30.976	14.956	33.1300110811819LJB
0018SEATERCT9701CL03R1	31.551	9.665	34.9000110811819LJB
0018SEATERCT9701CL03S1	27.983	13.362	32.1690110811819LJB
0018SEATERCT9701CL03SM	27.955	13.292	32.3020110811819LJB
0018SEATERCT9701CL03TL	31.813	15.239	31.5590110811819LJB
0018SEATERCT9701CL04L1	31.904	14.354	29.4780110811819LJB
0018SEATERCT9701CL04R1	32.366	11.244	32.2280110811819LJB
0018SEATERCT9701CL04S1	28.255	13.629	29.2290110811819LJB
0018SEATERCT9701CL04SM	28.716	13.667	29.6850110811819LJB
0018SEATERCT9701CL04TL	32.089	14.949	29.1530110811819LJB
0018SEATERCT9701CL05R1	32.554	11.286	29.5450110811819LJB
0018SEATERCT9701CL05TR	32.913	11.852	30.8540110811819LJB
0018SEATERCT9701CSACL1	29.770	15.372	19.2940110811819LJB
0018SEATERCT9701CSACLT	30.101	15.940	22.1320110811819LJB
0018SEATERCT9701CSACR1	30.895	12.539	18.2930110811819LJB
0018SEATERCT9701CSACRT	30.199	10.672	22.7690110811819LJB
0018SEATERCT9701CSACS1	29.090	12.855	24.2310110811819LJB
0018SEATERCT9701CSACSM	28.959	13.558	24.9650110811819LJB
0018SEATERCT9701CT01L1	24.752	11.928	73.5820110811819LJB
0018SEATERCT9701CT01R1	27.228	8.880	73.5620110811819LJB
0018SEATERCT9701CT01S1	23.043	11.561	73.6120110811819LJB
0018SEATERCT9701CT01SM	23.782	11.055	73.7890110811819LJB

0018SEATERCT9701CT01TL	26.475	12.202	74.2040110811819LJB
0018SEATERCT9701CT01TR	26.543	9.044	73.6770110811819LJB
0018SEATERCT9701CT04L1	23.898	13.662	67.5560110811819LJB
0018SEATERCT9701CT04R1	24.250	8.742	67.8320110811819LJB
0018SEATERCT9701CT04S1	21.492	12.250	67.5310110811819LJB
0018SEATERCT9701CT04SM	21.451	12.346	67.8430110811819LJB
0018SEATERCT9701CT04TL	24.803	13.246	69.7940110811819LJB
0018SEATERCT9701CT04TR	24.041	8.665	68.3160110811819LJB
0018SEATERCT9701CT08L1	22.527	13.859	55.0560110811819LJB
0018SEATERCT9701CT08R1	21.641	9.924	55.6890110811819LJB
0018SEATERCT9701CT08S1	20.303	13.410	54.9420110811819LJB
0018SEATERCT9701CT08SM	20.316	13.047	55.3670110811819LJB
0018SEATERCT9701CT08TL	22.120	15.079	55.9170110811819LJB
0018SEATERCT9701CT08TR	22.751	12.119	55.5260110811819LJB
0018SEATERCT9701CT11L1	24.949	15.173	45.9370110811819LJB
0018SEATERCT9701CT11R1	25.664	12.312	44.7430110811819LJB
0018SEATERCT9701CT11S1	23.994	13.766	44.5200110811819LJB
0018SEATERCT9701CT11SM	23.539	13.785	44.6310110811819LJB
0018SEATERCT9701CT11TL	26.115	15.340	46.1690110811819LJB
0018SEATERCT9701CT11TR	26.131	12.524	44.7340110811819LJB
0018SEATERCT9701CT12L1	26.985	14.205	43.0250110811819LJB
0018SEATERCT9701CT12R1	27.575	12.506	41.9920110811819LJB
0018SEATERCT9701CT12S1	25.222	13.440	40.8900110811819LJB
0018SEATERCT9701CT12SM	25.013	13.753	41.3130110811819LJB
0018SEATERCT9701CT12TL	27.092	14.569	43.0310110811819LJB
0018SEATERCT9701CT12TR	29.047	12.486	43.0740110811819LJB
0018SEATERCT9701GLROD1	83.035	9.266	50.0780110811819LJB
0018SEATERCT9701GLROD2	47.540	9.242	50.0780110811819LJB
0018SEATERCT9701QUBE01	61.657	6.151	58.7640110811819LJB
0018SEATERCT9701QUBE02	49.961	6.008	58.7760110811819LJB
0018SEATERCT9701QUBE03	61.479	21.268	58.7480110811819LJB
0018SEATERCT9701QUBE04	49.789	21.217	58.7610110811819LJB
0018SEATERCT9701QUBE05	61.660	6.085	49.5610110811819LJB
0018SEATERCT9701QUBE06	50.029	5.979	49.5160110811819LJB
0018SEATERCT9701QUBE07	61.549	21.229	49.3900110811819LJB
0018SEATERCT9701QUBE08	49.789	21.138	49.4490110811819LJB
0018SEATERCT9701STGSRP	30.368	12.288	9.9810110811819LJB
0018SEATERCT9701STGT02	21.697	1.452	42.5620110811819LJB
0018SEATERCT9701STGT03	18.904	5.356	53.5090110811819LJB
0018SEATERCT9701STGT07	21.724	24.682	44.6660110811819LJB
0018SEATERCT9701STGT08	18.894	28.353	56.2720110811819LJB
0018SEATERCT9701STGT13	18.876	4.318	53.8010110811819LJB
0018SEATERCT9701STGT17	21.620	24.056	45.3190110811819LJB
0018SEATERCT9701STGT18	18.789	27.831	56.6420110811819LJB
0018SEATERCT9701WIRE02	0.076	0.002	30.4650110811819LJB
0018SEATERCT9701WIRE03	0.050	0.002	60.9760110811819LJB
0018SEATERCT9701WIRE08	0.217	30.473	30.4080110811819LJB
0018SIDEBEND0201CINLIS	40.191	19.211	13.8820110812627LJB
0018SIDEBEND0201CINLPS	30.452	25.400	29.4170110812627LJB
0018SIDEBEND0201CINLPT	44.908	17.616	20.8470110812627LJB
0018SIDEBEND0201CINRAS	41.549	2.682	29.5470110812627LJB
0018SIDEBEND0201CINRPS	32.697	1.850	31.6270110812627LJB
0018SIDEBEND0201CINRPT	45.018	13.925	20.4410110812627LJB
0018SIDEBEND0201CL01L1	25.469	13.061	39.2900110812627LJB

0018SIDEBEND0201CL01S1	23.827	12.705	36.5350110812627LJB
0018SIDEBEND0201CL01SM	22.786	12.261	37.7580110812627LJB
0018SIDEBEND0201CL01TL	25.486	12.994	39.4050110812627LJB
0018SIDEBEND0201CL02S1	23.891	13.192	34.6010110812627LJB
0018SIDEBEND0201CL02SM	23.816	12.740	34.3950110812627LJB
0018SIDEBEND0201CL03L1	27.601	15.321	32.0960110812627LJB
0018SIDEBEND0201CL03R1	28.682	9.944	33.1440110812627LJB
0018SIDEBEND0201CL03S1	24.797	13.563	30.6810110812627LJB
0018SIDEBEND0201CL03SM	24.893	13.453	30.8310110812627LJB
0018SIDEBEND0201CL03TL	28.543	16.302	30.4840110812627LJB
0018SIDEBEND0201CL03TR	26.885	11.672	33.9640110812627LJB
0018SIDEBEND0201CL04L1	29.347	15.007	27.7200110812627LJB
0018SIDEBEND0201CL04R1	29.508	11.896	30.7910110812627LJB
0018SIDEBEND0201CL04S1	26.099	14.027	27.0480110812627LJB
0018SIDEBEND0201CL04SM	25.967	14.105	27.8090110812627LJB
0018SIDEBEND0201CL04TL	29.767	15.794	28.0160110812627LJB
0018SIDEBEND0201CL05R1	30.034	12.144	28.1430110812627LJB
0018SIDEBEND0201CL05TR	30.231	12.665	29.5090110812627LJB
0018SIDEBEND0201CSACL1	30.274	16.125	17.3190110812627LJB
0018SIDEBEND0201CSACLT	29.693	16.650	20.1220110812627LJB
0018SIDEBEND0201CSACR1	31.957	13.459	16.6590110812627LJB
0018SIDEBEND0201CSACRT	30.121	11.390	20.7490110812627LJB
0018SIDEBEND0201CSACS1	28.421	13.340	22.1710110812627LJB
0018SIDEBEND0201CSACSM	28.076	14.074	22.5140110812627LJB
0018SIDEBEND0201CT08L1	21.619	5.820	53.5970110812627LJB
0018SIDEBEND0201CT08R1	21.223	1.780	52.6820110812627LJB
0018SIDEBEND0201CT08S1	19.273	5.108	53.6210110812627LJB
0018SIDEBEND0201CT08SM	19.532	4.939	53.6450110812627LJB
0018SIDEBEND0201CT08TL	21.047	6.418	55.0240110812627LJB
0018SIDEBEND0201CT11R1	23.536	8.857	43.4240110812627LJB
0018SIDEBEND0201CT11S1	21.604	9.929	43.9780110812627LJB
0018SIDEBEND0201CT11SM	21.178	9.814	44.1160110812627LJB
0018SIDEBEND0201CT11TR	23.905	9.183	43.5040110812627LJB
0018SIDEBEND0201CT12L1	24.173	11.390	42.5010110812627LJB
0018SIDEBEND0201LT12R1	24.933	10.344	40.8460110812627LJB
0018SIDEBEND0201CT12S1	22.254	11.035	40.4100110812627LJB
0018SIDEBEND0201CT12SM	22.080	11.127	40.9280110812627LJB
0018SIDEBEND0201CT12TL	24.302	11.775	42.6290110812627LJB
0018SIDEBEND0201CT12TR	26.474	10.231	41.7490110812627LJB
0018SIDEBEND0201GLROD1	83.030	9.249	50.0720110812627LJB
0018SIDEBEND0201GLROD2	47.522	9.215	50.0720110812627LJB
0018SIDEBEND0201QUBE01	61.659	6.132	58.7550110812627LJB
0018SIDEBEND0201QUBE02	49.981	5.986	58.7540110812627LJB
0018SIDEBEND0201QUBE05	61.645	6.063	49.5610110812627LJB
0018SIDEBEND0201QUBE06	49.990	5.953	49.5020110812627LJB
0018SIDEBEND0201QUBE07	61.604	21.200	49.3870110812627LJB
0018SIDEBEND0201QUBE08	49.815	21.114	49.4440110812627LJB
0018SIDEBEND0201STGSRP	28.917	14.580	9.9460110812627LJB
0018SIDEBEND0201STGT02	20.537	3.590	42.5290110812627LJB
0018SIDEBEND0201STGT03	17.641	7.440	53.4700110812627LJB
0018SIDEBEND0201STGT06	25.420	29.333	23.8420110812627LJB
0018SIDEBEND0201STGT13	17.594	6.420	53.7630110812627LJB
0018SIDEBEND0201STGT16	25.445	28.713	23.7310110812627LJB
0018SIDEBEND0201WIRE02	0.083	0.017	30.4600110812627LJB

```
0018SIDEBEND0201WIRE03  0.055  0.004 60.9730110812627LJB
0018SIDEBEND0201WIRE08 -0.003 30.497 30.4170110812627LJB
 END
```

8.0 REFERENCES

Anderson, J.A.D and Sweetman, B.J. 1975. "A Combined Flexi-Rule/Hydrogoniometer for Measurement of Lumbar Spine and its Sagittal Movement." Rheumat. & Rehab. 14:173-179.

Andersson, G.B.J., Schultz, A., Nathan, A., and Irstam, L. 1981. "Roentgenographic Measurement of Lumbar Intervertebral Disc Height." Spine, 6(2):154:158.

Andriacchi, T., Schultz, A., Belytschko, T., and Galante, J. 1974. "A Model for Studies of Mechanical Interactions Between the Human Spine and Rib Cage." J. Biomechanics, 7:497-507.

Aronson, A.S., Holst, L., and Selvik, G. 1974. "An Instrument for Insertion of Radiopaque Bone Markers." Radiol. 113:733-734.

Bakke, S.N. 1931. "Röntgenologische Beobachtungen Uber die Bewegrengen der Wirbelsäule." Acta Radio., Suppl. 13, pp. 1-75.

Begg, A.C. and Falconer, M.A. 1949. "Plain Radiography in Intraspinal Protrusion of Lumbar Intervertebral Disks: A Correlation with Operative Findings." Brit. J. Surg. 36:225-239.

Belytschko, T., Kulak, R.F., Schultz, A.B., and Galante, J.O. 1974. "Finite Element Stress Analysis of an Intervertebral Disc." J. Biomechanics 7:277-285.

Blowers, D.H., Elson, R., and Korley, E. 1972. "An Investigation of the Sphericity of the Human Femoral Head." Med. & Biol. Eng. 10:762-775.

Brown, R.H., Burstein, A.H., Nash, C.L., and Schock, C.C. 1976. "Spinal Analysis Using a Three-Dimensional Radiographic Technique." J. Biomechanics 9:355-365.

Chandler, R.F., Clauser, C.E., McConville, J.T., Reynolds, H.M., and Young, J.W. 1975. "Investigation of Inertial Properties of the Human Body." Final Report, National Highway Traffic Safety Administration, DOT HS-801 430. U.S. Dept. Transportation, Washington, D.C.

Clarke, I.C., Fiske, C., and Amstutz, H.C. 1979. "Spherometer Measurements of Human Hip-Joint Geometry." Med. & Biol. Eng. & Comput. 17:155-160.

Clauser, C.E., McConville, J.T., and Young, J.W. 1969. "Weight, Volume, and Center of Mass of Segments of the Human Body." Technical Report, Aerospace Medical Research Laboratory, AMRL-TR-69-70. Wright-Patterson Air Force Base, Ohio.

Clayson, S.J., Newman, I.M., Debevec, D.F., Anger, R.W., Skowlund, H.V., and Kottke, F.J. 1962. "Evaluation of Mobility of Hip and Lumbar Vertebrae of Normal Young Women." Arch. Phys. Med. 43(1):8.

Cossette, J.W., Farfan, H.F., Robertson, G.H., and Wells, R.V. 1971. "The Instantaneous Center of Rotation of the Third Lumbar Intervertebral Joint." J. Biomechanics 4:149-153.

Damon, A., Stoudt, H.W., and McFarland, R.A. 1966. The Human Body in Equipment Design. Harvard Univ. Press, Cambridge, Mass.

Dempster, W.T. 1955. "Space Requirements of the Seated Operator: Geometrical, Kinematic, and Mechanical Aspects of the Body with Special Reference to the Limbs." Wright Air Development Technical Report, WADC-TR-55-159. Wright Air Development Center, Wright-Patterson Air Force Base, Ohio.

Egund, N., Olsson, T.H., Schmid, H., and Selvik, G. 1978. "Movements in the Sacrolilac Joints Demonstrated with Roentgen Stereophotogrammetry." Acta Rad. Diag. 19:833-846.

Frisch, G.D. and D'Aulerio, L.A. 1980. "Bioman - An Improved Occupant Crew Station Compliance Modeling System." Aviat. Space and Environ. Med. 51:160-167.

Froning, E.C. and Frohman, B. 1968. "Motion of the Lumbosacral Spine after Laminectomy and Spine Fusion." J. Bone Jt. Surg. 50-A(5): 897-917.

Geoffrey, S.P. 1961. "A 2-D Mannikin - The Inside Story." SAE #267A, Society of Automotive Engineers, New York.

Gregerson, G.G. and Lucas, D.B. 1967. "An In Vivo Study of the Axial Rotation of the Human Thoracolumbar Spine." J. Bone Jt. Surg. 49-A(2):247-262.

Hagelstam, L. 1949. "Retroposition of Lumbar Vertebrae." Acta Chirurgica Scand., Suppl. 143, pp. 1-152.

Hirsch, C. 1965. "Forces in the Hip Joint", pp. 341-350. In Kenedi, R.M. (ed.) Biomechanics and Related Bioengineering Topics. Pergamon Press, Ltd., Oxford.

Jensen, R.H. and Davy, D.T. 1975. "An Investigation of Muscle Lines of Action about the Hip: A Centroid Line Approach vs. the Straight Line Approach." J. Biomechanics 8:103-110.

Keegan, J.J. 1953. "Alterations of the Lumbar Curve related to Posture and Seating." J. Bone Jt. Surg. 35A(3):589-603.

Knutsson, F. 1944. "The Instability Associated with Disk Degeneration in the Lumbar Spine." Acta Radiol. 25:593-609.

Kroemer, K.H.E. 1973. "COMBIMAN: Computerized Biomechanical Man-Model." Aerospace Medical Research Laboratory, AMRL-TR-72-16. Wright-Patterson Air Force Base, Ohio.

Lanier, R.R., Jr. 1939. "The Presacral Vertebrae of American White and Negro Males." Amer. J. Phys. Anthrop. 25(3):341-420.

Loebl, W.Y. 1967. "Measurement of Spinal Posture and Range of Spinal Movement." Ann. Phys. Med. 9:103-110.

Marcus, J.H. 1980. "The accuracy of Screw Analysis Using Position Data from Anatomical Motion Studies." Master's Thesis. Michigan State University.

Martin, R. 1928. Lehrbuch der Anthropologie. G. Fischer, Jena.

Milne, J.S. and Lauder, I.J. 1974. "Age Effects in Kyphosis and Lordosis in Adults." Ann. Hum. Biol. 1(3):327-337.

Mohr, G.C., Brinkley, J.W., Kazarian, L.E., and Millard, W.W. 1969. "Variations of Spinal Alignment in Egress Systems and their Effect." Aerosp. Med. 40:938-988.

Olsson, T.H., Selvik, G., and Willner, S. 1977. "Mobility in the Lumbosacral Spine after Fusion Studied with the Aid of Roentgen Stereophotogrammetry." Clin. Orthop. & Rel. Res. 129:181-190.

Patrick, J.M. 1976. "Thoracic and Lumbar Spinal Curves in Nigerian Adults." Ann. Hum. Biol. 3(4):383-386.

Pennal, G.F., Conn, G.S., McDonald, G., Dale, G., and Garside, H. 1972. "Motion Studies of the Lumbar Spine: A Preliminary Report." J. Bone Jt. Surg. 54-B(3):442-452.

Pope, M., Hanley, E., Matteri, R., Wilder, D., and Frymoyer, J. 1977a. "Measurement of Interbertebral Disc Space Height." Spine 2(4):282-286.

Pope, M.H., Wilder, D.G., Buturla, E., Hatteri, R., Frymoyer, W.W., and Frymoyer, J.W. 1977b. "Radiographic and Biomechanical Studies of the Human Spine." Final Report, Air Force Office of Scientific Research, AFOSR-TR-78-0063. Bolling Air Force Base, D.C.

Rab, G.T. and Chao, E.Y. 1977. "Verification of Roentgenographic Landmarks in the Lumbar Spine." Spine 2(4):287-293.

Reynolds, H.M. 1976. "A Foundation for Systems Anthropometry, Phase I." Interim Scientific Report, Air Force Office of Scientific Research, AFOSR-TR-77-0911. Bolling Air Force Base, D.C.

Reynolds, H.M., Freeman, J.R., and Bender, M. 1977. "A Foundation for System Anthropometry, Phase II." Final Report, Air

Force Office of Scientific Research, AFOSR-TR-78-1160. Bolling Air Force Base, D.C.

Reynolds, H.M., Hubbard, R.P., Freeman, J.R., and Marcus, J. 1978. "A Foundation for Systems Anthropometry, Phase III." Annual Report, Air Force Office of Scientific Research. Bolling Air Force Base, D.C.

Reynolds, H.M., Marcus, J., and Batzer, L. 1981. "A Foundation for Systems Anthropometry." Final Report, Southeastern Center for Electrical Engineering Education, Orlando, Florida.

Reynolds, H.M. 1980. "Three-Dimensional Kinematics in the Pelvic Girdle." J. Amer. Ost. Assoc. 80(4):277-280.

Reynolds, H.M. and Hubbard, R.P. 1980. "Anatomical Frames of Reference and Biomechanics." Hum. Factors 22(2):171-176.

Reynolds, H.M., Hallgren, R., and Marcus, J. 1982. "Systems Anthropometry: Development of a Stereoradiographic Measurement System." J. Biomechanics 15(4):229-233.

Reynolds, H.M., Snow, C.C., and Young, J.W. 1981. "Spatial Geometry of the Human Pelvis." Memorandum Report, Federal Aviation Administration, AAC-119-81-5. Protection and Survival Laboratory, Civil Aeromedical Institute, Mike Maroney Aeronautical Center, Oklahoma City, Oklahoma.

Robbins, D.H. and Reynolds, H.M. 1975. "Position and Mobility of Skeletal Landmarks of the 50th Percentile Male in an Automotive Seating Posture." Final Report, Vehicle Research Institute, VRI7.1 SAE, Warrendale, Pennsylvania.

Rolander, S.D. 1966. "Motion of the Lumbar Spine with Special Reference to the Stabilizing Effect of Posterior Fusion." Acta Orthop. Scand., Suppl. 90, pp. 1-144.

Rydell, N. 1965. "Forces in the Hip Joint", pp. 351-357. In Kenedi R.M. (ed.) Biomechanics and Related Bioengineering Topics. Pergamon Press, Ltd., Oxford.

Schultz, A. 1974. "Mechanics of the Human Spine." Appl. Mech. Rev., pp. 1487-1497.

Schultz, A.B., Benson, D.R., and Hirsch, C. 1974a. "Force-Deformation Properties of Human Ribs." J. Biomechanics 7(3):303-309.

Schultz, A.B., Benson, D.R., and Hirsch, C. 1974b. "Force-Deformation Properties of Human Costo-Sternal and Costo-Vertebral Articulations." J. Biomechanics 7(3):311-318.

Selvik, G. 1974. "A Roentgen Stereophotogrammetric Method for the Study of Kinematics of the Skeletal System." Thesis, Department of Anatomy, University of Lund, Lund, Sweden.

Sherlock, R.A. and Aitken, W.M. 1980. "A Method of Precision Position Determination Using X-Ray Stereography." Phys. Med. Biol. 25(2): 349-355.

Snyder, R.G., Chaffin, D.B., and Schutz, R.K. 1972. "Link System of the Human Torso." Final Report, Aerospace Medical Research Laboratory, AMRL-TR-71-88. Wright-Patterson Air Force Base, Ohio.

Stokes, T.A.F., Medlicott, P.A., and Wilder, D.G. 1980. "Measurement of Movement in Painful Intervertebral Joints." Med. & Biol. Eng. & Comput. 18:694-700.

Suh, C.H. 1974. "The Fundamentals of Computer-Aided X-Ray Analysis of the Spine." J. Biomechanics 7(2):161-169.

Tanz, S.S. 1953. "Motion of the Lumbar Spine." J. Roentgen. 69(3): 399-412.

Todd, T.W. and Pyle, S.I. 1928. "A Quantitative Study of the Vertebral Column by Direct and Roentgenoscopic Methods." Amer. J. Phys. Anthrop. 12(2):321-338.

Troup, J.D.G., Hood, C.A., and Chapman, A.E. 1968. "Measurements of the Sagittal Mobility of the Lumbar Spine and Hips." Ann. Phys. Med. 9(8):308-321.

Weisl, H. 1954a. "The Ligaments of the Sacro-Iliac Joint Examined with Particular Reference to their Function." Acta Anat. 20(3):201-213.

Weisl, H. 1954b. "The Articular Surfaces of the Sacro-Iliac Joint and their Relation to the Movements of the Sacrum." Acta Anat. 22(1): 1-14.

Weisl, H. 1955. "The Movements of the Sacro-Iliac Joint." Acta Anat. 23(1):80-91.

White, A.A. III and Panjabi, M.M. 1978. "The Basic Kinematics of the Human Spine." Spine 3(1):12-20.

Wigh, R.E. 1980. "The Thoracolumbar and Lumbosacral Transitional Junctions." Spine 5(3):215-222.

Wilder, D.G., Pope M.H., and Frymoyer, J.W. 1980. "The Functional Topography of the Sacroiliac Joint." Spine 5(6):575-579.

*U.S.Government Printing Office: 1983 — 659-005/2044